STRATOSPHERIC OZONE CLIMATOLOGY AND VARIABILITY FROM GROUND-BASED AND SATELLITE OBSERVATIONS OVER IRENE, SOUTH AFRICA (25.5^{O}S; 28.1^{O}E)

by

JEREMIAH OGUNNIYI

212562297

June, 2014

Submitted in fulfilment of the academic

requirements for the degree of

Masters of Science in the

School of Chemistry and Physics,

University of KwaZulu-Natal

Durban

June, 2014

As the candidate's Supervisor I have/have not approved this thesis for submission

Signed: ..... Name: ..... Date: .....

Durban, June, 2014.

DECLARATION I

This thesis describes the work undertaken at the University of KwaZulu-Natal under the supervision of Prof. V. Sivakumar between February 2013 and June 2014.

I declare the work reported herein to be my own research, unless specifically indicated to the contrary in the text.

Signed: .....

On this.....day of.....2014

I hereby certify that this statement is correct

.....

Prof. V. Sivakumar (Supervisor)

DECLARATION II - PLAGIARISM

I, ..., declare that

1. The research reported in this thesis, except where otherwise indicated, is my original research.

2. This thesis has not been submitted for any degree or examination at any other university.

3. This thesis does not contain other persons' data, pictures, graphs or other information, unless specifically acknowledged as being sourced from other persons.

4. This thesis does not contain other persons' writing, unless specifically acknowledged as being sourced from other researchers. Where other written sources have been quoted, then:

(a) Their words have been re-written but the general information attributed to them has been referenced.

(b) Where their exact words have been used, then their writing has been placed in italics and inside quotation marks, and referenced.

5. This thesis does not contain text, graphics or tables copied and pasted from the Internet, unless specifically acknowledged, and the source being detailed in the thesis and in the References sections.

Signed: .....

DECLARATION III - PUBLICATIONS

Details of contributions to publications that form part and/or include research presented in this thesis (include publications in preparation, submitted, in press and published and give details of the contributions of each author to the experimental work and writing of each publication)

Signed: .....

ACKNOWLEDGEMENTS

I would like to express my sincere gratitude to my supervisor Prof. Venkataraman Sivakumar for his advice and contributions towards the successful completion of this research work. Your invaluable wealth of experience, patience and guidance throughout the period of this research has been of great help.

I would also like to thank the University of Kwa-Zulu Natal for the enabling environment for this research work to be carried out.

My gratitude goes to Dr. Adewumi for his help in securing my admission as well as Pastor Michael Olusanya, Pastor Joseph Adesina who were also instrumental.

I would like to thank all my friends who have been supportive throughout my study, Peter Merisi, Andronicus Akinyelu, Luke Joel, Jeremiah Oluleye, Olusola Bodode, Victor Ewuola, Tunde Awoniyi, Tola Awoniyi and many more whose names are too precious to mention. Members of DLCF are also acknowledged.

My family members are not left out for been there for me through thick and thin, the prayers, encouragements especially from my wonderful dad, my sweet mum, my darling sister, my inestimable brother, my lovely cousin.

Finally, all glory goes to the potentate of my faith.

Abbreviations

ECC**:** Electrochemical Concentration Cell

UV**:** Ultraviolet radiation

DU: Dobson Units

TCO: Total Column Ozone

UTLS: Upper Troposphere and Lower Stratosphere

TOMS: Total Ozone Mapping Spectrometer

EP-TOMS: Earth-Probe Total Ozone Mapping Spectrometer

GOME: Global Ozone Monitoring Experiment

OMI: Ozone Monitoring Experiment

IASI: Infrared Atmospheric Sounding Interferometer

MLS: Microwave Limb Sounder

ToZ: Total Ozone

QBO: Quasi-Biennial Oscillation

SHADOZ: Southern Hemisphere ADditional OZonesonde

H_2O: Water Vapour

CO: Carbon monoxide

$ClONO_2$: Chlorine Nitrate

O: Oxygen Atom

O_2: Oxygen Gas

O_3: Ozone

$OClO_3$: Perchlorate

HCOOH: Formic Acid

H_2CO_3: Carbonic Acid

HNO_3: Nitric Acid

CH_3OH: Methanol

CHOCHO: Ethanedione

Cl: Chlorine Atom

ClO: Hypochlorite

N: Nitrogen Atom

N_2: Nitrogen gas

NO: Nitric Oxide

NO_2: Nitrogen Dioxide

NH_3: Ammonia

N_2O: Nitrous Oxide

N_2O_5: Dinitrogen Pentoxide

HONO: Nitrous Acid

CH_4: Methane

CFC: Chlorofluorocarbon

$CFCl_3$: Freon-11

C_2H_4: Ethylene

SO_2: Sulphur dioxide

H_2S: Hydrogen Sulphide

BrO: Hypobromite

List of Tables

Pages

List of Equations Page

List of Figures

ABSTRACT

The climatological characteristic of ozone over Irene (25.5^{o}S, 28.1^{o}E) was assessed in this thesis using ground-based satellite observations. The aim of this was to examine the variability of both total and vertical ozone distribution over Irene. Ground based instruments were selected since they provide accurate measurement of ozone while satellite measurements were used for this study because they provide a wider coverage. Satellite data from Total Ozone Mapping Spectrometer (TOMS) from November 1978 to May 1993, Global Ozone Monitoring Experiment-1 (GOME-1) from August 1995 to June 2003, Earth Probe Total Ozone Monitoring Spectrometer (EP-TOMS) from January 1997 to December 2005, Microwave Limb Sounder (October 2004 to April 2013), Ozone Monitoring Interferometer (OMI) from October 2004 to December 2013, Global Ozone Monitoring Experiment-2 (GOME-2) from January 2007 to December 2013, and Infrared Atmospheric Sounding Interferometer (IASI) from June 2008 to December 2011 and ground-based measurements from Dobson Instrument (August 1989 to December 2011) as well as Ozonesondes (November 1978 to Decemeber 2007) were used. The seven satellites and two ground based instruments used for this study were selected as they provide long term ozone monitoring data. The above satellites measurements were collected when they overpass over Irene. The height profiles of ozone concentration obtained from ozonesondes and satellite (MLS) are in good in good agreement from 15 km and above. Maximum ozone concentration was found in the height region of 23 km to 27 km. Above this height, ozone concentration reduced with increasing height. The monthly variation of ozone concentration from ozonesondes and MLS showed maximum concentration during spring and minimum concentration during autumn. Maximum ozone concentration from ozonesonde corresponds to $4.5x10^{12}$ molecules/cm^3 while that from MLS satellite was ~ $4.1x10^{12}$ molecules/cm^3 during spring. A difference in the range of $4x10^{11}$molecules/cm^3 and $0.8x10^{12}$ molecules/cm^3 was obtained for all seasons except during winter when the difference was in the range of $0.6x10^{12}$ molecules/cm^3 and $0.9x10^{12}$ molecules/cm^3. Satellite measurements used to determine column ozone replicated spring maximum and autumn minimum. TOMS variation displayed higher value of total column ozone of about 7 DU when compared with other satellites but had good agreement with Dobson instrument. Combined satellite measurement of ozone was within 3 DU with Dobson mesurement. Satellite comparison with Dobson improved when both

GOME measurements were not used to within 1 DU while GOME comparison with Dobson was within 5 DU. EPTOMS and GOME-1 showed gradual increase in column ozone between 1995 and 2005 by ~2 DU which has increased to ~7 DU in the last decade as measured by OMI, GOME-2 and IASI satellites. Ozone variability over South Africa was consistent with the seasonal variability of spring maximum and autumn minimum. The lower part of South Africa had more total ozone compared to the central part and lower part of South Africa attributed to maritime activities taking place in the region as well as the impact of wind from ozone rich regions in the high latitudes to mid-latitude regions. The north eastern part of South Africa had ~5 DU more than other northern part. This is atributed to the impact of biomass burning in the surrounding regions. This study has shown that there was ozone loss between 1978 and 1991 in Irene but there has been gradual recovery of ozone by ~ 7 DU per decade.

Table of Content Page

CHAPTER 1

INTRODUCTION

1.1 The Earth's Atmosphere

The earth's atmosphere consists of gases surrounding the earth. The atmosphere protects life by absorbing ultraviolet solar radiation and warms the surface of the earth through the greenhouse effect. The gases present in the atmosphere are presented by volume in the pie chart in figure 1.1. Percentage concentrations of nitrogen, oxygen, argon in the atmosphere are 78 %, 20.9 % and 0.9 % respectively. Other gases include, Ne, He, $CH4_4$, H, NO and O_3 with percentage concentration of 0.036 %, 0.0018 %, 0.0005 %, 0.00017 %, 0.00005 %, 0.00003 %, 0.000004 % respectively. Though ozone concentration is the lowest and can be considered negligible compared to other gases, it is of great importance to living organisms. The earth's atmosphere is divided into four bands based on altitude as shown in figure 1.2: the troposphere (0 to ~15 km), the stratosphere (15 km to 50 km), the mesosphere (50 km to 90 km), and the thermosphere (90 km and above). The ionosphere is sometimes included. The ionosphere consists of the upper mesosphere, the thermosphere and the exosphere.

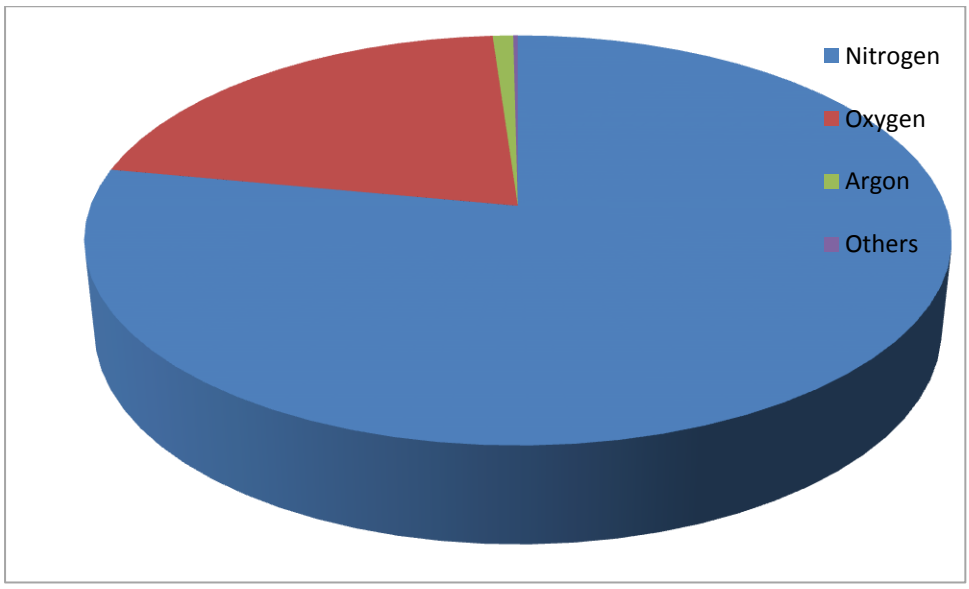

Figure 1.1- Pie chart showing gas constituents of the earth's atmosphere and their percentage volume

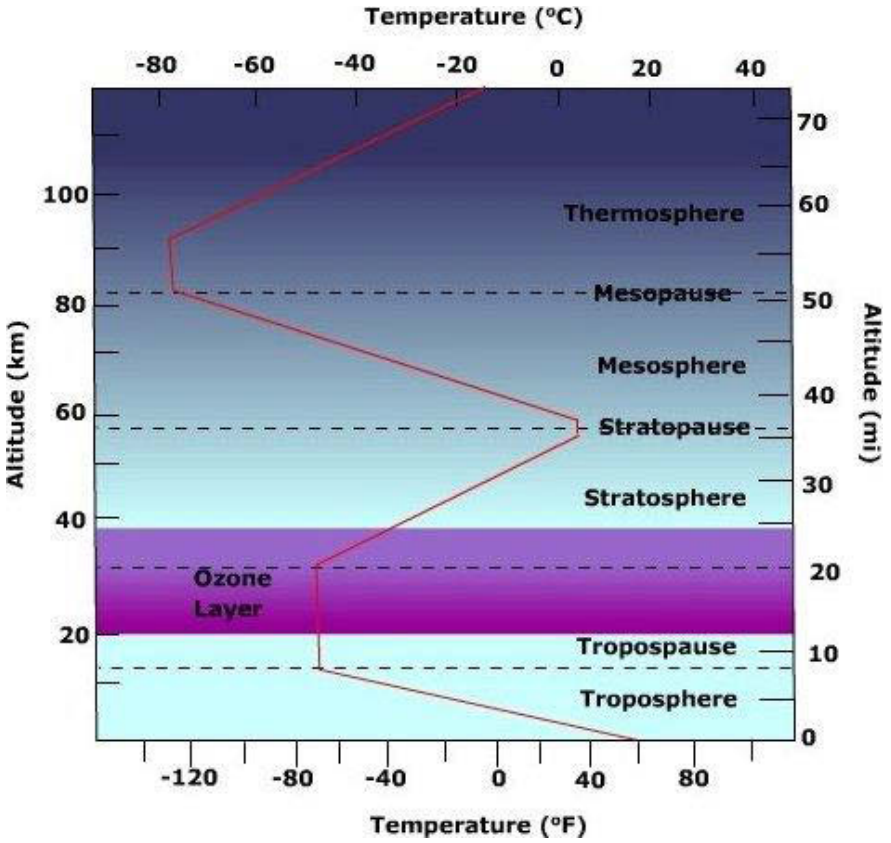

Figure 1.2: Height profile of temperature, illustrating different layers in the atmosphere as well as the ozone layer (sourced from http://www.aerospaceweb.org/question/atmosphere/q0059.shtml)

1.2 Ozone in the atmosphere

Ozone is an allotrope of oxygen having three covalently bonded oxygen atoms. It is the most important trace element in terms of its impact on living organisms (Wang Jun and Wang Hui-Jun 2010, Calkins and Thordardottir 1980). It makes up about 1 part in 10^6 of atmospheric elements. Ozone condenses to a dark blue liquid at -112^{o}C and freezes at -251.2^{o}C. Its chemical property is similar to that of oxygen, however, it is more reactive and it is a very powerful oxidizing agent. It is produced when sulphur (iv) oxide, nitrogen oxides are exposed to UVR of wavelengths less than 240 nm (Pyle and Shepherd 2007). It is also produced naturally during thunder storms which give rise to a characteristic pungent smell after storm (De Caria and Pickering 2005). It is an unstable gas, thus, its preparation is very difficult and its reactivity makes it dangerous to prepare. Ozone is found both in the troposphere and in the stratosphere regions of the atmosphere (see- Figure-1.2), but majorly found in the stratosphere ranging from 20-30 km known as the ozone layer (Van der Leun 2004). Maximum ozone concentration is found at altitudes between 22 km and 27 km over tropical

region (Sivakumar et al., 2007). Stratospheric ozone absorbs ultraviolet (UV) radiations within the wavelength region of 250 nm to 300 nm (Dobber et al 2006, Rusch et al., 1994) preventing dangerous effects due to excessive UV radiation exposure on the biological systems (Anton et al 2010, Bramstedt et al., 2003). As it absorbs UVR to protect living organisms, it also provides a mechanism of radiative heating in the stratosphere (Dufour et al., 2012). Anthropogenic sources of pollution mainly in the form of chlorofluorocarbons (CFCs) have constantly depleted the ozone layer (Lu and Sanche 2001). This depletion of global ozone concentration leads to an increase in ultraviolet flux on the earth with a resultant effect on man, plants and animals (Norval et al., 2007). In urban areas, tropospheric ozone is prominent. This gives rise to a second ozone maximum often observed at low altitudes (4 km or less). Tropospheric ozone is found to be harmful and dangerous with negative effects on the biological and ecological system such as eye and skin cancer in man and animals, cataracts, weakening of human immune system, degradation of wood, fabrics and plastics, stunted growth in plants, death of aquatic animals (Clain et al., 2009). Surface ozone concentration varies with both geographical locations and seasons (Chan and Vet 2010).

Researches into atmospheric ozone have increased since 1985 when total column ozone decreased by about 30 DU over southern mid-latitudes attributed to a combination of westerly phase QBO (Quasi-Biennial Oscillation) and the switch from easterly to westerly phase early in the year (Bodeker et al., 2007).

Between 1950 and 2000, about 23 million metric tonnes of chlorofluorocarbons, 11 million tonnes of methyl chloroform, 4 million tonnes of hydro fluorocarbon and 2.5 million tonnes of carbon tetrachloride have been released into the atmosphere (Harremoes et al., 2002). These gases deplete the amount of ozone in the atmosphere. The ozone layer was discovered in the 1970s when fears of threats to human were raised. This was due to the exhaust gas emission coming from aircrafts flying within the stratosphere. This exhaust gases contained various nitrogen oxides known to catalyse the destruction of ozone. Supersonic jets containing methane and other gases to reduce the rate of this depletion were proposed to be launched. However, due to economic reasons, this could not materialize. Sherwood Rowland and Mario Molina proposed the use of chlorine atoms to replace nitrogen oxides. It was later realized in 1985 that chlorine induced ozone depletion.

1.3 Formation of ozone

The atmospheric composition ranges with altitudes its interaction with incoming solar radiation determines the presence of ozone in that range (Browell et al., 2003). Though Nitrogen and Oxygen gases are abundant in the atmosphere, they do not react at normal temperatures. However, they react in cylinders of automobiles. In the troposphere, when there are vehicular activities, both Nitrogen and Oxygen gases react to form NO which then reacts with O_2 in the atmosphere to produce NO_2. When NO_2 reacts with light, it dissociates to form NO and O. The free oxygen atom and diatomic oxygen combines to form ozone.

$$N_2 + O_2 \rightarrow 2NO \quad (1.1)$$

$$2NO + O_2 \rightarrow 2NO_2 \quad (1.2)$$

$$NO_2 + UV \rightarrow NO + O \quad (1.3)$$

$$O + O_2 \rightarrow O_3 \quad (1.4)$$

In the stratosphere, ozone is produced by photochemical reactions involving oxygen molecules. When oxygen molecule absorbs UVR less than 240 nm, it breaks to form two oxygen atoms. The oxygen atom and diatomic oxygen combines to form ozone.

$$O_2 + UV \rightarrow O + O \quad (1.5)$$

$$O + O_2 + N \rightarrow N + O_3 \quad (1.6)$$

N is usually molecular nitrogen which acts as a catalyst.

When ozone absorbs UVR greater than 250 nm, it dissociates again to form oxygen gas and oxygen atom.

$$O_3 + UV \rightarrow O_2 + O \quad (1.7)$$

Therefore, the concentration of oxygen atom for the formation of ozone determines the rate of photolysis of oxygen gas and the variation in oxygen gas concentration with altitude (Oum et al., 1998). These processes of ozone formation and destruction are summarized in figure 1.3. Though stratospheric ozone is produced by solar radiation, conventionally, maximum ozone concentration should be at the tropics while minimum ozone concentration at the polar regions. However, this is not so with maximum ozone concentration found in the mid-to-high latitudes of both the northern and southern hemispheres. Maximum and minimum ozone

concentrations are found to be in the winter/spring and summer/autumn both in the northern and southern hemisphere (Charles Welch 2014).

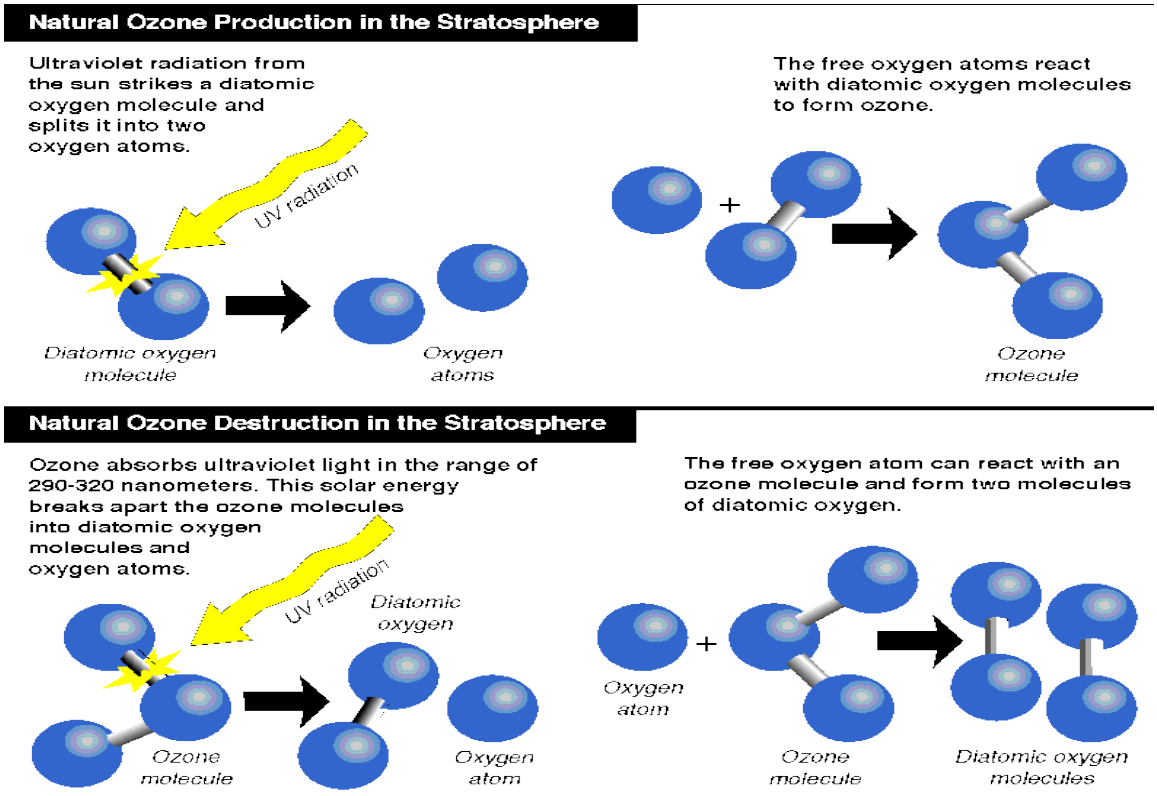

Figure 1.3: natural production and destruction of stratospheric ozone (sourced from Rod Jenkins, 2006 - http://www.ozonedepletion.info/education/ozone.html)

Atmospheric dynamics role in the redistribution of ozone cannot be over-emphasized. This causes ozone carrying air to circulate from high altitudes in the tropics to the poles. This circulation continues to the pole in the northern hemisphere with a spring maximum of about 450 Dobson Unit (DU) but stops at 60^{o} in the southern hemisphere with a spring maximum of about 380 DU.

1.4 Destruction of ozone

The major cause of ozone depletion is the increase in atmospheric Chlorine. Chlorine enters the atmosphere in the form of chlorofluorocarbons (CFCs). Chlorofluorocarbons are carbon compounds containing Chlorine, Fluorine and Bromine atoms. They are synthetically prepared as they do not occur naturally. CFCs are not easily oxidized nor reduced as they are chemically non-reactive, non-toxic and non-flammable. They have high industrial usage as they are used in the manufacture of polyurethane foams, cleaning solvents for electronic equipment, fire extinguishers and cooling fluids in refrigeration.

When equipment or instrument containing chlorofluorocarbons are used, they gradually escape to the troposphere. Due to their inert nature, dynamical atmospheric processes have no impact on them as they slowly rise to the stratosphere. In the stratosphere, UVR arising from the sun is strong enough to dissociate them. By the time photo dissociation occurs, chlorine mixes with ozone and the layer gets depleted.

$$CFCl_3 + UV \rightarrow CFCl_2 + Cl \quad (1.8)$$

$$Cl + O_3 \rightarrow ClO + O_2 \quad (1.9)$$

Nitrogen oxides also play their role in ozone depletion.

$$NO + O_3 \rightarrow NO_2 + O_2 \quad (1.10)$$

These reactions are the main cause of ozone depletion.

Montreal protocol was introduced in 1987 and its enforcement started in 1989 to protect the ozone layer. The purpose was to gradually reduce and phase out the use of compounds containing fluorocarbons in industries. Since this protocol, the atmospheric compositions of most chlorofluorocarbons have decreased as shown in figure 1.4. After 25 years of signing this agreement, 98 % of ozone depleting substances present in ~ 100 dangerous chemicals worldwide has been phased out. If international agreements are applied and adhered to, by 2050, total ozone layer recovery is expected. Without the Montreal protocol, by the year 2042, ozone layer would have depleted to an extent that the ecosystem would be at risk. Figure 1.5 shows how the earth would be by 2042 with and without the Montreal protocol.

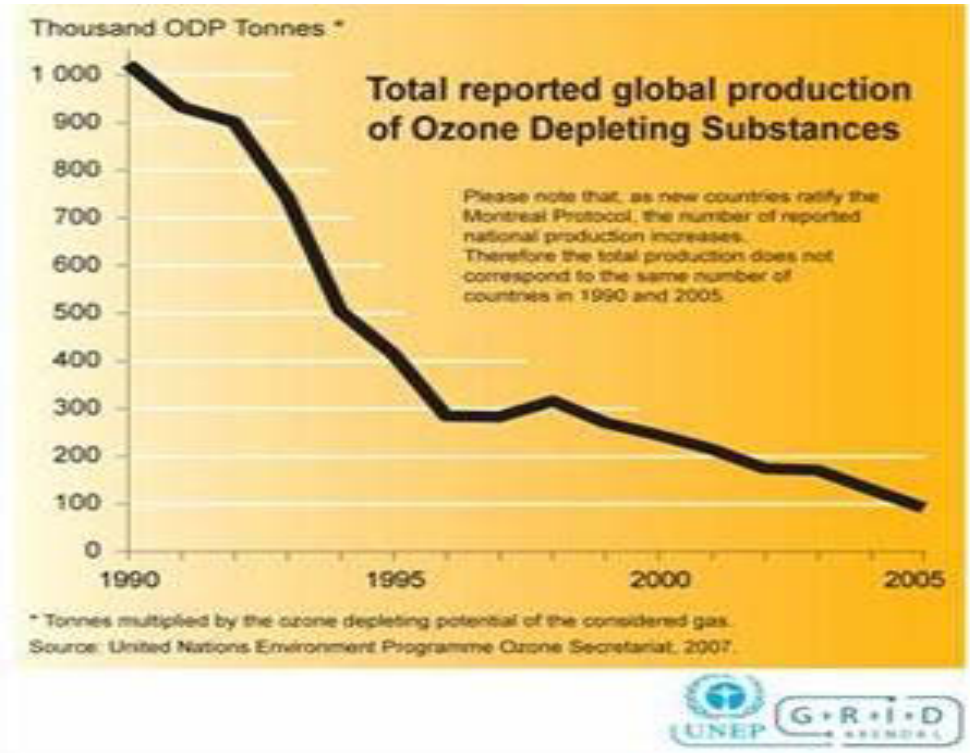

Figure 1.4: Graph showing global reduction of ozone depleting substances since the Montreal protocol (adapted from http://www.climate.org/topics/ozone-depletion.html)

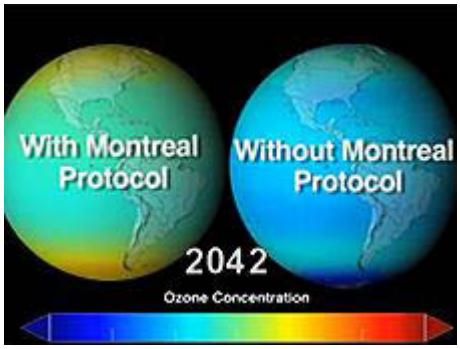

Figure 1.5: Figure showing what earth would look like in 2042 with and without Montreal protocol (sourced from http://www.nasa.gov/topics/earth/features/ozone-hole-2012.html)

1.5 The Antarctic ozone hole

The first major evidence of the result of anthropogenic activities on the ozone layer is the Antarctic ozone hole. Ozone concentration is measured in Dobson Units (DU) by calculating the total column ozone. Total column ozone is the thickness of the ozone layer at Standard Temperature and Pressure (STP). One DU is ~2.69 x 10^{16}molecules/cm^2. At STP, average ozone concentration corresponds to 300 DU, about 3 mm. Between 22 km and 27 km where maximum ozone concentration is expected, ozone concentration at this height region is about

10ppmv. The Antarctic ozone hole is due to the unique climatological conditions prevalent in the Southern Hemisphere which is both chemical and dynamical (Susan Solomon 1988). Ozone concentration depends on the amount of O, ClO, HCl, and ClONO2. At maximum ozone concentration O and ClO are low while HCl and $ClONO_2$ are high.

During winter, there is a loss of sunlight over the polar region, this makes temperature to fall significantly leading to the formation of polar vortex. Temperature during this polar winter drops to about -90^{o}C. This facilitates the formation of polar cloud in the Antarctic stratosphere. During the formation of these clouds, HNO_3, NO_2 are removed from the atmosphere. No ozone depletion takes place during this period because there is high chlorine reservoir. At the end of the winter, solar radiation returns to the Antarctic which initiates photochemical reactions. Mixing of stratospheric air with its boundaries is prevented by the polar vortex. Chlorine reacts photochemically to liberate free molecular chlorine on the surface of the polar stratospheric cloud. Molecular chlorine then reacts with ozone, which results in ozone loss. Bromine can also lead to ozone loss either through interaction with oxygen or a couple of reactions with chlorine. This depletion ends at the beginning of the summer as polar stratospheric cloud evaporates and molecular chlorine is converted to other compound. This recovery continues to winter and the whole chain starts again during spring.

Planetary waves play important role in ozone recovery in the Southern Hemisphere. Break in the polar vortex causes redistribution of ozone over the Antarctic by dynamical processes. With this break in polar vortex, ozone rich air from low altitudes replaces ozone poor air at high latitudes. With the annual formation of the ozone hole, global ozone concentration does not fully recover from previous spring depletion. This reduces the global ozone concentration. This annual depletion has been well documented. Between 1979 and 1991, at the equatorial region, little or no ozone loss was recorded while 3 to 5 % loss was recorded in the mid latitude and 4 to 8 % at high latitudes.

Solar cycle also contributes to variation in ozone concentration. Ozone concentration is directly proportional to solar cycle. Therefore, maximum ozone concentration corresponds to maximum solar activity. Stratospheric aerosols especially from volcanic eruptions also impact ozone concentration. However, chemical and dynamical processes are the major players in ozone concentration variability (Clain et al., 2009).

1.6 Research aims and objectives

The aim of this study is to examine the rate of ozone depletion and recovery over Irene, South Africa. This study also focused on ozone climatological characteristics over Irene from 1978 to 2013 with the use of two ground-based instruments and seven satellite measurements. Ozone monthly distribution and interannual variability over Irene is also examined. This study also focuses both on the vertical distribution of ozone as well as ozone column distribution. This study also examined the accuracy of the instruments used for this study with the aim of recommending the best for future studies. In addition to Irene studied as a location, ozone variation over South Africa is also examined in this study.

1.7 A brief history of study area

The present study address the climatological results of vertical ozone and the total column ozone over Irene (25.5^{o}S ; 28.1^{o}E), South Africa. The unique location of the station Irene, is by the fact that the availability of height profile of ozone by regular launch of combined radiosonde with ozone sensor (generally referred as ozonesonde). Irene is also one of the Southern Hemisphere Additional OzoneSonde (SHADOZ) network (Thompson et al., 2003). Irene is located between two highly industrialized cities of Pretoria and Johannesburg in the subtropical region of the Southern Hemisphere. It represents an area of relevant interest due to the observation of high and low latitude influences attributed to the transport processes (Semane et al., 2005). Like other Southern Hemisphere, Irene displays Southern Hemisphere tropospheric seasonality which is the austral spring time maximum different from other ozonesonde stations in the African tropics like Ascension, Brazzaville (Diab et al., 2004). Biomass burning is more evident in South Africa than many other Southern Hemisphere regions and it is more affected by subtropical jet stream (Clain et al., 2009). According to Yasmine et al., (2001), biomass burning contributes 26 % of stratospheric ozone and 16 % of tropospheric. Figure 1.5 shows the location of Irene in South Africa.

South Africa (latitude 22^{o}S to 35^{o}S and longitude 16^{o}E to 32^{o}E) is located in the southernmost part of the African continent. South Africa shares borders with Namibia in the north western part, Botswana in the north-north, Zimbabwe and Mozambique in the north eastern part. An overview of ozone measurements over South Africa was presented in a poster by Coetzee et al (2012) and showed that ozone sounding launches in South Africa commenced in 1992 with the station situated in Irene with two monthly measurements till date (2014). There were data gaps between 1994 and 1996 and between2007 and 2012 when

there were no soundings. South Africa has regularly taken part in special soundings for a number of campaigns such as SAFARI 1992, 1994 and 2000. The South African Weather Service (SAWS) was also involved in THESO/TRACAS project with an ozone station in Reunion Island. Apart from ozone vertical profile, total column ozone over South Africa has also been measured. The first total column ozone measurement over South Africa was with the Dobson instrument from 1964 to 1972 operating from Pretoria (World Meteorological Organisation). Continuous ozone measurements have continued over South Africa with South Africa now operating two Dobson instruments. The first Dobson instrument in South Africa was at Irene (25.5^{o}S; 28.1^{o}E) near Pretoria (25.7^{o}S; 28.2^{o}E) near the nation's capital while the other is located in Springbok (29.7^{o}S; 17.9^{o}E), located in the country's northern part. Both of these instruments are regularly calibrated with reference to the world Dobson standard. There is also an ozone observatory in Cape Point (34.2^{o}S; 18.3^{o}E), about 60km south of Cape Town (33.9^{o}S; 18.4^{o}E) in the southernmost part of South Africa. This location is noted for occasional biomass burning in the surrounding areas as well as moderate temperatures, dry summer and increased precipitation during winter. Thermo electron instruments are used for ozone measurement in Springbok. These have been operational since 1995 and are regularly calibrated with respect to the world's calibration standard. During the 1990 and early 2000, a SAOZ (Système D'Analyse par Observation Zènithale) instrument was operational in Durban but no more in operation now.

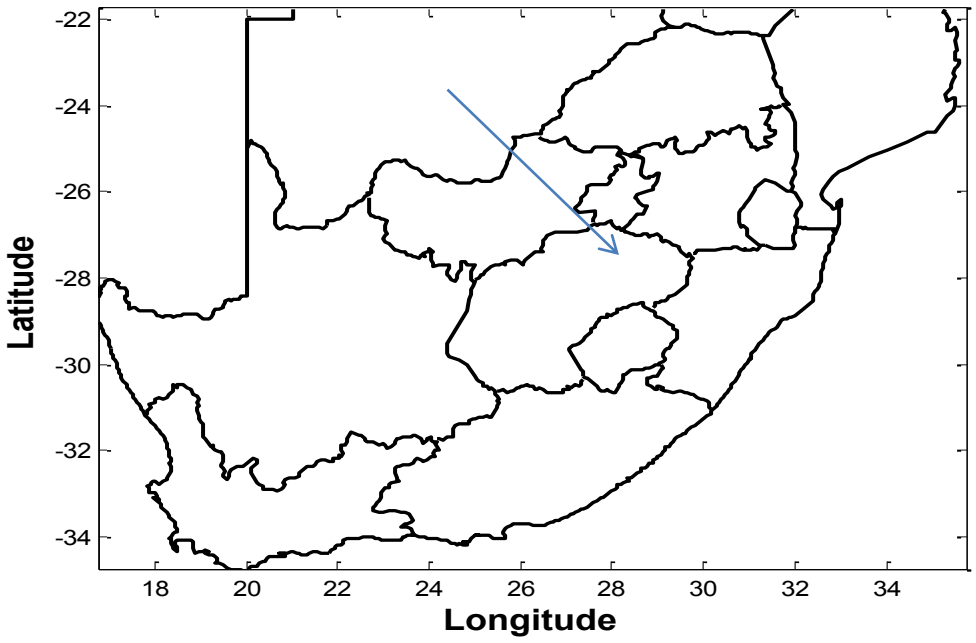

Figure 1.6: Geographical map of South Africa with an arrow showing the location of Irene (Study area)

1.8 Synopsis/overview of the thesis

This thesis is divided into five chapters. The first chapter gives brief details on the earth's atmosphere and ozone. The formation and destruction of ozone, the impact of ozone depleting substances on the earth's atmosphere, the Antarctic ozone hole and the location of the study are all discussed in this chapter.

Chapter two presents various ozone measuring instruments. It is divided into two sections. The first focuses on ground based instruments while the second focuses on satellite measurements. The specifications of some of these instruments are also discussed. Previous studies that have been carried out using some of these instruments are also presented. These studies were selected based on their relevance to this study and were limited to the last twenty years. This chapter is divided into two sections. The first focuses on the vertical variation of ozone, while the second presents the review of works done on total column ozone.

Chapter three focuses on research methods. The instruments used for this study, the years of measurements, data filtering carried out and data combinations are all discussed in this chapter.

The fourth chapter of this thesis is on the results and discussion. The results obtained are discussed under three sections. The first part is on the vertical distribution of ozone over Irene, the second is on total column ozone variation and climatology over Irene while the third section discusses the variation of ozone over South Africa

The last section gives the summary of this thesis. The summary is divided into three sections based on the results obtained in the thesis.

CHAPTER 2

OZONE MEASUREMENT

The qualitative analysis of atmospheric ozone started in 1913 by Charles Fabry and Henri Buisson, the French Physicists and was later explored by G.M.B. Dobson, the British Meteorologist. He later developed an instrument for measurement and analysis of ozone from ground level called the spectrometer. Since the late 1920s, ground-based measurements have been made using the Dobson Spectrophotometer and more recently the Brewer (Fioletov et al., 1999). The details of ozone measuring instruments are presented in this chapter. These instruments are divided into two categories: the ground-based measurements and satellite observations.

2.1 Ground-based measurements

Ground-based instruments refer to in-situ instruments measuring ozone. Some of these instruments are the Dobson and Brewer spectrophotometer, Lidars and ozonesondes. Both the Dobson and Brewer spectrometers measure total column ozone in the atmosphere while Lidars, ozonesondes measure ozone vertical distribution.

2.1.1 Dobson spectrophotometer

The Dobson spectrophotometer is the standard instrument to measure total column ozone on earth (Van Roozendael et al., 1998). Its measurement of total column ozone is reliable. Dobson spectrometers were substituted with automated Brewer spectrometer in the late 1980s and 1990s (Fioletov et al., 2002). The world standard Dobson spectrophotometer is the Dobson 83 which has been established in 1962 as the standard for total ozone measurement. It is the standard for all Dobson instrument calibration. Between 1962 and 1989, 15 American based and 75 foreign based Dobson instruments have been calibrated. The Dobson spectrophotometer 83 was calibrated 10 times between 1962 and 1987 by direct sun observation. Results from the calibration show that Dobson 83 maintains a precision of ± 0.5 % in long term ozone measurements. This result shows high accuracy and precision of the Dobson instrument for global network which is a reference for comparing and validating satellite measurements (Komhyr et al., 1989). With proper maintenance and regular

calibrations, ozone column from Dobson instrument estimated accuracy is ~1 % for direct sun observation and 2-3 % for zenith sky observation of sun elevation higher than 15^{o}. Dobson spectrophotometer is based on differential absorption method in the ultraviolet Huggins band (Balis et al., 2007) where ozone exhibits maximum absorption feature (Komhyr et al., 1989). Its measurement principle relies on the ratio of direct sunlight intensities at two standard wavelengths. The most common combination used is the double pair which is the recommended international standard for mid-latitudes (Balis et al., 2007; Anton et al., 2010).

The Dobson network temporal and spatial coincidences cover wide geographical area which helps to validate satellite sensor. This network has provided a number of total column ozone data for both trend analysis and satellite validation of total ozone data. In middle latitudes, there is a seasonal error of ± 0.9 % in Dobson measurements as ozone absorption coefficient used in retrievals depends on temperature. Systematic error constitutes about 4 % (Balis et al., 2007). A typical example of a Dobson instrument is shown in figure 2.1 below.

Figure 2.1: Dobson spectrophotometer (adapted from NOAA - http://www.ozonelayer.noaa.gov/action/dobson.htm)

2.1.2 Light Detection And Ranging (LIDAR)

Lidar is a remote sensing instrument that operates in the optical range. It measures atmospheric ozone, temperature and aerosols with the use of light-matter interactions such as Rayleigh, Mie and Raman Scattering. Lidar was first developed in the early 1960s but it was in 1991 people became aware of its usefulness and accuracy. Lidars are similar in principle to Radars (Radio Detection and Ranging) but uses laser light for measurements instead of radio waves. Lidars emit laser pulses into the atmosphere. These pulses are scattered by aerosols

and air molecules, some of which returns to the Lidars which analyses the scattered pulses to detect the aerosol layer, wind velocity and ozone concentration.

Lidars measure ozone vertical distribution by the Differential Absorption Laser (DIAL) technique. This technique requires the emission of two laser beams characterised by different ozone absorption cross section simultaneously. To measure atmospheric ozone, the laser wavelength depends on the altitude range to be measured. Ozone absorption is more efficient in the ultraviolet but the selected wavelength depends on whether tropospheric or stratospheric ozone is to be measured. An example of a mobile Lidar is shown in figure 2.2

Components of the Lidar system

- Laser for scientific applications, 600-1000 nm laser are used. If the Lidar receiver detectors and electronics have sufficient bandwidth, better target resolution is achieved with shorter pulses. The purpose of the Lidar determines the wavelength to be used
- Scanners and optics. The speed at which images are scanned determines how fast the images are developed
- Photo detector and receiver electronics. Solid state detectors such as silicon avalanche, photodiodes or photomultipliers are the photo detectors used
- Position navigation system. Sensors are mounted on airplane, satellites, mobile platforms to determine the position of the Lidar sensor

Figure 2.2: Mobile Lidar (sourced from Wikipedia - http://en.wikipedia.org/wiki/Lidar)

2.1.3.1 Ozonesondes

Ozonesonde is a balloon-borne instrument attached to a meteorological radiosonde. It is light weight. There is always a station receiving the ozone information and other quantities such as temperature, pressure, humidity. As the balloon carrying the instrument moves high through the atmosphere and it sends the measurements to the receiving station. Ozonesondes contain Electrochemical Concentration Cells (ECC) as shown in figure 2.3. The Electrochemical Concentration Cell is an electrochemical cell with two half cells made of Teflon serving as the cathode and the anode chamber. Both cells contain potassium mesh electrodes and are immersed in a potassium iodide solution of different concentrations. The two chambers are connected together by an ion bridge to provide an ion pathway and to prevent the mixing of the cathode and anode electrolytes. As the Electrochemical Concentration Cell reacts with the potassium iodide solution, it produces a weak current as it senses the ozone equivalent to the concentration of ozone in the sampled air

2.1.3.2 Ozonesonde preparation and launching

The procedure for ozonesonde preparation by the South African Weather Station is presented here using a Vaisala DigiCORA Sounding System MW31. Vaisala DigiCORA Sounding System is a sounding ground station which produces upper-air data for climatology and

meteorology research. Meteorology parameters such as humidity, temperature and pressure are measured by sensors integrated in the radiosonde attached to a free flying balloon. Wind speed and direction are determined using GPS navigation satellites. The system also provides synoptic upper-air messages for numerical weather prediction models and weather forecast. It uses the latest technology to ensure accuracy.

As presented in the guide, the important characteristics are given here:

Pump characteristics:

Pump Voltage (12-13 V)

Pump Current (90-120 mA)

Pump Pressure (>670 hPa)

Pump Vacuum (>670 hPa)

The cathode and the anode are both drained with the cathode replaced first.

The pump and the sensor are then flushed with NO O_3 for 5 minutes and the sonde also with NO O_3 for 10 minutes. The sonde is the conditioned along with the sensors with 5µA O_3 for another 10 minutes. After 10minutes of 5µA LO O_3, the sensor output current is recorded and then LO O_3 is changed to NO O_3 and the rate of sensor impulse is also recorded.

2.1.3.3 Balloon and DigiCORA preparation

The battery of the radiosonde box is connected to the radiosonde.. After this connection, the background sensor's current is checked. The sensor's current takes about 10 minutes to stabilize. After about 8 minutes with 2 minutes left, the battery is inserted inside distilled water for 2 minutes. The insertion of the battery in the radiosonde box should not be more than 20 minutes before flight. After 10 minutes, the final ozone current background value is recorded along with the surface pressure, wind direction, wind speed, temperature and cloud group. The sounding will start automatically once the pressure falls.

Once everything is in place, the radiosonde is connected to the balloon and released. As its goes high up through the atmosphere, it telemeters its readings to the receiving station for analysis. The balloon bursts at about 35 km or below. I was privileged to witness ozonesonde preparation and launching at the meteorological observatory Lindenburg, Germany 4th July, 2013. Figures 2.4-2.6 were taken by me during this time

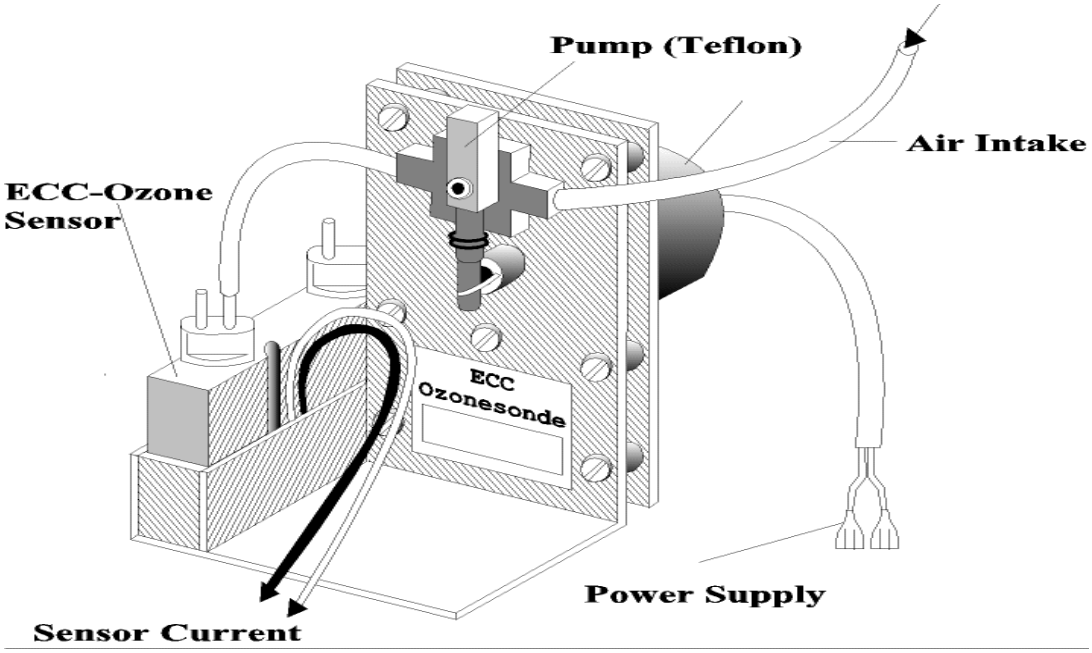

Figure 2.3 The Schematics on an Electrochemical Concentration Cell (SAWS - http://www.wmo.int/pages/prog/arep/gaw/documents/GAW_201.pdf)

Figure 2.4: Ozone generator with an ECC attached to it (picture taken by me)

Figure 2.5: ECC is to be attached with a balloon just before launch (picture taken by me)

Figure 2.6 The ECC and balloon after launch into space (picture taken by me)

2.1.4 Importance of the SHADOZ program

Ozonesonde role in monitoring the lower atmospheric ozone is very important as it has proved to be accurate and effective in these atmospheric regions. In a cause to monitor ozone, during the 1990s, tropical and subtropical stations in the southern hemisphere launched ozonesondes, although samplings were scattered and the geographical coverage was uneven. During the Southern African Fire Atmospheric Research Initiative/Transport and Atmospheric Chemistry near the Equator-Atlantic (SAFARI/TRACE-A), five sites were selected over a six weeks period in 1992, and over 50 launched were made. However, only one of these stations remained operational by the end of 1993. This lack of consistency in operational stations and gaps in ozonesonde operations limits the trends in research as data base are not comprehensive enough. Ground-based stations that can fix the features in tropical ozone variability associated with climate, dynamic and zonal wave one feature in satellite ozone are very few. This limitation brought about the Southern Hemisphere Additional Ozonesondes (SHADOZ) project. This project was meant to correct lack of consistency in tropical ozonesonde observations at operational sites by the enhancement of balloon launches. SHADOZ is meant to augment ozonesonde launches at existing stations with international partners on a cost share basis and also for zonal distribution of sites for wave number one pattern is observed in equatorial total ozone (Thompson et al., 2003). Irene became part of SHADOZ program in 1998. Since Irene joined SHADOZ, there has been an average of two monthly measurements over the years. However, due to financial reasons, measurements were stopped in 2007 but resumed in September 2012 and since 2013, there has been weekly measurements are made over Irene.

2.1.5 Rockets

Atmospheric column ozone has been of interest since the 1920s. Satellites help to determine total ozone from ground levels as ozone vertical distribution is made possible by balloon carrying instruments. However, most balloons burst at maximum height of 35 km. At this altitude region, ozone is basically controlled by meteorological factors. Above this height region, ozone production is by photochemical reactions where balloons cannot reach. Umkehr effect has been used for the vertical ozone distribution for wider altitude range with low accuracy (Johnson et al., 1951).

1n 1946, Vergeltungswaffe-2 rockets were made available to measure ozone vertical distribtion to altitudes balloons could not reach and to study the top edge of the ozone layer

with prevailing photochemical equilibrium. Between 1946 and 1948, four flight were successfully flown to measure ozone vertical distribution. These rockets meaured ozone to about 67 km above sea level

2.1.6 Aircrafts

The Measurement of Ozone and Water vapour by Airbus In-service Aircraft (MOZAIC) programme commenced in 1993 to collect data. Its main objective was to understand the anthropogenic effects on the atmospshere with the effects os aircrafts being the major aim of the study. MOZAIC programme has five long range Airbus A340 aircrafts flying throughout the world which measured watervapour and ozone automatically and regularly. The aim is to validate global chemistry of transport models by building a large data base of measurements to enhance studies on physical and chemical processes in the atmosphere and it has proved to be an effective tool for climate and regional air quality models as well as satellite products validation (Poberaj et al., 2009). Regular flights commenced in 1994 and by December 1997, 7500 flights had been flown corresponding to 54000 flights hours of observations. (Marenco et al., 1998). The MOZAIC data covers majorly 9-12 km where global ozone distribution is quite difficult to describe. According to Marenco et al (1998), there are four reasons why ozone between 9 km and 12 km is difficult to analyse accurately

- Satellites have poor vertical resolution and accuracy in the troposphere, therefore, it is difficult for these instruments to look through the uttermost cirrus clouds to measure ozone and water vapour.
- Ground based Lidars and vertical ozone sounding instruments are limited in number and they do not have global coverage
- The accuracy and precision of standard meteorological humidity sensors are not well known because they are not validated above 500 mbar
- Dedicated scientific aircrafts or balloon sounding campaigns that accurately estimate ozone and water vapour in the middle and upper tropshere are limited

2.2 Satellite measurements

Satellites have been launched into space for global measurements of ozone and other trace gases. Some of the satellites are: Nimbus-7 carrying Total Ozone Mapping Spectrometer (TOMS) and Solar Backscatter Ultraviolet Version (SBUV) satellites, Application Explorer Mission (AEM-2), Solar Mesospheric Explorer (SME) and (Earth Radiation Budget Satellite

(ERBS). Satellites have been used to measure both the total column ozone and the vertical distribution of ozone.

2.2.1 Total Ozone Mapping Spectrometer (TOMS)

TOMS is an instrument that measures the total column ozone present in the earth's atmosphere aboard Nimbus-7. It was first launched on October 24, 1978 using Nimbus-7 spacecraft followed by the Meteor-3 in 1991. The Earth Probe was launced in 1996 (NASA). The Nimbus-7 satellite carried eight different experiments and instruments to observe the earth surface, atmosphere, oceans and the sun in the ultraviolet, visible, near infrared and microwave region of the spectrum. Three of the instruments on board were launched to measure global ozone concentration. Total Ozone Mapping Spectrometer (TOMS) was designed to measure global total column ozone while Solar Backscatter Ultraviolet System (SBUV) was designed to quantify the vertical profile of ozone on daily basis. The Limb Infrared Mirror of the Stratosphere (LIMS) was also on board to measure ozone.

The Nimbus-7 satellite has an orbital period of 104 minutes as it was launched into a local nooon, sun-synochronous, near polar orbit at an altitude of 950 km. TOMS satellite can also be used to determine cloud cover for study areas. It measures in 6 wavelength bands (313 nm, 318 nm, 331 nm, 340 nm, 360 nm, 380 nm) at swath angle of 51^{o} on either side of the satellite and a resolutionfrom50-280 km at the extreme scan angle. Wavelengths between 360^{o} and 380^{o} are outside the major ozone absorption bands, therefore, when they are backscattered, ultraviolet irradiances are inverted to obtain the total column ozone to a Solar Zenith Angle (SZA) of 88^{o}. TOMS satellite on board Nimbus-7 gives a daily measurement in a 50 km x 50 km field of view at nadir and 250 km x 250 km at extreme off nadir (Anton et al., 2010). TOMS satellite looks down at the atmosphere (nadir viewing) to quantify the amount of backscattered UVR. It has a spatial resolution and swath width of 3^{o} and 2700 km respectively with a design life of 2 years.

2.2.2 The Earth-ProbeTotal Ozone Mapping Spectrometer (EP-TOMS)

The Earth Probe Total Ozone Mapping Spectrometer (EP-TOMS) was launched 2nd July, 1996 and was operational till December 2005. It provides a daily survey of the earth's atmosphere. It operates at nadir viewing. It has a mass of 295 kg and power of 130 W with a size of 1.16 m in diameter and 1.77 in height. It had an initial altitude of 500 km and inclination angle of 99.3^{o} and an Equator crossing time of 12 noon. To increase its daily coverage and reach a stable orbit in 4 years, EP-TOMS was re-boosted in December 1997

with its new height reaching 750 km. It was decommissioned 30th May, 2007 after about 37 years of measurements starting with the first launch on the Nimbus-7 spacecraft.

Meteor-3 was launched in August 1991 to succeed the Nimbus-7, however, an electrical problem caused it to fail as it stopped retrieval from December 27, 1994 (Herman et al., 1996). The spacecraft carrying the ADEOS malfunctioned on 30th June, 1997 due to power loss, thereby ending retrieval.

2.2.3 Solar Backscatter Ultraviolet Version (SBUV)

The SBUV is a nadir viewing non scanning instrument used to determine total ozone and ozone profile in the atmosphere in the spectral region of 160 nm to 400 nm. The purpose of the SBUV instruments are to measure global and profile distribtuion of stratospheric ozone, the dynamics and structure stratospheric ozone, photochemical processes and the influence of trace constituents on the ozone layer as well as the long term solar activity in the ultraviolet spectrum. SBUV consists of a monochrometer and a Cloud Cover Radiometer (CCR. The SBUV contains four major mechanisms:

- A deployable diffuser for selecting solar radiation measurements
- A movable grating for wavelength selection
- A deployable mercury lamp for wavelength calibration and
- An optical chopper mechanism for converting incoming radiation to pulses

All signals entering the SBUV are chopped at a frequency of 50 Hz by the optical chopper. The chopped optical signal from the monochrometer strikes the cathode of the multiplier tube which makes the reflective beam divider separate the signal into two components. Some of the signals are sent to the cathode of the reference photodiode while the rest goes to the photomultiplier tube. The photodiode allows calibration independent of the mainphotomultiplier tube to be carried out. The SBUV instrument has minor surfaces which have high finishes for low light scatter which are aluminised and coated with Mg_2F for 80 % refelctance at 160 nm. The monochrometer gratings have a grating constant of 2400 groves per mm and a 52 mm x 52 mm ruled area. An approximately 0.4 % per year linear drifts is found between Dobson instrument and SBUV (Gregory et al., 1988). Figure 2.7 shows the SBUV instrument in space with various instruments on board.

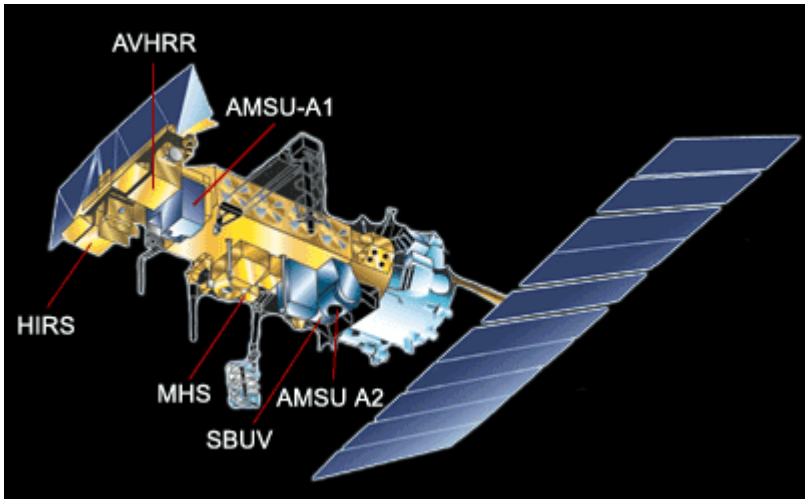

Figure 2.7: SBUV satellite in space showing different instruments on board (adapted from NOAA - http://www.star.nesdis.noaa.gov/smcd/spb/ozone/NOAA18.php)

2.2.4 Application Explorer Mission (AEM)

The first American Explorer satellite, the Explorer I-V was launched on 31st January, 1958 by the Army Ballistic Agency. The first successful explorer lauched was the Explorer VI. The satellites were named science series before launch, provided the launch is successful, their nomeclature would change to Explorer. However, most explorer satellites failed to archieve orbit. The explorer satellites were for scientific purposes such as energy particle exploration through ionospheric and atmospheric studies, investigations of micrometeroids, geodesy, gamma ray astronomy, air density, radio astronomy, solar monitoring, interplanetary monitoring amongst others. A comprehensive list of explorer satellites with their mission, purpose and launch dates can be obtained from the website., www.history.nasa.gov/explorer.html. The latest explorer satellite was the Explorer 59, launched 6th October, 1981 to study reactions between sunlight, ozone and other constituents of the atmosphere.

2.2.5 The Solar Mesospehric Explorer (SME)

The Solar Mesospheric Explorer Satellite was launched on 6th Ocober, 1981 to determine the processes which create and destroy ozone in the earth's stratosphere and mesosphere. Its goals were to investigate the effects of variation in solar ultraviolet flux on ozone densities in the mesosphere, the correlation between nitrogendioxide and ozone, the relationship between water vapour, temperature and ozone in the messophere and upper stratosphere. The spacecraft had a cylindrical body approximately 1.7 m x 1.25 m which had two modules.

SME was first housed on a spacecraft bus and it carried a solar proton alarm detector which measured integrated solar flux ranging from 30 to 500 MeV. It has a mass of 145 kg. Due to energy considerations, all instruments on board the SME were switched off in December 1988 and on 14th April, 1989, it lost contact permanently due to battery failure.

2.2.6 The Earth Radiation Budget Satellite (ERBS)

The Earth Radiation Budget Satellite was first launced on 5th October, 1984 to study stratospheric aerosol gases and earth radiation budget. The radiation budget represents the balance between incoming energy from the sun and outgoing thermal and reflected (long wave and short wave) energy from the earth. Scientific data about the ozone layer was also provided by the mission. It was developed to examine how energy from the sun is absorbed and reflected by the earth. ERB Experiment (ERBE) is designed around three earth orbiting satellites- the ERBS and two NOAA satellites. This satellite also determines the impact of anthropogenic activities such as biomass burning and the use of cholorfluorocarbons and natural occurences like volcanic eruptions on the earth's radiation balance. ERBS also carried the Stratospheric Aerosol Gas Experiment (SAGE II). SAGE II uses solar occultation technique to estimate attenuated solar radiation of the earth's limb. SAGE II measures ozone in the height range of 0.5 km to 70.5 km. The second ERBE instrument was launched January 1985 on board NOAA-9 while the third was launched October 1986 aboard NOAA-10 satellite. Due to budgetory reasons, the instrument stopped operational in 2005 although non-scanning instruments are still functioning as only scanning instruments on board stopped functioning.

2.2.7 The Upper Atmosphere Research Satellite (UARS)

The Upper Atmosphere Research Satellite was launched 12th September, 1991. It was meant to study the protective ozone layer. The UAR satellite carried 10 instruments on board, four of which were designed to measure atmospheric composition and temperature (Cryogenic Limb Array Etalon Spectrometer, Improved Stratospheric And Mesospheric Sounder, Halogen Occultaion Experiment and the Micorwave Limb Sounder) shown in figure 2.8, High Resolution Dopple Imager (HRDI) and Wind Imaging Interferometer (WINDII) were to observe atmospheric wind while the Solar Steller Irradiance Comparison Experiment (SOLSTICE), Solar Ultraviolet Spectral Irradiance Monitor (SUSIM) an Particle Environment Monitor (PEM) were to measure the energy inputs from solar radiation and charged particles. The last instrument was the Active Cavity Radiometer Irradiance Monitor

Satellite (ACRIMII) which was to continue NASA's solar constant measurement. UARS was 35 feet long, 15 feet wide and it weighed 1300 0pounds. It had an orbital inclination of 57^{o} and operational altitude of 600 km. Most atmospheric composition measured by UARS are now being measured by EOS AURA while Solar Radiation and Climate Experiment and Active Cavity Radiometer Irradiance Monitor Satellite now measure UARS solar irradiance.

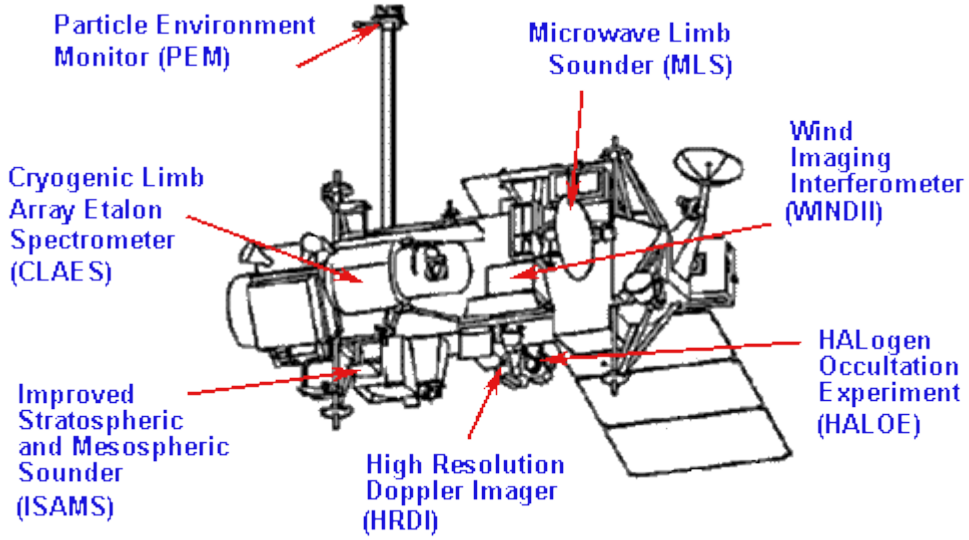

Figure 2.8: UARS instruments showing satellittes on board (adapted from BADC - https://badc.nerc.ac.uk/data/uars/figures/uars_schematic.html)

2.2.8 The Cryogenic Limb Array Etalon Spectrometer (CLAES)

The Cryogenic Limb Array Etalon Spectrometer (CLAES) was one of the 10 instruments on board the Upper Atmospheric Research Satellite (UARS) launched in September 1991. The aim of the CLAES was to investigate the energy balance, global photochemistry and dynamics of the stratosphere and mesosphere. It measures the height profiles of trace gases sch as NO, O_3, H_2O, N_2O, NO_2, N_2O_5, HCl, HNO_3, CH4, ClONO2, CFC 11, CFC 12 as well as temperature, pressure and aerosol absorbtion coefficient at various wavelengths. CLAES has a vertical resolution between 10 and 60 km. Its horizontal grid size is 500 km and it is between latitudes 80^{o}S to 80^{o}N. According to Roche et al (1993), ozone retrieval accuracy at 35 km is ~8 % with 4 % precision where the accuracy is the root sum square (rss). Data products for CLAES are available from 21st October 1991 to 5th May, 1993.

Improved Stratospheric and Mesospheric Sounder (ISAM) measured global temperature and composition profiles both in the stratosphere and mesosphere. The objective of the ISAM was

to determine atmospheric temperature with respect to pressure, to determine nitrogen oxide origin and their impacts on ozone and to study water vapour variability in the middle stratosphere. ISAM also determines ozone concentration, carbon monoxide, methane, dinitrogen pentoxide and aerosols in the middle atmopshere.

2.2.9 Halogen Occultation Experiment (HALOE)

The Halogen Occultation Experiment (HALOE) was another instrument on board the Upper Atmopsheric Research Satellite (UARS) launched in 1991. It uses solar occultaion technique to determine the vertical distribution of ozone and trace gases such as hydrogen chloride, hydrogen fluoride, methane, water vapor, nitric oxide, nitrogen dioxide that affects global ozone distribution by measuring the reduction in the sun's energy intensity in selected spectral bands. From the NASA's website, HALOE had four objectives which were to :

- Improve the understanding of stratospheric ozone depletion. This would be ensured by collecting and analysing global profile distribution of ozone and trace gases of important in its destruction.
- Study chlorofluoromethane's impact on ozone. This would be done by measuring hydrogen chloride and hydeogen fluoride and other chemical compounds with data from Freon 11 and Freon 12 obtained from other UARS experiment.
- Investigate sources and depositories of trace gases, transport mechanisms, dynamics and the validation of atmospheric and photochemical dynamic models.
- Measure hydrogen chloride, hydrogen fluoride, methane and nitric oxide using gas filter correlation radiometry and to measure water vapour, nitrogen dioxide, ozone and carbon dioxide using broad band filter radiometry.

HALOE measurements begins at an altitude of 150 km (where there is no atmospheric interference) to the earth's surface till the sun is obscured by clouds. HALOE data collection is from 11th October 1991 to 21st November, 2005.

2.2.10 Microwave Limb Sounder (MLS)

MLS is one of the four satellites on board Aura. It has three objectives which are to track the stability of stratospheric ozone layer, predict climate change better with its variability and to improve comprehension of global air quality. MLS measurements are made both day and night with atmospheric constituents such as temperature, humidity, cloud, water vapour and ice also measured. It uses stratospheric emission for tropospheric, stratospheric and even

mesospheric constituents. Scientifically, MLS improves the understanding of ozone depletion with a critical monitoring of the stratosphere when the atmosphere is saturated with Chlorine. It helps in understanding the climate change for both seasonal-to-interannual and long-term variability and the variation of both troposheirc and stratospheric ozone.

MLS specificiation

It has spectal bands at millimeter and sumbillimeter wavelength with spatial resolution performed along the sub-orbital track varying for different constituent to be measured. Its thermal operating range is between 10^{o} and 35^{o}, telescope angle between 60^{o} and 70^{0} relative to nadir. MLS sounder has a mass of 490 kg, duty angle of 100 %, power of 550 W and a data rate of 100 kbps. It observes in five spectal regions from 118 GHz to 2.5 THz. Comparison between MLS data measurements and balloon flight shows between 5 % and 10 % agreement (Lucien et al., 2006), while according to Livesey (2008), its accuracy is about 5 %. Figure 2.9 shows the Aura satellite and the instruments on board in orbit.

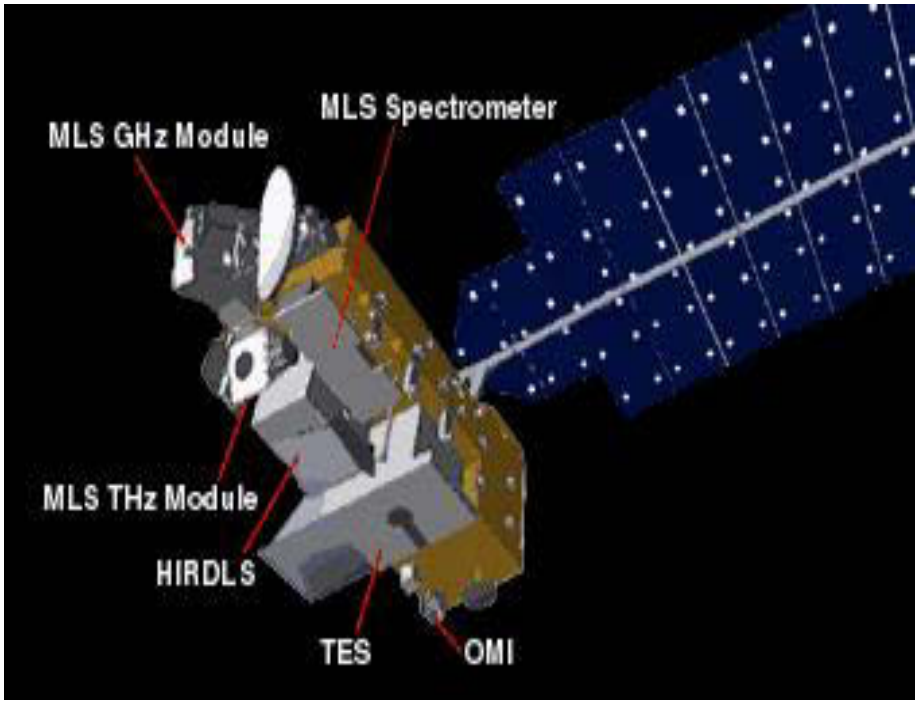

Figure 2.9- Aura satellite showing instruments on board (adapted from http://en.wikipedia.org/wiki/Aura_(satellite)

2.2.11 Ozone Monitoring Instrument (OMI) Satellite

OMI was launched in July 2004 on a sun-synchronous polar orbit on the Aura satellite of NASA with an Equator crossing time of 13.45 Local Time on the ascending node. It is a

nadir viewing imaging spectrometer which measures atmospheric backscattered sunlight in the wavelength region of 270-500 nm with a spectral resolution of 0.5 nm. OMI provides data to derive ozone as well as to measure cloud pressure and coverage. It can also differentiate aerosol types such as dust, smoke and sulphates.

OMI has high spectral capability which improves the level of precision and accuracy of total column ozone. It gives a better ground resolution than GOME satellite and it measures more atmospheric constituents than the TOMS satellite. It observes the earth atmosphere with 114^{o} viewing field distributed over 60 different viewing angles proportional to the flight direction unlike GOME-2 which has only a scanning mirror and one dimensional photodiode array detectors. OMI has a spatial swath of 2600 km and pixel ranging from 13 km x 24 km to 13 km x 128 km (NASA). It uses a linear fit algorithm for the retrieval of total column ozone. This technique uses OMI data at different wavelengths to determine total column ozone and SO_2.

OMI specifications

OMI measures in the wavelength region of 270-500 nm (UV-1 to visible). It has a spectral resolution of 1.0 nm to 0.45 nm and spectral sampling 2 to 3. It has a telescope angle of 114^{0} (2600 km on ground) and a two-dimensional Charged-Couple Device detector of 780 x576 (spectral x spatial) pixels. OMI has a mass of 65 kg, power of 66 W and a data rate of 0.8 Mb/s on the average. Figure 2.10 shows the components of the OMI satellite.

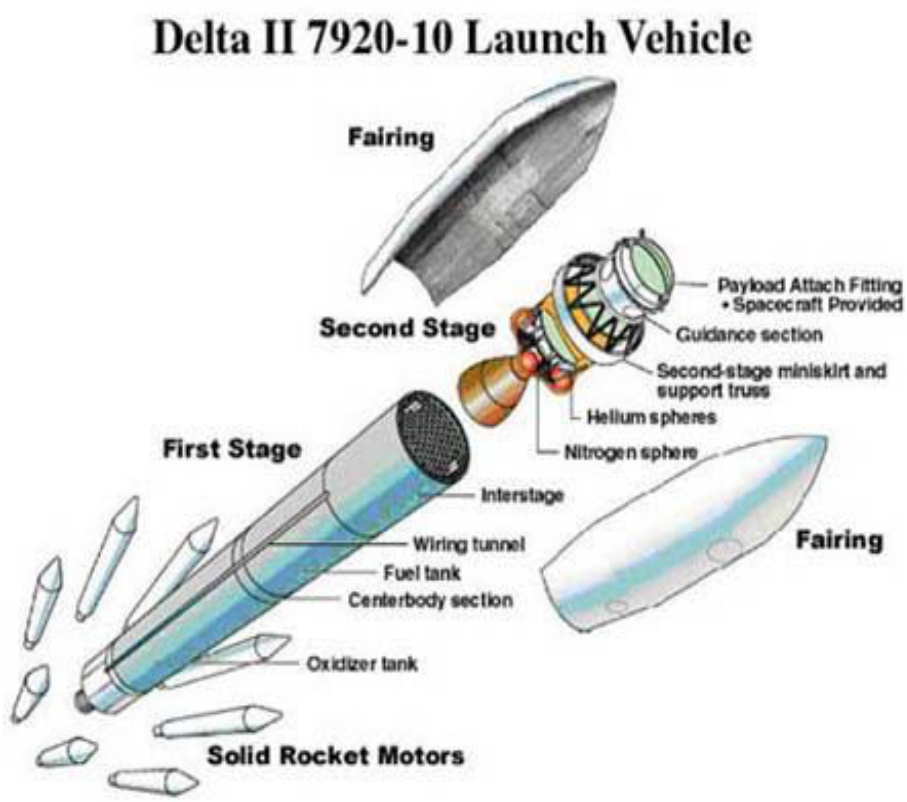

Figure 2.10- Components of OMI satellite (sourced from spaceflight now - http://spaceflightnow.com/delta/d322/061212delta2.html)

2.2.12 High Resolution Dynamics Limb Sounder (HIRDLS)

High Resolution Dynamics Limb Sounder (HIRDLS) was lauched on the Earth Observatory Satellite AURA in 2004. During its launch, engineering studies reveal that a piece of thermal blanketing material broken off from the back of the satellite which blocked 80 % of the optical path of the aperture viewing the earth. However, with the 80 % blockage, high resolution measurements can be made at a single scan. Efforts to remove this material mirror were frutile. HIRDLS measures temperature as well as trace gases such as CH4, O3, H_2O, N_2O_5, N_2O, NO_2, HNO_3, CFC11, $ClONO_2$, CFC12 and aerosols. HIRDLS can also be used to determine polar stratospheric cloud locations. It is a 21 channel limb scanning infrared radiometer which measures altitude range of 8 km to 100 km. It has a spectral range of 6 mm to 18 mm and a standard profile of 5^o longitude and 5^o latitude with 1km vertical resolution. It has a spatial resolution spacing of 500 km horizontally (5^olat) x 1 km vertically. It has a mass of 220 kg, power of 220 W and a data rate of 65 kbps.

2.2.13 Global Ozone Monitoring Experiment (GOME)

GOME was first launched on European Remote Sensing (ERS-2) in April 1995. It is a visible spectrometer used for global observation of atmospheric ozone, trace gases as well as UVR. It covers 240-790 nm wavelength intervals and has a spectra resolution of 0.2-0.5 nm (Theys et al., 2013). An improved GOME-1 satellite, GOME-2 was launched in October 2006 on board the Meteorological Operational Satellite-A (MetOp-A. This new GOME satellite which is an improved GOME-1 is to make more remarkable contribution towards climate and atmospheric research with regular data for use in air quality and forecasting. The scanning swath of GOME-2 is 1920 km allowing almost daily global coverage (NASA). The retrieval of absorbing trace gases such as O_3, SO_2, NO_2, H_2CO, CHOCHO, OClO, H_2O, BrO, cloud and aerosol parameter is made possible by its spectral range and resolution.

GOME-2 Specifications

It has a spectral band of 240 nm to 790 nm with a spectral resolution of 0.26 nm to 0.51 nm and a spatial resolution of 80 km x 80 km. Its earth coverage is from 120 km to 1920 km. It has 4096 spectral channels with 30 polarization channels. Its calibration system is done with the spectral lamp, white lamp and solar diffuser. The GOME-2 satellite has a spectral dimension of 600 mm x 800 mm x 500 mm and a weight of 68 kg. Its main bus voltage is 22 V to 37 V, power consumption of 50 W and data rate of 400 kbit/s.

To determine its orbit accurately, a Precision Range and Range-Rate Equipment (PRARE) and a Laser Rectro-reflector were included in the satellite. The reflector was used to calibrate the Radar Altimeter to within 10 cm though PRARE has not been operational since its launch.

2.2.14 Infrared Atmospheric Sounding Interferometer (IASI)

IASI is a new French satellite with high level of accuracy and precision designed for meteorological soundings. It was first launched on board Meteorological Operational Satellite Program-A (METOP-A) on 19th October, 2006 while the second program was launched in 2012 on board METOP-B satellite. It is a nadir-viewing spectrometer operating in the thermal infrared (Dufour et al., 2012) It measures the infrared spectrum released by the earth. It provides infrared soundings of temperature profiles both in the stratosphere and troposphere as well as important chemical components involved in climate change and temperature chemistry aimed at estimating trace gases such as O_3, Carbon dioxide, CH_4, CO, H_2O,

HCOOH, CH_3OH, NH_3 and other gases on a sporadic basis such as HONO, C_2H_4, SO_2, H_2S (Clarisse et al., 2004). IASI interferometer has a spectral coverage from 645-2760cm^{-1}, spectral resolution of 0.5cm^{-1} and instrumental noise of 0.2 k below 2000 cm^{-1} (Theys et al., 2013).IASI has a spectral range of 3.7-15.5 µm, size of 1.2 m x 1.1 m x 1.1 m and a mass of 210 kg. IASI optical configuration is based on a Michelson Interferometer.

A validation exercise performed on IASI using balloon sonde measurements indicated that there is no significant bias in total column measurement and that the retrieval errors of less than 5 % are consistent with the standard deviation difference between ozonesondes and IASI (Keim et al., 2009). The diagrams in figure (2.12) were obtained from the NASA website.

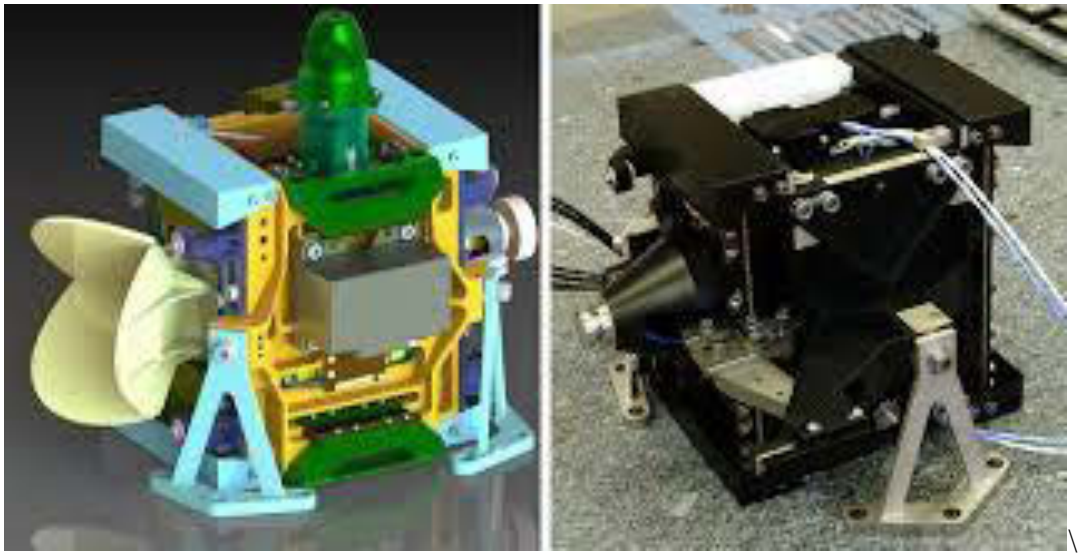

Figure 2.11- IASI satellite prepared for launch (sourced from http://www.csem.ch/site/card.asp?bBut=yes&pId=20169)

The ozone measuring instruments have been discussed. Instruments used for vertical ozone measurements have been presented as well as instruments used for total column ozone measurements. Both ground based instruments and satellite instruments have also been presented. Researchers have made use of these instruments at various geographical locations to investigate ozone variability and climatology over time. Some of the reasearches carried out with relevance to this study are reviewed under literature review.

2.3 LITERATURE REVIEW

Researchers have made use of different ground based and satellite measurements explained above to understand the variation and climatology of ozone at different altitudes and at

various geographical locations. Some of their works are reviewed here based on their relevance to this study. The review work has been restricted within the last 15 years which might provide us an overview of most recent studies on the subject.

The first sets of the works reviewed focuses on the vertical (both tropospheric and stratospheric) variation of ozone at different sites. For this section, only relevant studies carried out in the last decade are reviewed.

Tropospheric Ozone

Diab et al (2004) presented the climatology of tropospheric ozone over Irene, South Africa during two time periods, 1990 to 1994 and from 1998 to 2002 using ozonesonde profiles. 172 profile measurements were obtained for the first period while for the second period, 122 profile measurements were used. The time of soundings was also different as for the first period, soundings were made at 8 am local time while for the second period, and soundings were made at about 10 am. Ozonesonde proves to be the most effective instrument for both tropospheric and lower stratospheric ozone measurement (Diab et al., 2004). However, a review of Barnes et al (1998) shows that though ozonesonde provides effective and precise ozone measurement, it does not provide a global coverage. Ozonesonde limitation is complimented by satellite measurements which provides both global coverage and with low frequency of observation required for particular geographical location. Ozone concentrations from ground to 16 km were integrated to obtain total column ozone. They estimated total ozone present in the troposphere by dividing the troposphere into two 2 km layer each. The result of their monthly mean showed a spring maximum of ~40 DU which is in agreement with the well-established spring time ozone maximum in the Southern Hemisphere. For the vertical variation of total ozone, the same spring maximum was evident for each layer below 10 km. Their result also revealed steady ozone values from January to June with a steady rise during mid-winter, it then peaks at spring and then reduces. May minimum was evident between 4 km and 8 km corresponding to ~3.5 DU. Above 10 km, their result showed that there was neither clear ozone maximum nor a clearly defined seasonal cycle. The result of their comparison of the two separate periods of measurements showed that during the first period, there was a broad maximum experienced during spring which had turned to mid-spring maximum in the second period. They also observed little difference in measurements between the two periods below 8 km except for a sharp mid-spring maximum in the second period which was best developed between 0 and 4 km. Their low measurements obtained in low altitudes were attributed to an increase in surface-based photochemical sources of ozone.

For altitudes above 10 km, they observed a small increase of ~1 DU in total ozone measurements in the second half of the year.

They also presented the vertical distribution of tropospheric ozone using the mean annual and mean seasonal profiles from the two time periods. They showed an increase of ~10 ppbv in surface ozone except for summer months. They attributed this to the effects of increased anthropogenic sources. Their results suggested an increase in the emission of ozone precursor gases due to increased industrialization and population. The population of Pretoria in 1991 was estimated to be ~0.5 million which had increased to ~2 million in 2001. This increase in population would have a resultant effect on both industrial and vehicular activities in the region.

The climatology of tropospheric ozone over Irene and Reunion Island was also presented by Clain et al (2009) with measurements from ozonesondes, LIDAR and aircrafts. They used data from 1998 to 2006 with 20 to 25 monthly profiles over the eight year period. 577 MOZAIC data and 265 LIDAR profiles were used for their work. Positive ozone trend of ~1.97 DU per decade was observed in their study. They showed that Irene is influenced by biomass burning as well as stratospheric-tropospheric exchange between 4 km and 16 km. For measurements in Reunion Island, they established that biomass burning was maximum between September and October while the stratospheric-tropospheric exchange from subtropical jet stream was maximum during summer and minimum in autumn. Their results on tropospheric ozone measurements obtained from Lidar and ozonesondes showed that both instruments are in good agreement in the lower troposphere but their agreement in the upper troposphere was not very good. This they attributed to the possibility of inaccurate Lidar measurements under cloudy conditions.

Boynard et al (2009) used measurements from IASI and GOME-2 satellites, ground-based instruments as well as ozonesonde observation to compare tropospheric ozone and total ozone measurements. Their study period was between June 2007 and August 2008. Their result showed that IASI and GOME-2 satellites exhibited similar structures for total column ozone with latitudes. Both instruments measured maximum column at high latitudes while minimum ozone values were obtained in the tropics. However, there was a positive bias of ~4.9 DU to ~13 DU in total ozone measurements from IASI and GOME-2 satellites with an average bias of ~9 DU in 2008. A positive bias of ~9.3 DU was also obtained when measurements from IASI was compared with both Dobson and Brewer spectrophotometers. They attributed this bias to the varying observation methods of the instruments.

Ziemke et al (2011) presented a global climatology of tropospheric and stratospheric ozone using Ozone Monitoring Instrument (OMI) as well as Microwave Limb Sounder (MLS) measurements by combining six years of measurements from October 2004 to December 2010. These instruments were validated with SHADOZ and measurements from the World Ozone and UVR Data Centre (WOUDC) by comparing their monthly averages. Total column ozone measured by these instruments was converted to volume mixing ratio for comparison. Satellite measurements were compared with ozonesonde measurements from 2004 to 2009 and WOUDC measurements from 2005 to 2008. They selected twenty eight stations in the Northern Hemisphere and ten stations in the Southern Hemisphere for their study. They obtained larger Root Mean Square difference in the Northern Hemisphere high latitudes. This they attributed to the limited numbers of monthly measurements from both satellites as well as in situ measurements. They also opined that OMI measurements in higher latitudes may be inconsistent due to high Solar Zenith Angles (SZA).

They also made use of Labow-Logan-McPeters (LLM) climatology for tropospheric ozone climatology. They derived this climatology by combining ozonesonde and satellite measurements from Stratospheric Aerosol and Gas Experiment (SAGE II) and Microwave Limb Sounder (MLS). The result showed consistency with the seasonal transition peak of total ozone in the Northern Hemisphere from tropics to mid-latitudes and from spring to summer months. In their climatology, they observed the lowest total column ozone in the Southern Hemisphere tropics around 10^{o}S from January to April corresponding to ~24 DU. Their measured value in both hemispheres for mid-latitudes was ~30 DU. In the Northern Hemisphere, the highest values were in June and July corresponding to ~42 DU while that of the Southern Hemisphere was ~39 DU between September and November.

For stratospheric column ozone, they observed maximum ozone in the Northern Hemisphere during winter and spring months corresponding to ~40 DU while their observed summer stratospheric ozone was ~220 DU in the tropics. At latitudes within 10^{o} in both hemispheres, ozone values measured was ~150 DU between September and October, attributed to the Antarctic Ozone Hole. They also showed in their work that their derived ozone climatology is useful for many purposes such as; the global circulation models of ocean-atmosphere, the evaluation of 3-D chemistry transport model performance, identification and correction of problems in various models involving errors in coded photochemical reaction rates, errors in wind fields, stratosphere-troposphere exchange, boundary layer dynamics and chemistry.

Stratospheric Ozone

Semane et al (2006) observed an unusual stratospheric decrease in ozone over Irene in May, 2002. 178 ozonesonde profiles from 1998 to 2005 were used for the study. They used total column ozone from EPTOMS satellite to provide diurnal ozone distribution for the study period. Their study focused on 12th May when extremely low stratospheric ozone was observed. Their average monthly total ozone over Irene between 1999 and 2005 was 249 ± 12 DU at 1σ standard deviation. However, EPTOMS measurement on 12th May was 219 DU, 30 DU lower than the climatological mean in May. There was no ozonesonde measurement on 12th May but ozonesonde launched 15th May measured 226 DU total ozone which was still lower than the climatological mean. The role of isentropic transport of polar and tropical air masses was investigated using high resolution PV-maps on selected isentropic surfaces. They made use of the MIMOSA model and its analysis to show how polar air masses were injected to the mid-latitudes area as well as the subtropics. They then related the unusual stratospheric decrease on total ozone in May, 2002 to the isentropic transport of air masses both in the lower and middle stratosphere.

Sivakumar et al (2007) presented the ozone climatology and variation in the stratosphere in Reunion Island using in situ measurements from ozonesondes (from September 1992 to February 2005) and Système D'Analyse par Observations Zénithales - SAOZ (from January 1993 to December 2004). Satellite measurements from HALogen Occultation Experiment - HALOE (from January 1991 to February 2005), Stratospheric Aerosol and Gas Experiment - SAGE II (from October 1984 to February 1999) and Total Ozone Mapping Spectrometer - TOMS (from January 1978 to December 2004) were also used. Height ranges from 0 km to 30 km were used for ozonesonde measurements. Ozone measurements for their study were converted to molecules/cm^3 to examine the ozone concentration. They used TOMS measurements to normalise ozone profiles in order to compare with SAOZ measurements and OAS - Ozonesondes And SAGE II. The normalization was done by integrating profile measurements from ozonesondes and SAGE II. The result of their height profile indicated maximum ozone concentration of about $4.5x12^{12}$ molecules/cm^3 at 26 km. This height maximum was displayed by all instruments. Their results also revealed that ozonesonde measurements of ozone were higher compared with SAGE II and HALOE by ~3 % in the lowers troposphere. They attributed this underestimation of ozone by these satellites to be due to the way they measure ozone. They expected the errors to increase down the troposphere.

For ozonesonde measurement bias in the troposphere, their result illustrated 4 % to 6 % and 10 % to 12 % bias in the lower troposphere and upper troposphere/lower stratosphere altitude

range respectively. Their seasonal ozone variation showed a spring time maximum in the height region of 24 km to 28 km. This was replicated by HALOE measurements. They also obtained the percentage difference between measurements from HALOE and ozonesondes by making ozonesonde the reference. HALOE measurements were subtracted from ozonesonde measurements and then divided by ozonesonde measurements. They then multiplied the result by 100 to obtain the percentage difference. The result revealed a percentage difference ranging from -20 % to +6 0% for all monthly measurements. They observed that the height region of 15 km and 17.5 km had the highest positive bias. The result of their comparison of monthly ozone from TOMS satellite and the normalized ozone profiles obtained were within ±5 %. They however obtained low measurements between 1992 and 1995 which they attributed the spread of aerosol in the Southern Hemisphere from the Mount Pinatubo eruption.

Total column ozone

The following review studies are mostly confined to the total column ozone variations. Since the total column ozone has been measured for the past five decades, the review presented here are only few and those were relevant to the present study.

The Dobson instrument has been effective in determining total column ozone. McPeters and Labow (1996) assessed the accuracy of TOMS measurements with Dobson for 14.5 years and showed that TOMS agreed with the average ozone from 30 ground stations used to within ± 1 % throughout the years of measurements. They also showed TOMS time dependent drift with Dobson as 0.29 % per decade. Bonawentura et al. (2006) compared OMI satellite measurement with Dobson and showed a bias and standard deviation of normalized difference between them as 1 % and 2 to 3 % respectively. Fioletov et al. (2008) compared Dobson with EPTOMS, OMI and GOME satellites and their studies revealed that their difference were within ± 2 % and very rarely outside ± 3 % envelope depending on the season and region. They also showed that the differences between satellite measurements and ground based instruments are larger under cloudy conditions compared to clear sky condition.

McPeters et al., (1997), used satellites to derive an ozone climatology using balloonsonde to estimate total ozone. Total ozone from SBUV instrument from 1979 to 1990 were used for latitudes between 70^{o}N and 70^{o}S. They however did not use data from 1982 due to its contamination with aerosols from El Chichon volcano which made SBUV measurements inaccurate for lower stratosphere ozone retrieval. The data used were filtered to within 10 %,

measurements outside this range were not used for their study. Their estimated values of total ozone were within ± 2 % accuracy for tropical regions and ± 5 % for high latitudes where larger ozone variability is expected.

They also derived total column ozone from balloonsondes by assuming a constant mixing ratio from the altitude where the balloon burst to the top of the atmosphere by extrapolation. They selected a worst case scenario where the balloon bursted close to the maximum ozone mixing ratio profile which however led to an overestimation in the upper atmosphere. They also revealed that an improvement in the correlation between balloonsonde total ozone and Dobson measurements can be gotten when accurate and stable climatology of column ozone is used because ozone variability is much more predictable in the upper stratosphere compared with the lower stratosphere.

Since the 1980s, satellite measurements have shown a negative trend in total column ozone measurements specifically in middle and high latitudes of both the southern and northern hemisphere (Solomon et al., 1996). Chandra et al. (1996) used ~14 years of TOMS measurement to study total ozone in the northern mid latitude and showed that ozone trend are influenced by annual variability associated with dynamical perturbations in the atmosphere. They also presented an ozone trend reduction of 1 to 3 % per decade.

Fioletov et al (2002) estimated the global and zonal ozone variations from satellites and ground based measurements between 1964 and 2000. The ground-based instruments used were the Dobson and Brewer spectrophotometer and data from the World Ozone and UVR Data Centre. TOMS satellite was used to provide diurnal global measurements. Measurements from EPTOMS as well as SBUV satellites were also used. The monthly averages of the data used were subtracted from the monthly measurements to remove the seasonal ozone trend on the estimated data. In the Northern mid-latitudes, there was an agreement of 1 % between ground-based measurements and satellites data while over the tropical, equatorial and Southern mid-latitudes, a systematic difference of ~2 % to 3 % was observed. They also showed the effects of Quasi Biennial Oscillation (QBO) on ozone fluctuations between 25^{o}S and 25^{o}N in their work. Their estimate of global ozone trend showed a decrease of about 3 % in measurements taken between late 1970s and 1990s between 60^{o}S and 60^{o}N. They presented the percentage decline in ozone over mid-latitudes at about 2.5 % per decade from 1979 to 2000.

They also analysed the long term stability of EPTOMS data separately for the Northern and Southern Hemispheres and showed that there was no significant drift in measurements from 1996 to June 2001. From late 2001, they observed an increasing drift in total ozone measurement in both hemispheres by ~3 %. They attributed the drift in measurements to degradation of the EPTOMS satellite. This drift was corrected using data from NOAA 16 and 17 SBUV. They observed significant improvement in the measurements from the corrected EPTOMS. They however suggested that despite the remarkable success in the calibration and correction of EPTOMS measurements by NASA TOMS, data from this instrument should not be used for global ozone trend due to the fact that the data relied on NOAA16 and 17SBUV data trend. The data can however be used for diurnal and seasonal total ozone variability study. For ozone seasonality, they revealed that EPTOMS satellite overestimated ozone compared with Brewer measurements for small solar zenith angles and under estimation of ozone for large zonal zenith angles.

Thompson et al (2003) used SHADOZ measurements, Dobson and TOMS measurements to present a tropical ozone climatology. Over 1000 ozone profiles from 10 Southern Hemisphere tropical and subtropical stations from 1998 to 2000 were used. They also provided measurements of temperature, pressure and humidity for ozonesonde measurement. They observed that the temperature measured had good accuracy but suggested that humidity at temperatures below -60^{o}Cshould be ignored for analysis. Their results showed a good agreement to within 2 % to 4 % between SHADOZ measurements and those from TOMS satellite in five of the stations. Their work revealed the best agreement between TOMS, Dobson and SHADOZ was at Nairobi and Irene - the stations with the highest terrain. Ozonesonde data were converted to Dobson units and compared with TOMS tropospheric ozone. The result revealed good agreement at all stations within 15^{o} of the equator.

Bodeker et al (2007) presented the Southern Hemisphere mid-latitude anomaly of the 1985 total column ozone using Dobson instruments and TOMS satellite. Four mid-latitudinal sites ranging from 32^{o}S to 45^{o}S were used for the study. For their data to be valid, they put their monthly mean value at a minimum of five daily measurements while a minimum of eight monthly means were required for their annual mean to be valid. They made use of TOMS satellite to show the spatial structure of the 1985 anomaly. They suggested that the 1985 total ozone column anomaly was due to reduction in maximum ozone values and not an increase in minimum ozone values. They also suggested the influence of QBO for the change in spatial pattern of ozone from 1984 to 1985. They suggested a QBO switch from easterly to

westerly phase to be an important factor in explaining the 1985 anomaly. The further concluded that minimum solar cycle also contributed to the low ozone observed in 1985 over the Southern mid-latitudes.

Mahendranth and Bharathi (2012) estimated tropical annual and seasonal trends of TCO and showed an increasing trend of 1.88 DU per year or 0.61 % per year. They also presented the maximum and minimum diurnal variability of TCO as 28 DU (9.19 %) and -36 DU (-11.8 %) respectively. McPeters et al (2007) presented ozone climatological profiles for satellite retrieval algorithm and showed that the new climatology agrees with TOMS TCO measurements to within 4 % except for areas close to the Antarctic ozone hole. They attributed better agreement in measurements to calibration improvements and improved climatology. Kirchhoff et al (1991) presented 10 year ozone climatology for a subtropical site and showed maximum concentration during spring in September/October. This maximum was about 5 % higher than the annual average for TCO.

Nair et al (2013) derived an ozone trend for both total column ozone and ozone vertical profiles at a Northern mid-latitude station. Total column ozone used for this study were from Dobson instrument (from 1984 to 2010) and SAOZ (from 1992 to 2010). Profile measurements were from Lidar (1985 to 2010), SAGE II (from 1984 to 2005), HALOE (from 1991 to 2005) and MLS (from 2004 to 2010). They analysed the long term evolution of monthly mean ozone using a regression model. This was obtained by subtracting the monthly climatological measurements from the monthly mean ozone for the same period. Their result suggested that it was better to combine measurements from Dobson and SAOZ than using measurements from both instruments individually. They revealed that combining measurements from both instruments provide stable long term ozone data. Their result on trend analysis showed a negative trend in total ozone measurements before 1997 which was attributed to increase in the amount of ozone depleting substances. However, after 1997, they observed positive ozone trend in total column ozone measurements attributed partly to the decreased amount of ozone depleting substances. Their study also revealed that the reduction in ozone depleting substances was not only limited to the middle stratosphere but in the whole stratosphere which suggested that total ozone recovery was taking place.

For the vertical distribution of ozone, their result showed similar ozone anomalies to within ± 10 % except for altitude range between 16 km and 20 km. They then used QBO to explain the variability of stratospheric ozone during winter and spring. Their study also showed that there was maximum heat flux as well as North Atlantic Oscillation (NAO) during winter.

CHAPTER THREE

RESEARCH METHODOLOGY

This chapter focuses on the data sets used for this study

3.1.1 DATASETS USED

3.1.1.1 Ozonesonde data

10 years of ozonesonde data collected over Irene from 1998 to 2007 (archived on the SHADOZ web site: http://croc.gsfc.nasa.gov/shadoz) is used. Ozonesondes were launched twice monthly for the years of study. There was however no launch from January to October 1998, February 2004, January 2006, July 2006 to Novemeber 2006, June 2007 and November 2007. Some months had just a single launch as there were only 8 launches in September 2000. Table 3.1 shows monthly distribution of data used for the present study. All ozonesonde data used for this study are filtered to within 2 sigma for better data quality. Data whose standard deviaitions are more or less than the range selected for this study are not used. However, the future works are planned for addressing these anomaly (high or low) in ozone and the dates of such anomaly occurrence are given in the appendix.

3.1.1.2 Aura MLS data

We have used the vertical profile of ozone for ~10 years (from August 2004 to May 2013) for this study (see- Table-3.1: monthly distribution of data over Irene). This data is obtained from Aura archive where some selected sites data are archived including Irene geographical location with latitude ranges from 25.885^{o}S to 25.873^{o}S and longitudes over 28.213^{o}E to 28.234^{o}E. Further information on MLS can be obtained from the website: http://mls.jpl.nasa.gov/index-eos-mls.php. MLS data used was subjected to qualitative analysis and data outside ±2σ were not used.

Months	Aura MLS	SHADOZ
Jan	2177	17
Feb	1933	17
Mar	1657	22
Apr	1888	20
May	2002	21
June	1872	18
July	1908	17
Aug	2053	17
Sep	2089	21
Oct	2160	20
Nov	2078	19
Dec	2137	19

Table-3.1. Table showing the monthly distribution of ozonesonde and Aura MLS observations over Irene.

Combined MLS and ozonesonde

The data used for addressing the combined ozone variations are from ozonesonde measurements and MLS from the year 2004 to 2007. This is due to the fact that only these years have common profile measurements, i.e., SHADOZ data is from 1998 to 2007 while MLS Aura data available is from 2004 to 2013, thus, only similarities in years of measurement is between 2004 and 2007. The ozone values from the two instruments are combined and averaged to determine the average ozone seasonal variability. The combined measurement shows the average vertical distribution of ozone for Irene for the common years of measurements.

3.2.1.1 Satellite overpass data

The total number of satellite measurements (overpass over Irene) used for this study are tabulated in table-3.2 with their respective years of operational. The number of measurements depends on the total number of years each satellite operational and the obervational frequency of daily measurements. TOMS had very high number of measurement due to the number of years of measurements (~15 years) and the number of daily observation (four) while IASI had the lowest measurements as its operational begun recently (2008) with one observation daily. A brief detail on each satellite is discussed below. All satellites used for this study have been subjected to qualitative analysis to within ±2 σ for better data quality. As prescribed earlier, heretoo, the data outside this range were not used for the study.

Total Ozone Mapping Spectrometer (TOMS)

The data used for this study is from the day of its first launch using the Nimbus-7 space craft from November 1978 to May 1993. TOMS provides four daily measurements corresponding to the overpass over Irene as shown in table 4.2. The daily mean of these measurements are calculated and used for this study. TOMS calibration error is estimated at ±1 % (Jaross et al., 2005) while its measurement error is about 12 DU depending on cloud cover, relative humidity and other atmospheric parameters. The Earth Probe Total Ozone Mapping Spectrometer (EP-TOMS) provides a daily survey of the earth's atmosphere as it is also nadir pointing. The data used for this study is from January 1997 to December 2005. More information with regards to TOMS data can be referred to http://www.badc.rl.ac.uk/data/toms and http://toms.gsfc.nasa.gov/adeos/adeos.html

Ozone Monitoring Instrument (OMI)

Ten years of data are used for this study from October 2004 to December 2013. Four daily measurements corresponding to the overpass over Irene are made (see: – Table 3.2 for period of operational as well as the frequency of launches used for this study). It has a measurement error of ~6 DU and instrument error of about 2 %. Details on OMI can be obtained from http://aura.gsfc.nasa.gov/instrument/omi.html.

Global Ozone Monitoring Experiment (GOME)

Similar to TOMS, four sets of data are measured by GOME over a day and their corresponding mean is derived which is compared with other satellite measurements (see: – Table 3.2 for period of operational as well as the frequency of launches used for this study).

GOME data used for this study are from August 1995 to June 2003 (GOME-1) and from January 2007 to December 2013 (GOME-2). Instrument error is about 3.3 % while the mean measurement error over the period is ~6 DU.

Infrared Atmospheric Sounding Interferometer (IASI)

The data used for this study are from June 2008 to December 2011 and the monthly distributions are given in table 3.2. A validation exercise performed on IASI using balloonsonde measurements indicated that there is no significant bias in total column measurement and that the retrieval errors of less than 5 % are consistent with the standard deviation difference between the Ozonesondes and IASI (Keim et al., 2009). (Details on IASI can be sourced from www.osdpd.noaa.gov/IASI ; www.smsc.cnes.fr/IASI ; www.wdc.dlr.de/sensors /iasi**)**

Dobson instrument measurements

Monthly mean measurements from ground based Dobson instrument from 1989 to 2011 are also used for this study. The data are obtained from the Dobson instrument situated and operated at Irene. The data obtained are filtered to within 2 σ standard deviation for better quality. Datasets outside this range are not used and are presented in appendix 2 as anomalies. The frequency of Dobson measurements as well as other instruments used for this study is presented in table 3.2.

	Dobson	**TOMS**	**GOME-1**	**EPTOMS**	**GOME-2**	**OMI**	**IASI**
Month/ Years	Aug.1989-Dec.2011	Nov.1978-May1993	Aug.1995-June2003	Jan.1997-Dec.2005	Jan.2007-Dec.2013	Oct.2004-Dec.2013	June2008-Dec.2011
Jan	22	1860	992	266	868	1116	93
Feb	21	1696	908	243	792	1016	84
Mar	21	1860	992	269	868	1116	93
Apr	22	1800	960	263	840	1080	90
May	22	1860	992	261	868	1116	93
Jun	20	1680	960	262	840	1080	110
Jul	21	1736	868	251	868	1116	124
Aug	23	1736	992	298	868	1116	124
Sep	23	1680	980	277	840	1080	120

Oct	23	1736	992	290	868	1364	124
Nov	23	1800	960	241	840	1320	120
Dec	22	1860	992	256	868	1364	110
Total	263	21304	11588	3177	10228	13884	1285

Table-3.2. Monthly averaged distribution of ozone observation over Irene from satellites and Dobson instrument. The first row of the table indicates the month and years of operational of the corresponding instrument.

Integrated ozone

Integrated ozone was obtained using the method adopted by Sivakumar et al (2007). SHADOZ measurements and MLS measurements were stepped down to 1 km and merged together. The result is then integrated to retrieve the corresponding total column ozone in terms of Dobson Units (DU). The results obtained are then compared with the total ozone from both Dobson instruments and satellite measurements in Dobson units.

3.3 Geospatial

South Africa Seasons

South Africa has four distinct seasons: summer (December, January, February), autumn (March, April, May), winter (June, July, August) and spring (September, October, November). Meteorological parameters such as temperature, wind speed, precipitation, relative humidity varies throughout the seasons. Laakso et al., (2012), presented the meteorological characteristics of South Africa. Their result showed that wind speed is highest over South Africa is spring. This can be a possible reason for maximum ozone observed in spring as winds transfer ozone from the ozone rich regions in the higher latitudes to the middle latitudes. They result also showed that temperature is highest during spring and summer months. This would increase the photolysis of oxygen, hence, the production of more ozone. The impact of precipitation and relative humidity on ozone concentration has not been established in this work but their result showed that precipitation is higher in summer and lowest in winter as well as relative humidity.

In this section, we have managed to study the geo-spatial variation of ToZ over complete South Africa using OMI satellite data and the obtained results are presented here. South Africa was divided into three parts as illustrated by the earlier study on aerosol climatology over South Africa by Tesfaye et al., (2011). They have classified with respect to aerosol

loading in South Africa and is shown in figure 4.10. We pre-assume that the similar classification would hold good for the ozone variations and is adopted for this study to examine the ozone climatology over South Africa.

	Latitude		Longitude	
	Minimum	Maximum	Minimum	Maximum
South Africa	22	35	17	32
Lower Part A	31	35	18	31
Central Part B	27	31	17	33
Upper Part C	22	27	20	32

Table 3.4: Latitudes and longitudes for the division of South Africa to three parts

The data used for this section are obtained from OMI satellite from October 2004 to December 2013. OMI instrument was selected due to its close measurements of total ozone with the Dobson instrument (Balis et al., 2007). OMI has also been noted for accurate total ozone measurements (Liu et al., 2009). The data are filtered to within 2σ for better quality.

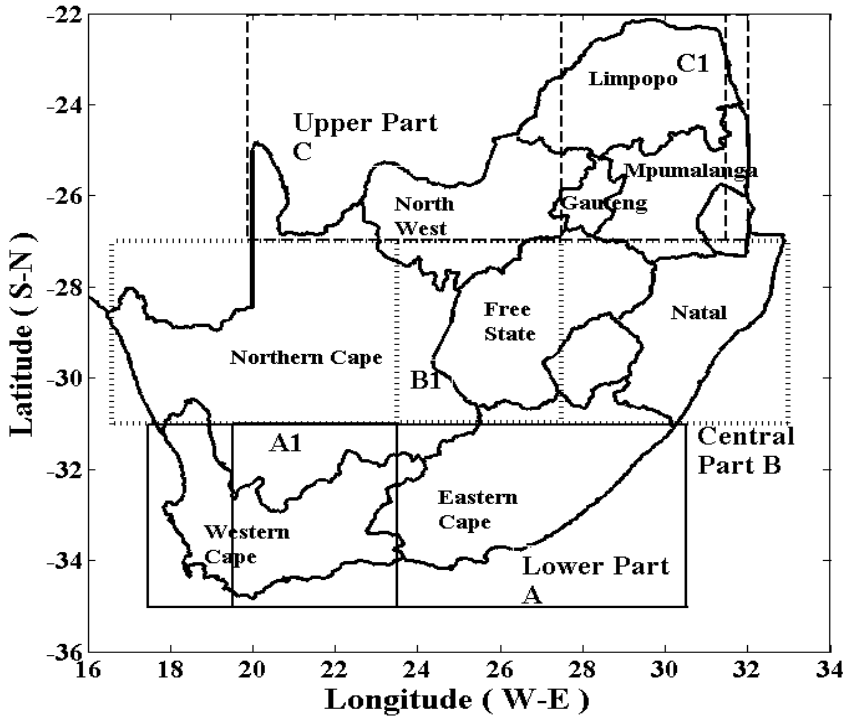

Figure 3.1:- Geographical map of South Africa with the three different regions of classifications (as adopted from Tesfaye et al., 2011)

CHAPTER 4

Results and Discussion

The results obtained in this thesis are presented in this chapter. The results are divided into three sections. The first shows the vertical variation and climatology of ozone over Irene using both ground-based and satellite observations. The second is on total column ozone variability and climatology using in-situ measurements and space-borne measurements while the third section shows ozone climatology over South Africa. The datasets used for each section are briefly described for better understanding.

4.1. Vertical ozone climatology and its variability

In this section, the vertical ozone variability of ozone over Irene is examined. The height profile (vertical) of ozone is divided into two: tropospheric ozone from 0 to 15 km and stratospheric ozone from 15 km to 30 km. Ozone found between 0 to 4 km is referred to as surface ozone for this study. Surface ozone is found due to photochemical reactions as well as biomass burning. However, the main ozone precursor in the troposphere is the anthropogenic emission of NO_x. The location of Irene also plays an important role in the abundance of ozone at the surface. Its location between two highly industrialized cities (refer to chapter-1, section 6 – a brief history of study area) where there is a constant release of hydrocarbons and NO_x from industries as well as its proximity to the main power generating region of South Africa makes ozone concentration high. It is noted here that the description of instruments used are already provided in the earlier chapter. Thus, to avoid the repeated information, we have provided only the datasets used.

4.1.2 Monthly climatology of tropospheric ozone from ozonesonde data

To address the monthly climatology, the ozonesonde data over Irene are combined and their average mean of corresponding months (irrespective of years) were determined. Figure (4.1a) shows the monthly mean ozone from 0 to 15 km. The vertical variations are from $0.5x10^{12}$ molecules/cm^3 to $2.5x10^{12}$ molecules/cm^3. Most concentrations are found between 1 km and 3 km and are more prominent from August to December. Average surface ozone concentration during this period is ~$1.1x10^{12}$ molecules/cm^3. The presence of more surface ozone compared to higher altitudes from 5 km to 10 km can be attributed to urban industrialization which has been on the increase each year (Diab et al., 2004). Increase in the

number of industries, increase in population, vehicular activities as well as human activities have all contributed to increase in the production of ozone. Above 4 km, there is a decline in ozone concentration, this is attributed mainly to surface deposition of the ozone formed and fast titration by species emitted from the surface. This reduction in ozone concentration can also be attributed to the presence of water vapour in the atmosphere. Water vapour is involved in the reaction that produces hydroxides in the atmosphere. These hydroxides are formed by the photolysis of ozone and other chemicals in the troposphere. When water vapour combines with gaseous oxygen (though they do not react with each other but gaseous oxygen acts as an oxidizer) OH^- is produced. There is however an increase in ozone concentration above 12 km, this height region corresponds to the tropopause where many activities are taking place. Isentropic exchanges are attributed for this increase in ozone concentration. In terms of tropospheric ozone seasonality, ozone concentration is minimum in May which corresponds to the season of low maritime air masses conveyed across the continent in relation to mid-latitude westerly waves (Diab et al., 2004). Spring time maximum was experienced as expected in both the lower and upper troposphere due to biogenic (vegetative and microbial) emissions, lightning production, photochemical sources and most importantly biomass burning. The burning pattern is distributed from North to South from 10^o to 20^o and then in a more easterly direction at 25^o where Irene is located from June to October. This is one of the major reasons for spring time ozone maximum in the southern hemisphere.

Figure (4.1b) shows the monthly average standard deviation for tropospheric ozone. The vertical variations of ozone concentrations varied are from 0.05 x 10^{12} molecules/cm^3 to 0.6x10^{12} molecules/cm^3. This range of variation is selected to show properly the measured standard deviation for better readability of variations in color bar. The result shows that there is not much variability for a few meters above ground level. This can be due to the limited number of profiles available at this altitude. Maximum standard deviation with an average values of ~ 0.4x10^{12} molecules/cm^3 is observed in July which is the beginning of biomass burning period over South Africa. Average standard deviation is found at the surface below 3km corresponding to ~0.4x10^{12} molecules/cm^3 in July. Since surface ozone is dominant in the troposphere, maximum standard deviation is expected at this altitude range. The initialization of the instruments (between the sensor to decoder) also might cause a small percentage of the error). However, the observed standard deviation is small compared to measured mean ozone concentration (see. Figure 4.1a) by ozonesondes, revealing the high

accuracy of ozonesonde measurements. Above this height region, the standard deviation values have been decreased with increasing height.

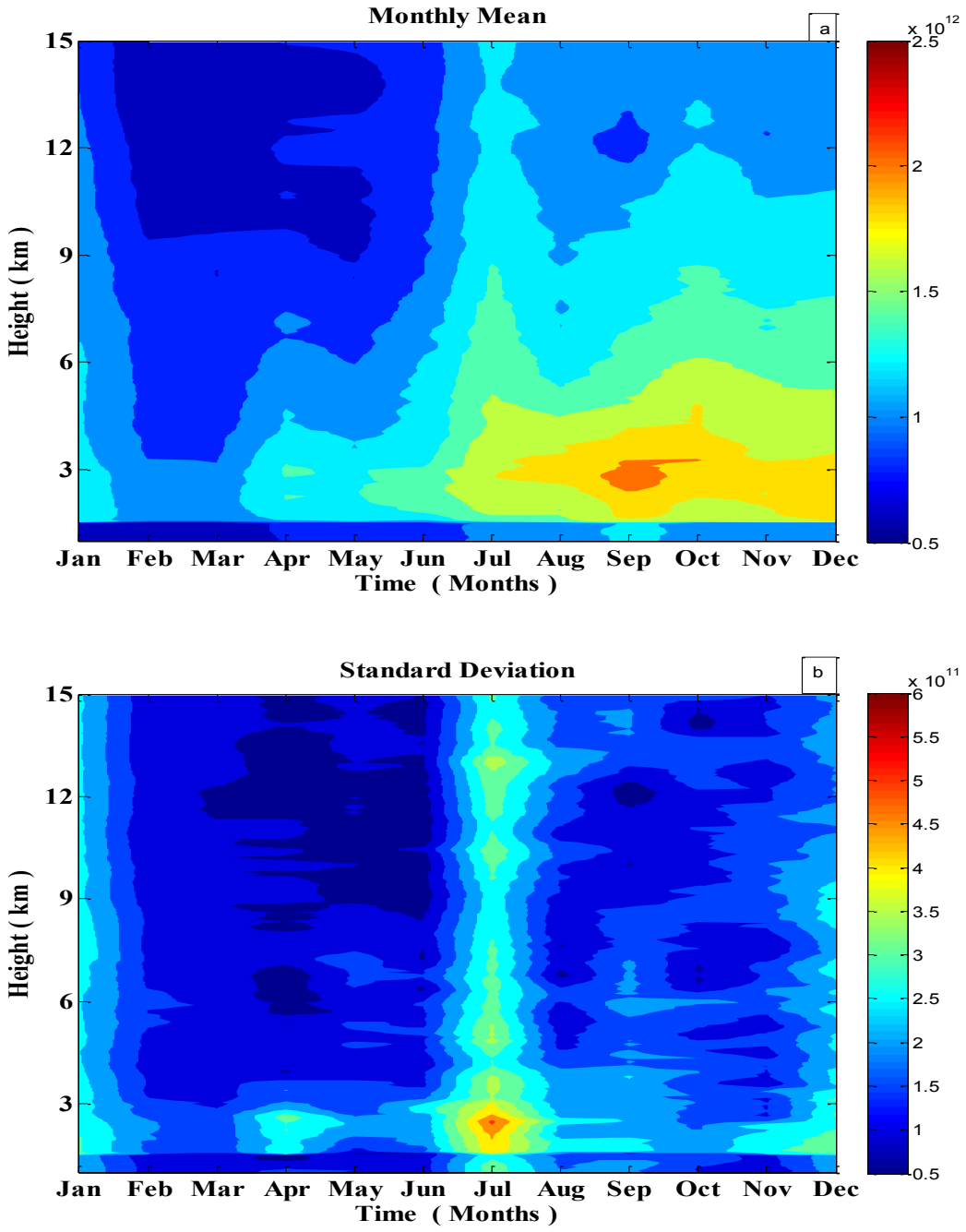

Figure 4.1(a) Height-Month colour map of monthly mean tropospheric ozone (b) Monthly mean standard deviation of tropospheric ozone. Note the changes in exponential scale between figure (a) and (b). Figure (b) scale is one order of ten less than (a).

4.1.3 Monthly climatology of stratospheric ozone from ozonesonde data

In this part of section presents the stratospheric ozone climatology and its variability over Irene. Figure (4.2a) shows the monthly mean variation of ozone for the height region from 15 km to 30 km. These monthly mean are obtained by grouping the data in terms of months irrespective of the year of measurement and their corresponding mean is calculated. The vertical ozone variations are from $1x10^{12}$ molecules/cm^3 to $5x10^{12}$ molecules/cm^3 for the height region from 15 km to 30 km. Ozone values for such height region from 15 km to 18 km is ~$1x10^{12}$ molecules/cm^3 as it increases to about $2x10^{12}$ molecules/cm^3 between 18 km and 21 km. Maximum ozone concentration is found to be within the height region of 22 km to 27 km ($4.5x10^{12}$ molecules/cm^3). Above 27 km, ozone concentration reduces. Maximum ozone concentration is found to be in the spring begin from late winter while the miminum is found during the summer / autumn months. The wave propagation into the stratosphere when the wind is westerly can be related to the seasonal variation in Irene (Sivakumar et al., 2007). According to Thompson et al., 2007 zonal wave is greatest during spring which enhances ozone concentration as ozone is transported and recirculated from African burning regions. There is also pronounced midlatitude influences due to stratospheric-troposheric ozone injection during winter (Thompson et al., 2003).

The monthly standard deviation for SHADOZ data is presented in figure (4.2b). The vertical variations are within $0.1x10^{12}$ molecules/cm^3 and $0.9x10^{12}$ molecules/cm^3. This range of variation is selected to show properly the measured standard deviation. Low standard deviation is recorded for the height region where maximum ozone concentration is recorded (Sivakumar et al., 2006) for all the months of the year. Maximum standard deviation are obtained in the height region of 17 km to 21 km. This height region corresponds to the tropopause height where much deviation is expected due to dynamical and chemical processes taking place in that region (Sivakumar et al., 2007; 2011; Wang Jun and Wang Hui-Jun 2010).

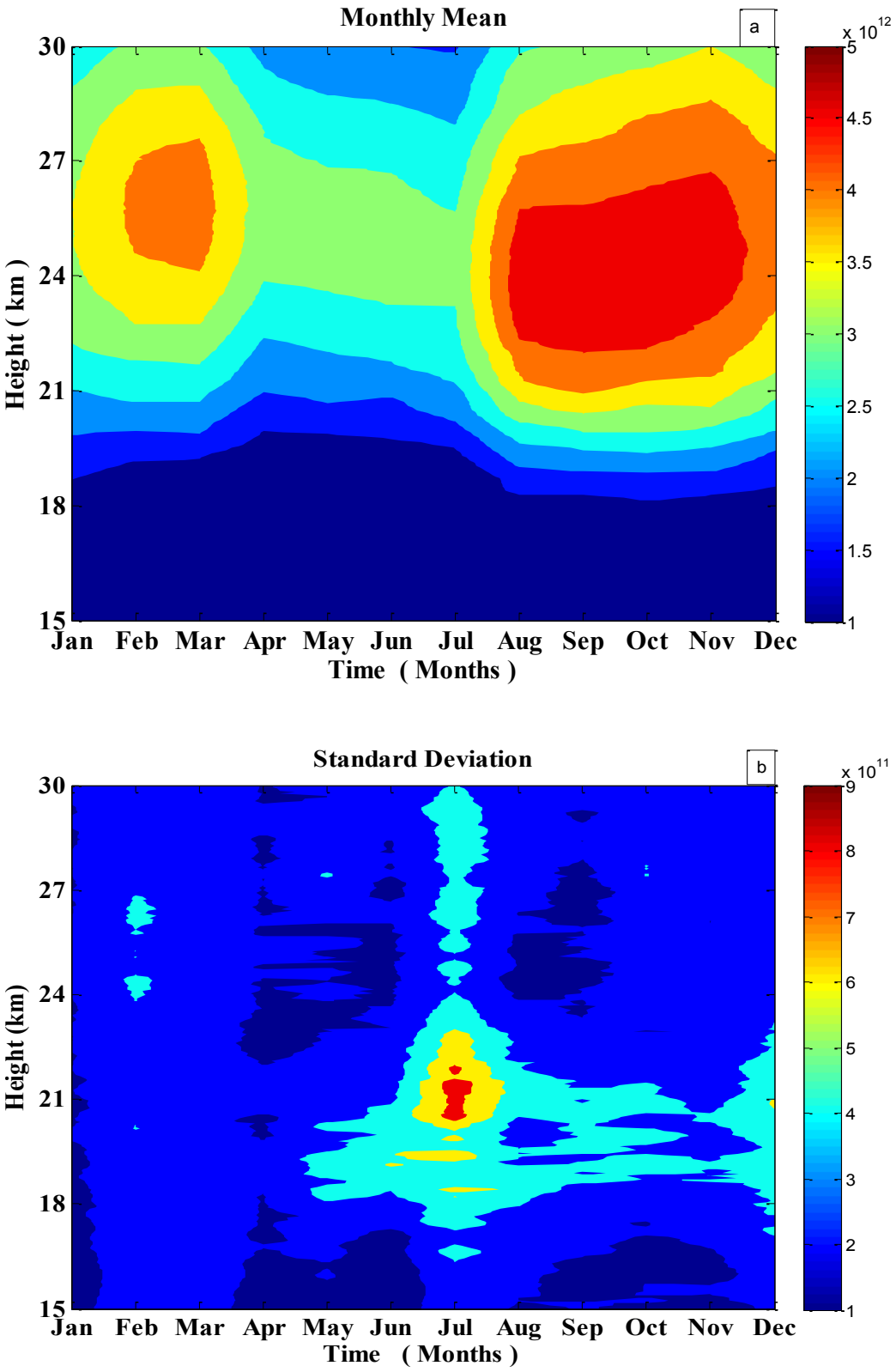

Figure 4.2(a) Height-Month colour map of monthly mean stratospheric ozone (b) Monthly mean standard deviation of stratospheric ozone. Note the changes in exponential scale between figure (a) and (b). Figure (b) scale is one order of ten less than (a).

4.1.4 Comparison of Aura-MLS and Ozonesonde profile

The annual mean ozone was obtained by compiling all the 10 year's of data. Ozone measurements used for this study were converted from ppmv to molecules/cm^3 to determine the ozone molecular concentration. The height region used for this section are from 15 km and 30 km. The height resolution was interpolated to every 50 m from 15 km to 30 km. The years are limited to 4 years (2004 to 2007) for comparison because these are the years both instruments had in common. Though MLS measurements are from 10 km to 60 km, the height variations from 15 km to 30 km are used to compare with ozonesonde measurements within these height. Figure (4.3a) shows the annual mean profile for ozonesondes and MLS for 2004 and 2005. Ozone concentration for 2004 and 2005 measured from Ozonesondes are higher than those measured by MLS. Ozonesonde measurement in 2004 is much more higher than its measurement in 2005. The size of the ozone hole for 2005 may be attributed for the low measurement as ozone hole was bigger in 2005 compared to 2004 (NOAA). The time of launch may contribute to some percentage increase in ozone concentration. For 2005, the average time of launch is 8.00 am while in 2004, the time of launch is 10.30 am, by this time of the day, the intensity of sunlight is higher. This brings about photolysis of oxygen leading to more ozone formation. For the height concentration of stratospheric ozone, ozone increase with an increase in height from ~22 km to 27 km where maximum ozone concentration is expected. Above this altitude, ozone concnetration reduces with height. MLS profile replicates the same stratopsheric ozone profile of gradual increase with height from the tropopasue to ~ 27 km. Maximum ozone concentration is also between 22 km and 27 km (stratospheric maximum), after this altitude range, ozone concentration decreases with increasing height.

Figure(4.3b) presents the height profile of ozone concentration for 2006 and 2007 measurements from Ozonesondes and MLS. The results of the height variation of ozone concentration agrees with those in figure(4.3a) except that the stratospheric maximum stepped up by 1 km to a range between 23 km and 28 km. Just above the tropopause, ozone concentration increased with an increase in height till it got to the height region between 23 km and 28 km where maximum ozone concentration is expected (stratospheric maximum). For both measurements, ozone concentration in 2007 is found to be higher than 2006. This is in relation to the stability of atmospheric chlorine and bromine and the proposed stratopsheric ozone recovery in the 21st century (Ziemke and Chandra 2012). However, more years of data sets may needed to access the level of recovery of ozone over the last decade.

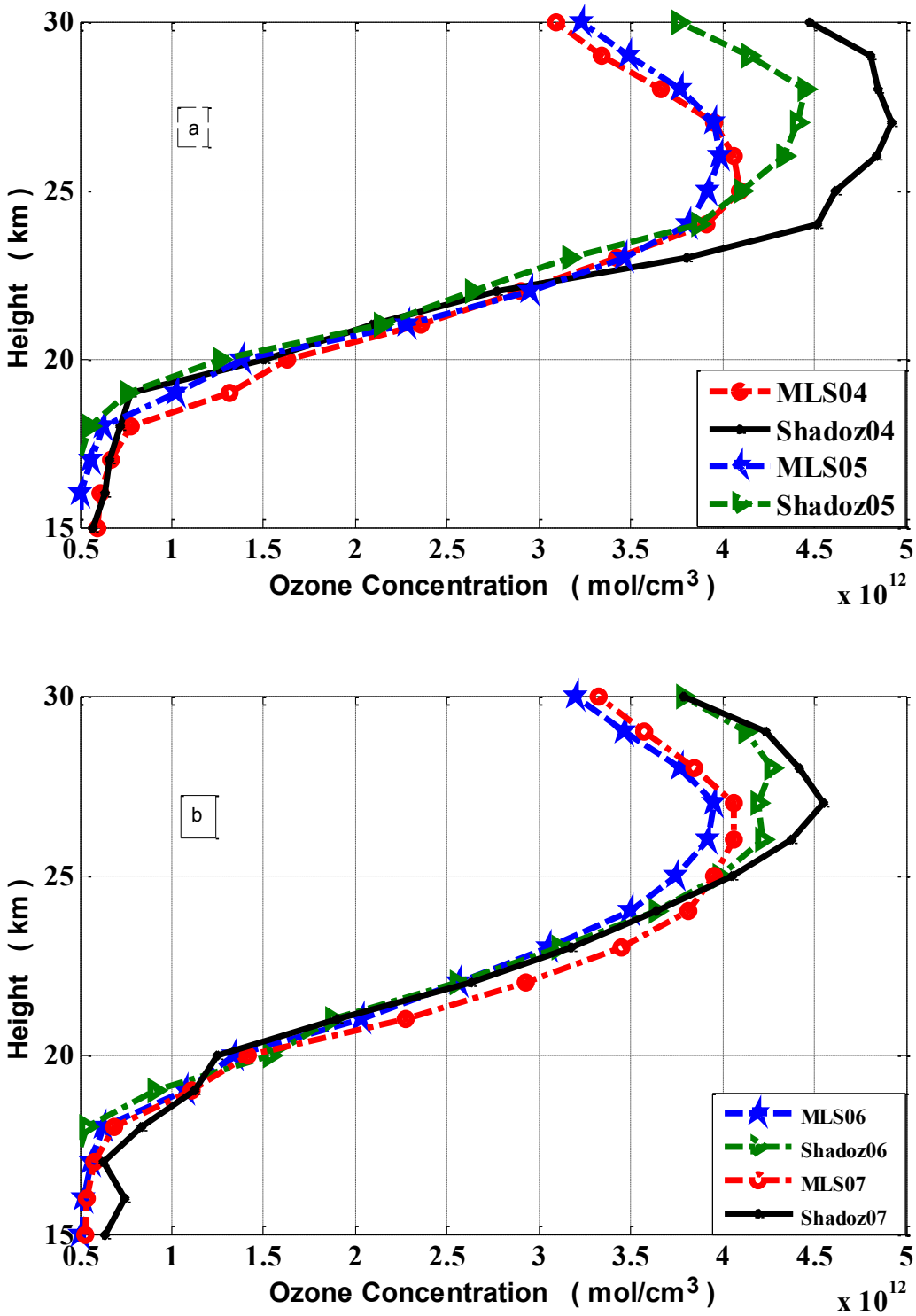

Figure. 4.3: Height profile of annual mean ozone obtained from ozonesonde and MLS (a) for 2004 - 2005 (b) for 2006 - 2007

4.1.5 Monthly variations of stratospheric ozone from MLS Aura satellite measurements

Similar to the ozonesonde, the data used here is also 10 years period of ozone measurement from the MLS Aura satellite overpass over Irene. The data are grouped according to the months of measurements irrespective of the year and their corresponding mean is calculated. The monthly mean obtained for MLS is smoother when compared with that from ozonesondes. This can be due to the height resolution of MLS data. Maximum ozone concentration is found to be within the height region of 22 km and 28 km and is about $4x10^{12}$ molecules/cm^3. This value is smaller when compared with ozonesonde concentration within these height regions. These low ozone values are in agreement with the global ozone climatology for MLS satellite for 25^oS to 30^oS (Ziemke et al., 2011). Stratospheric ozone measured are however quite low for the winter months which is not expected. Besides this, there is no significant difference in the measurement of MLS and ozonesonde for the height regions (Jiang et al., 2011). Above 28 km, the ozone concentration is reduced as expected.

The monthly standard deviation for MLS AURA is presented in figure (4.4b). The vertical height range of the deviation is $0.1x10^{12}$ molecules/cm^3 and $0.6x10^{12}$ molecules/cm^3. Maximum standard deviation of ~ $0.4x10^{12}$ molecules/cm^3 is observed in August between 18 km and 20 km which corresponds to the tropopause height range (Sivakumar et al., 2010) where maximum deviation is expected. High deviation at low height region during spring may be due to low accuracy of measurement at this height region.

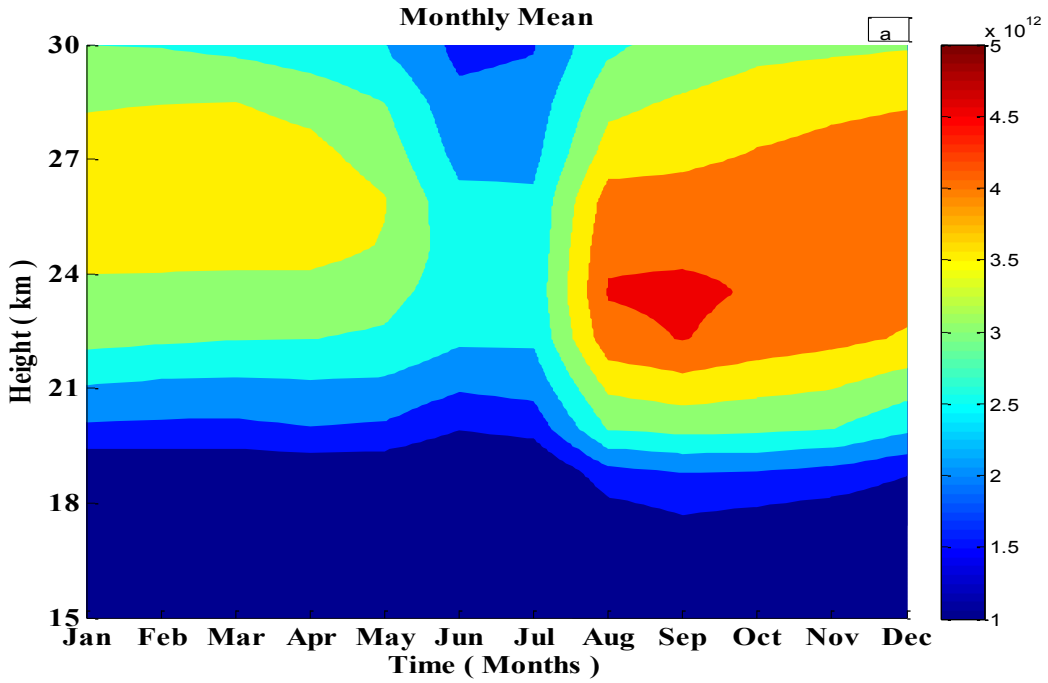

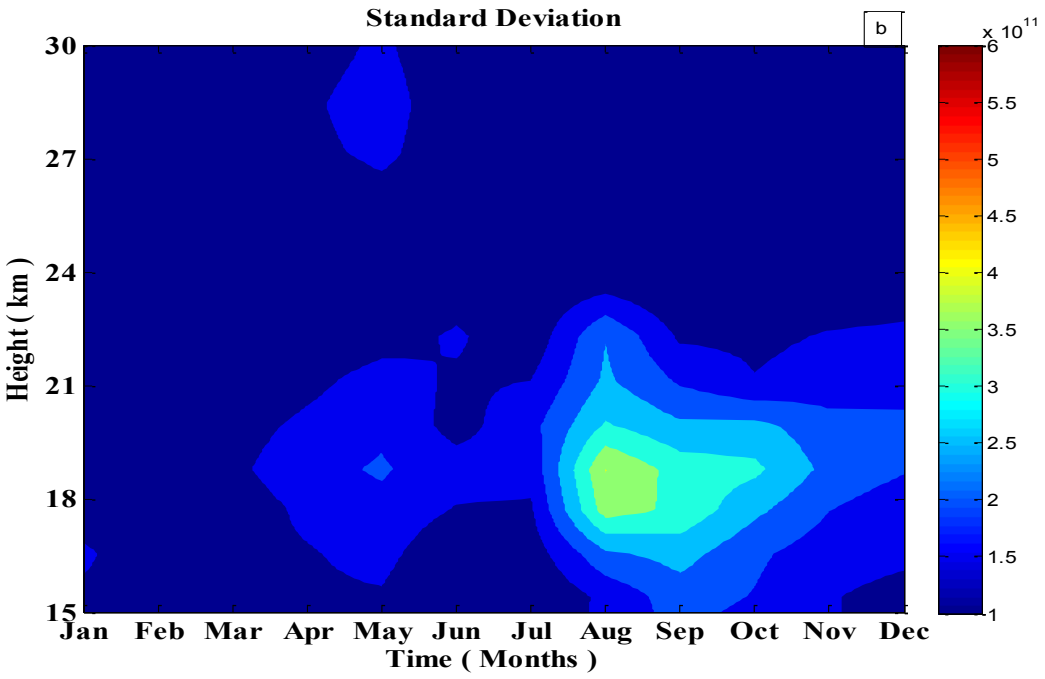

Figure 4.4 (a) Height-Monthly-Mean Ozone Concentration plot for MLS (b) and the Corresponding Standard Deviation

4.1.6 Monthly variations of stratospheric ozone by combined MLS and Ozonesonde observations

The monthly mean values are obtained by grouping the data with respect to months and irrespective of the years of measurements by which the corresponding mean is calculated. The vertical ozone variation is from $1x10^{12}$ molecules/cm^3 to $5x10^{12}$ molecules/cm^3. There is no significant variation in ozone concnetration from 15 km to 18 km as obtained earlier from both instruments separately. Ozone concentration in this height region is between $1x10^{12}$ molecules/cm^3 to $1.5x10^{12}$ molecules/cm^3. For the height region between 18 km and 21 km, a steady increase in stratospheric ozone is observed from $1.5x10^{12}$ molecules/cm^3 to $2.5x10^{12}$ molecules/cm^3. Maximum ozone concentration is found in the height region of 23 km to 27 km with spring ozone concentration corresponding to ~$4.7x10^{12}$ molecules/cm^3. During autumn, low ozone concentration is obtained, about $3.5x10^{12}$ molecules/cm^3, almost the same concentration is also obtained during the summer. All the four seasons replicated the same height variation of maximum ozone concentration. At height regions above 28 km, ozone concentration reduced with increasing height.

The monthly standard deviation for both Ozonesonde and MLS is presented in figure 4.5b. The vertical variations are within $0.05x10^{12}$ molecules/cm^3 and $0.6x10^{12}$ molecules/cm^3. This range of variation is selected to show properly the measured standard deviation. Low standard deviation is recorded for the height region where maximum ozone concentration is recorded (Sivakumar et al., 2006) for all the months of the year. Maximum standard deviation is obtained in the height region from 17 km to 21 km corresponding to $0.45x10^{12}$ molecules/cm^3. This height region corresponds to the tropopause height where much deviation is expected due to dynamical and chemical processes taking place in that region (Sivakumar et al., 2007; Wang Jun and Wang Hui-Jun 2010). Biomass burning could also be responsible for the observed high standard deviation in July as that is when it begins in the southern hemisphere tropics.

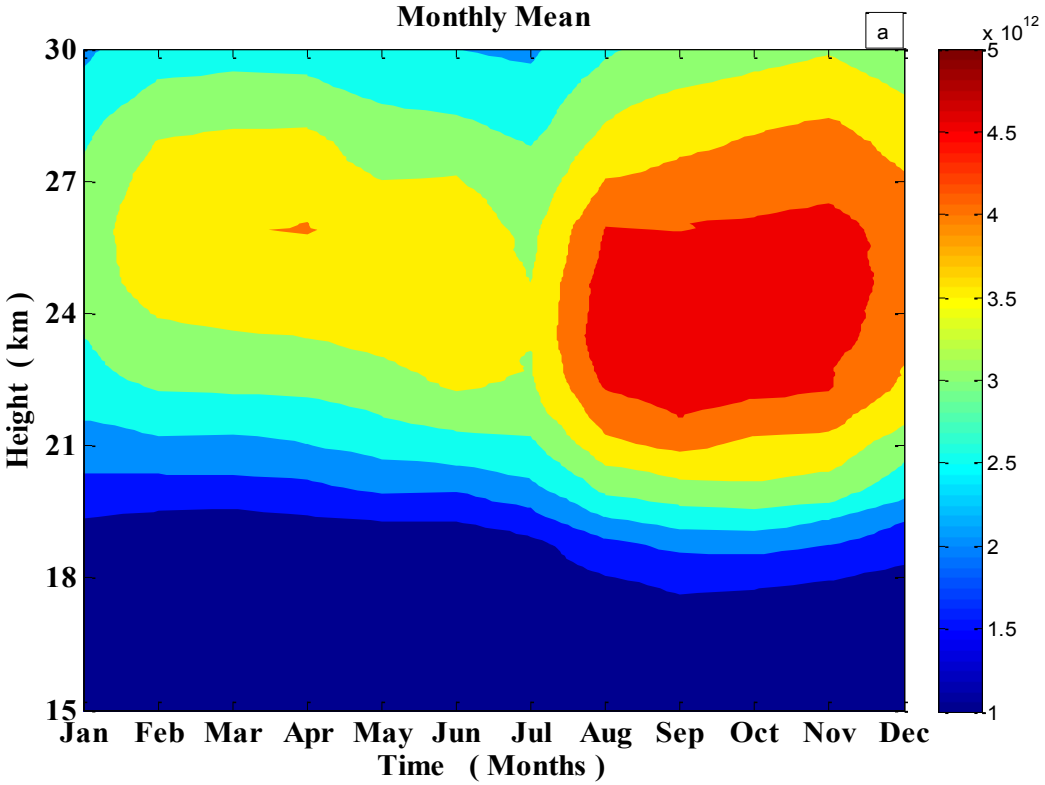

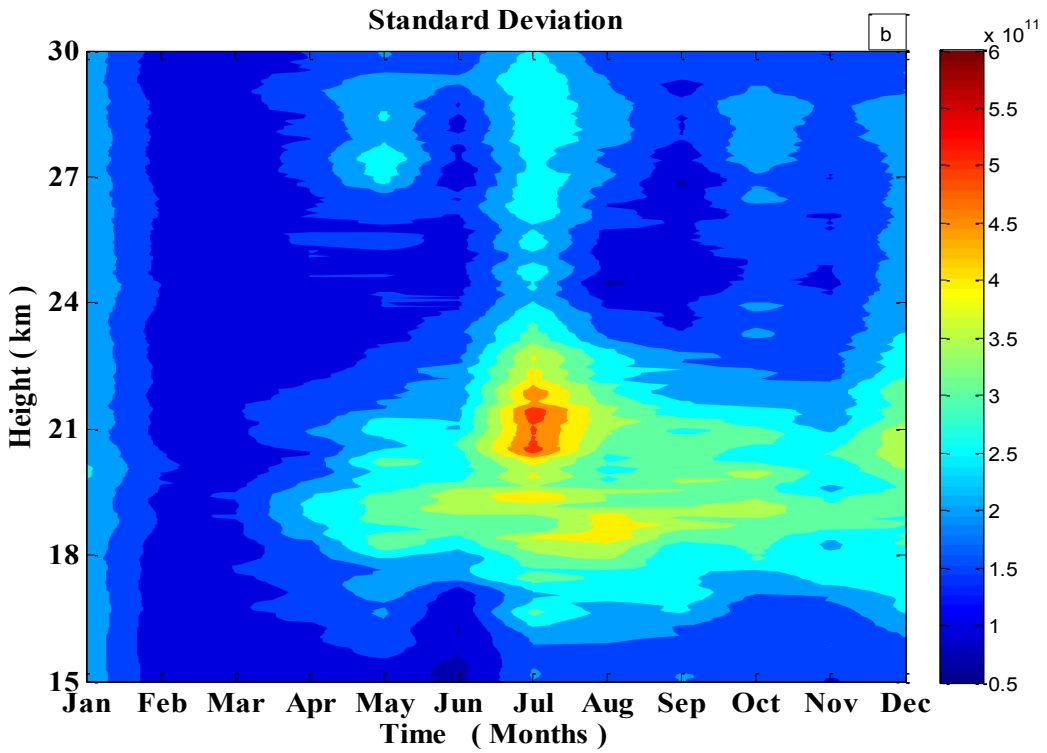

Figure 4.5 Height-Month colour map of monthly mean for combined ozone concentration from SHADOZ and MLS.

4.1.7 Difference Between Ozonesonde and MLS Aura

Figure 4.6 shows the difference between combined ozone concentration measured from ozonesondes and MLS. This is obtained by subtracting the measured ozone values of MLS from that of ozonesondes. The result shows very low difference between the measurements except in the stratospheric height where maximum ozone concentration is expected. Vertical ozone concentration difference is varied from $0.1x10^{12}$ molecules/cm^3 to $0.8x10^{12}$ molecules/cm^3. A difference of $0.2x10^{12}$ molecules/cm^3 is obtained for spring, autumn and early winter below 23 km and ~$0.5x10^{12}$ molecules/cm^3 above 23 km during spring, a difference in the range of $0.6x10^{12}$ molecules/cm^3 to $0.8x10^{12}$ molecules/cm^3 is obtained between 20 km and 23 km while above this altitude, a difference of $0.5x10^{12}$ molecules/cm^3 is obtained. Difference between these instruments may be due to difference in the instruments, time overlap of measurements, method of retrieval etc., However, Froidevaux et al., (2006), found that there is a low accuracy in MLS measurements in this height region.

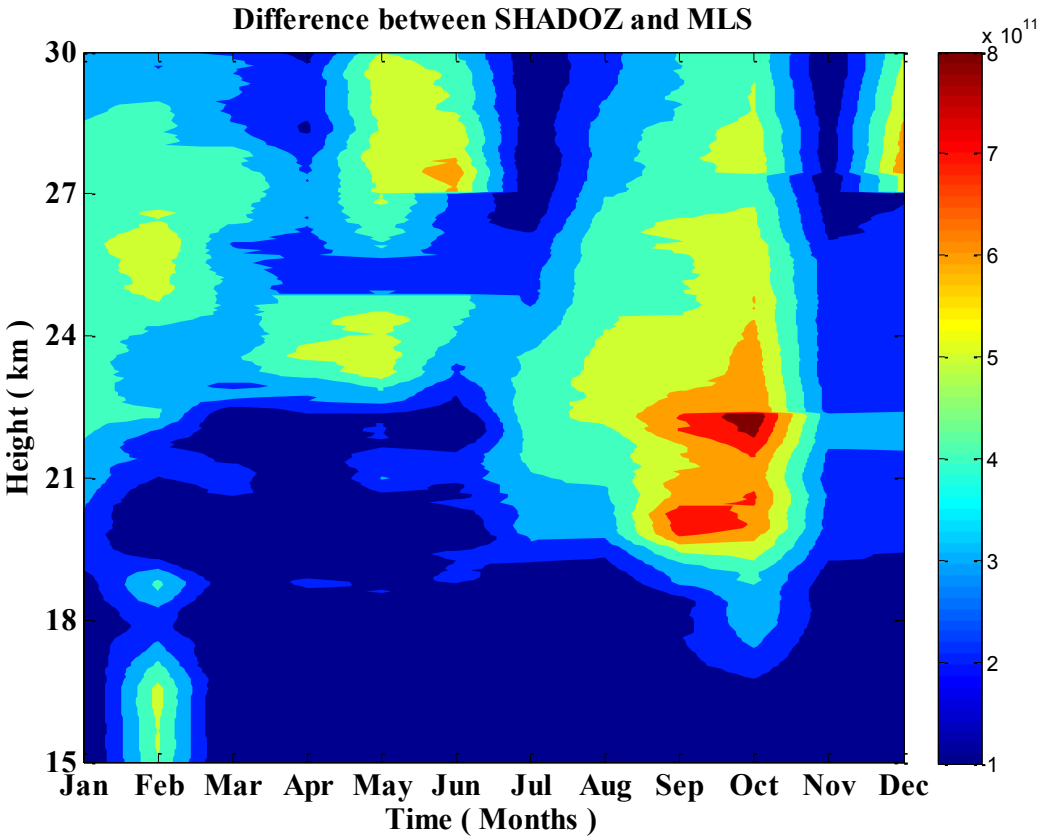

Figure (4 .6) Seasonal Difference between SHADOZ and MLS Aura Height Monthly Mean

4.2 Total column ozone climatology and variability

In this section, total ozone (hereafter referred as ToZ) variation and climatology over Irene, South Africa is examined using the Dobson instrument for ground-based measurements while TOMS, EPTOMS, GOME-1, GOME-2, OMI, IASI satellites are used. These satellites are carefully selected to provide 35 years of continuous measurements over Irene. The only data gap in this study was between June 1993 and July 1994 when none of these satellites was in operational.

4.2.1 Results

4.2.2.1 Monthly variability of ToZ from satellite measurements

Figure 4.7a shows the monthly satellite measurements from overpasses over Irene. This was obtained by grouping the data in terms of monthly measurements irrespective of the years of satellite measurements from the overpasses over Irene and their corresponding mean is determined. This is to show the variability of ozone over the years as measured by various satellites. TOMS has the highest total column ozone (ToZ) measurement compared to other satellites. TOMS ToZ measured during mid spring (Oct.) is about 297 DU. It also had the highest values for all seasons (Bramstedt et al., 2003) except for late autumn (May) where IASI had a higher value. IASI has been found to overestimate ozone when compared to ground-based measurements (Anton et al., 2011; Boynard et al., 2009). High ozone measurement from TOMS satellite can also be due to the years of overpass (1978 to 1993) when ozone concentration was relatively high in the atmosphere (Bojkov and Fioletov 1995). Minimum ozone concentration was experienced in May during late autumn of about 259 DU which is in agreement to the findings over a similar southern sub-tropics site, Reunion (Sivakumar et al., 2007).

Other satellite measurements replicated a spring time maximum and an autumn minimum. EPTOMS measurememements were higher than GOME-1 whose overpass time were similar (see. figure 4.7a). This is in agreement with the work of Anton et al. (2010) where they showed that despite EPTOMS instrumental degenerations, its measurements were still higher than GOME-1, although both satellite measurements are within the same standard deviation. There was also a good agreement between EP-TOMS and GOME-1 measurements as their measurements were consistent throughout the years of operational in terms of ozone seasonality. EPTOM measured a late autumn minimum of 259 DU and its spring maximum is

about 283 DU. There is a systematic difference of about 2 to3 % over tropical and equitorial regions and over southern midlatitudes in the estimate of global and zonal total ozone from GOME when compared to ground-based measurements (Fioletov et al., 2002). This is shown in GOME-1 measurements as ToZ has a peak value in September and October and had an early minimun in late summer (Feb.) of about 259 DU. This measurement of late summer minimum is also replicated by GOME-2 satellite as shown in figure 3.7b. GOME-2 also had another minimum during late autumn (May) and a mid spring maximum of total ozone in Ocotber. Though according to Balis et al. (2001), OMI overestimates total column ozone in the Southern Hemisphere, the result of this showed consistency with other measurements where it had a spring time maximum of 280 DU and an autumn minimum of 260 DU. TOMS, EPTOMS, OMI and IASI all measured a late autumn (May) minimum with a gradual increase through winter as it reaches a mid-spring maximum in October. GOME-2 replicated similar mid-spring maximum. GOME-1 have shown a month early maximum during september and minimum during late summer and late autumn (February and May). IASI measurement is quite different from other satellites measurements in terms of both seasonal minimum and average minimum, although its measurement is still within the same standard deviation with other satellites. It measures a winter minimum of ~264 DU. Its spring time maximum of 280 DU is in agreement with other satellite measurements. The result of this monthly mean total column ozone is in agreement with earlier studies made in the Southern Hemisphere where spring time maximum and an autumn minimum ozone concentration is expected (Sivakumar et al., 2007).

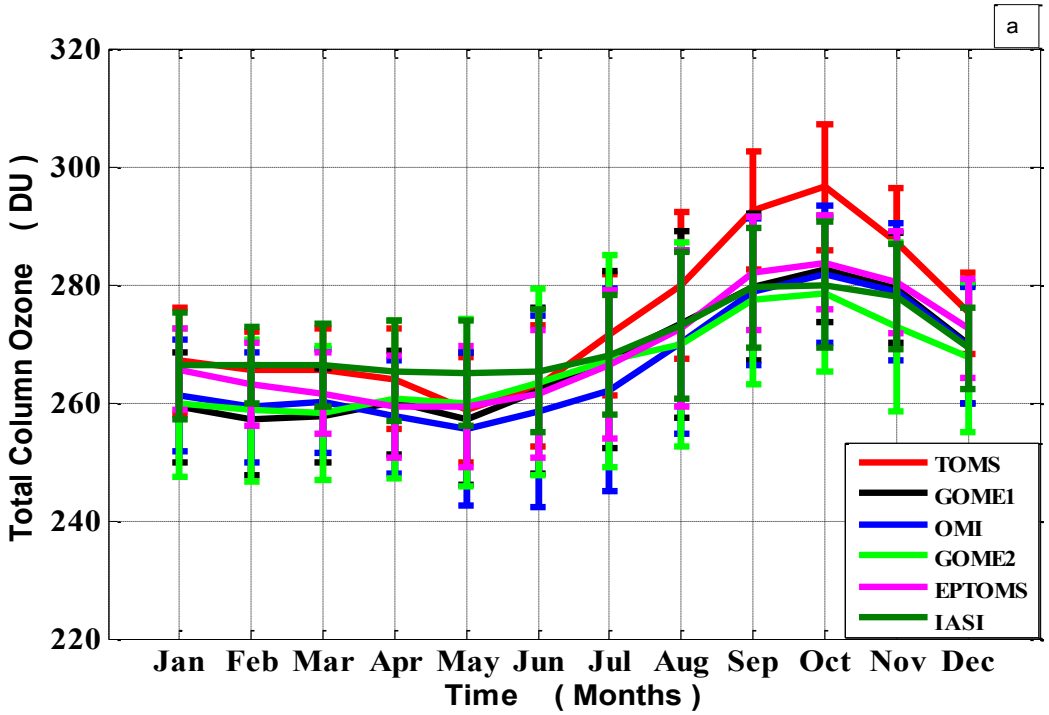

Figure 4.7 Monthly ozone variations and their corresponding standard deviations from (a) TOMS, EPTOMS, GOME-1, GOME-2, OMI and IASI

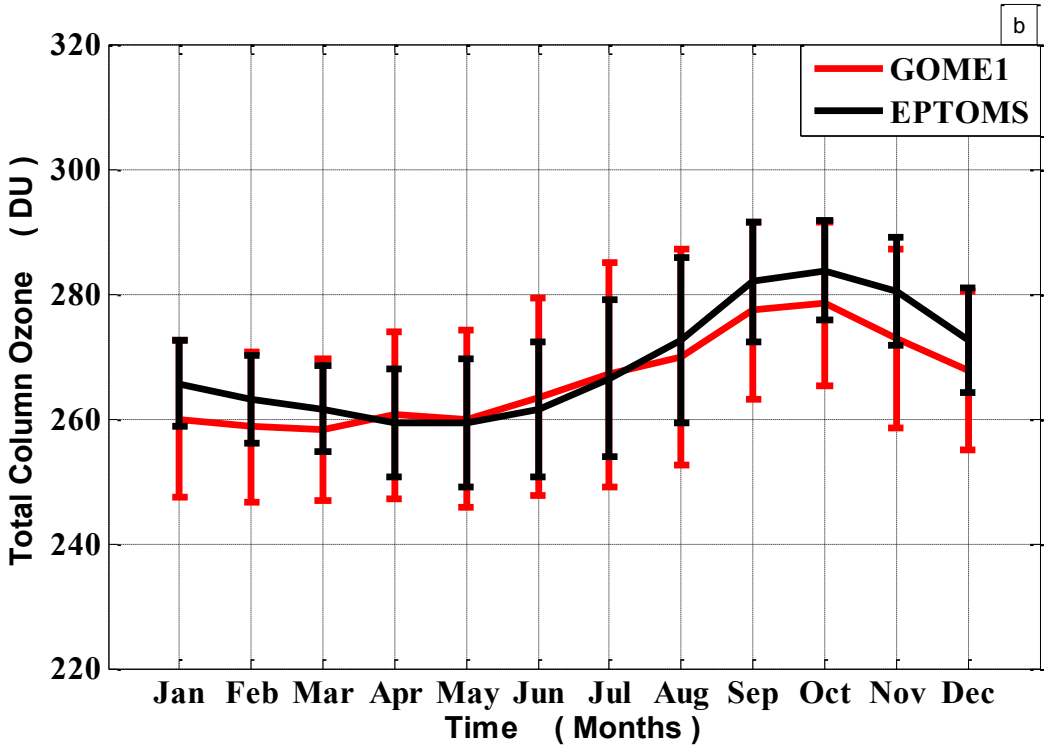

Figure 4.7 Monthly ozone variations and their corresponding standard deviations from (b) EPTOMS and GOME-1

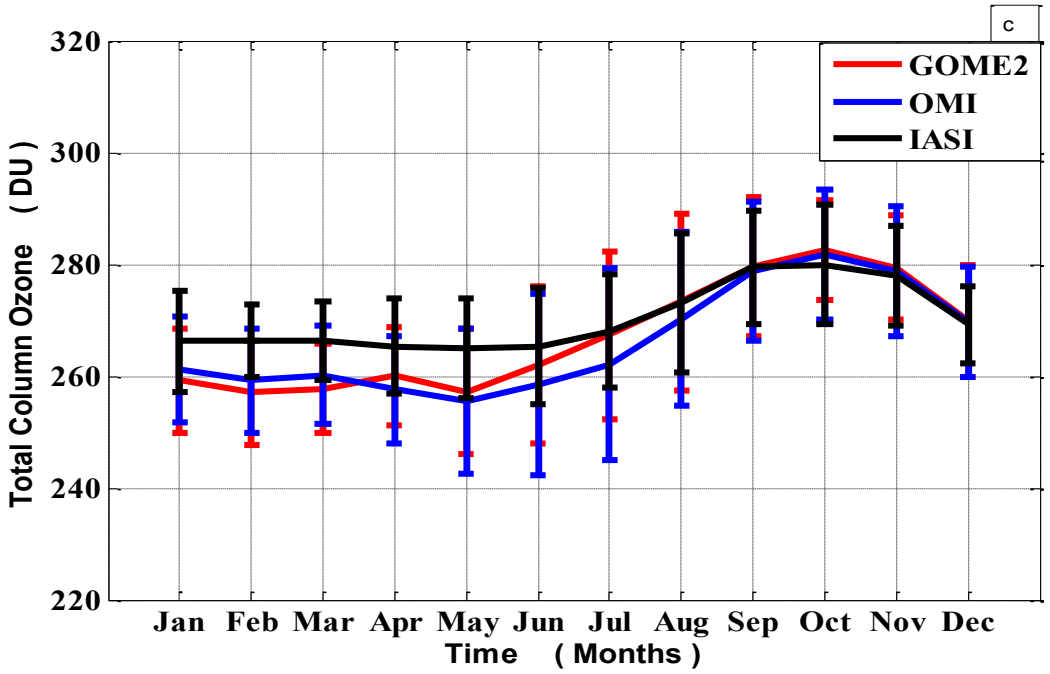

Figure 4.7 Monthly ozone variations and their corresponding standard deviations from (c) OMI, GOME-2 and IASI.

4.2.2.2 Interannual variability of total column ozone

The yearly mean values for each satellite was obtained by grouping the data in terms of yearly measurements and their corresponding mean is calculated. Ozone was uncharacteristically low in 1985 which agreed with the global data (Jones and Shanklin 2002). That was the year the ozone hole was first discovered by Joesph Farman and his collegues (Hamil and Brian Toon, 1991). TOMS satellite was the only satellite available for the study from 1978 to 1993 when it stopped operational (McPeters and Labow 1996). Yearly mean from TOMS is within 270 DU and 280 DU with the exception of 1985 when it was as low as 265DU (Jones and Shanklin 2002). However, in 1992, there was a significant decrease in total column ozone. This can be attributed to the volcanic eruption at Mt. Pinatubo in Philippines which caused a global decrease in ozone concentration (Gleanson et al., 1992). The eruption circulated aerosols globally within five months (Stowe et al., 1992), a major factor in the ozone loss. Figure 4.8a shows a downward trend in ozone measurements from 1978 to 1993. This is due to TOMS data available as it stopped operational in May which is the period minimum total ozone is expected (Newman et al., 1997). For late 1993 and 1994 where no data was available for this study due to lack of satellite retrieval used for this study,

total ozone continued to decline during this years (Hofmann et al., 1994). From 1995, the average ozone concentration in the atmosphere continued to flunctuate due to various dynamical processes and the magnitude of the various transport processes occuring each year (Houghton et al., 2001). For both EPTOMS and GOME-1 whose years of overpass are similar, they showed an average yearly ozone mean of about 267 DU and 263 DU respectively for the late 90s. The yearly mean however increased to about 271DU and 266 DU respectively in the 21st century. GOME-2 and OMI measured a yearly average of 269 DU and 273 DU respectively. This gradual increase and stability in total column ozone in the 21st century is attributed to the stability in the atmospheric amount of chlorine and bromine. Also, ozone depleting gases such as chlorofluorocarbons are removed from the atmosphere through natural processes, though at a very slow rate.

4.2.2.3 Temporal variation of ToZ

The temporal ozone variation for each satellite was done by calculating the monthly mean for the corresponding of years of the satellite overpass data. The purpose of this is to show if there is any pronounced variation(s) in the expected values of total column ozone overpass for the years of study. The flunctuations in figure 4.8 shows the seasonal variation in ozone as it increases gradually from autumn (where minimum ozone concentration is expected) to winter and then reaches a spring time maximum (linked to biomass burning activities) before it reduces through summer (Clain et al., 2009). TOMS ozone overpass had an average maximum ranging from 295 DU to 300 DU and a minimum of ~260 DU for most years. A spring time maximum averaging 284 DU was measured for EPTOMS throughout the years of overpas except in 1998 and 2004 when ozone maximum was about 278 DU. GOME-1 satellite also replicated low ozone measurement in 1998 but had been decommissioned by 2004 to determine if it would also measure low ozone over 2004. Reasons for the anomalies in these years are not discussed in this study which shall be addressed in the future.

The result of trend analysis of ozone over Irene shows a significant decrease in total ozone from 1978 to 1993 by ~8 DU as shown in figure 4.8a. This is attributed to the discovery of the ozone hole and the abundance of chlorofluorocarbons in the atmosphere. However, since the Montreal Protocol which placed a ban on chlorofluorocarbon compunds, atmospheric chlorine has reduced gradually over the years. This has brought about the stability and gradual recovery of the ozone layer as shown in figure 4.8b where there is an increase of ~2DU in total ozone from 1995 to 2005 measured by both GOME-1 and EPTOMS. A further

increase by about 7 DU to 9 DU is observed for measurements from OMI and IASI still revealling the gradual recovery of the ozone layer.

For GOME-2 satellite, data between November 2009 and May 2011 were not used for this study. Although the measurements were within the standard deviation used to filter the data, measurements during this period did not agree with the well established seasonality of ozone in the Southern Hemisphere. This can be attributed to instrumental errors as a new satellite GOME-2B was launched in 2012 for better monitoring of ozone and other trace gases in the atmosphere. Higher ozone peaks are measured by GOME-2 in 2012 and 2013 than OMI satellite, this can be attributed to the change in algorithm from GOME-2A to GOME-2B (Hao et al., 2014).

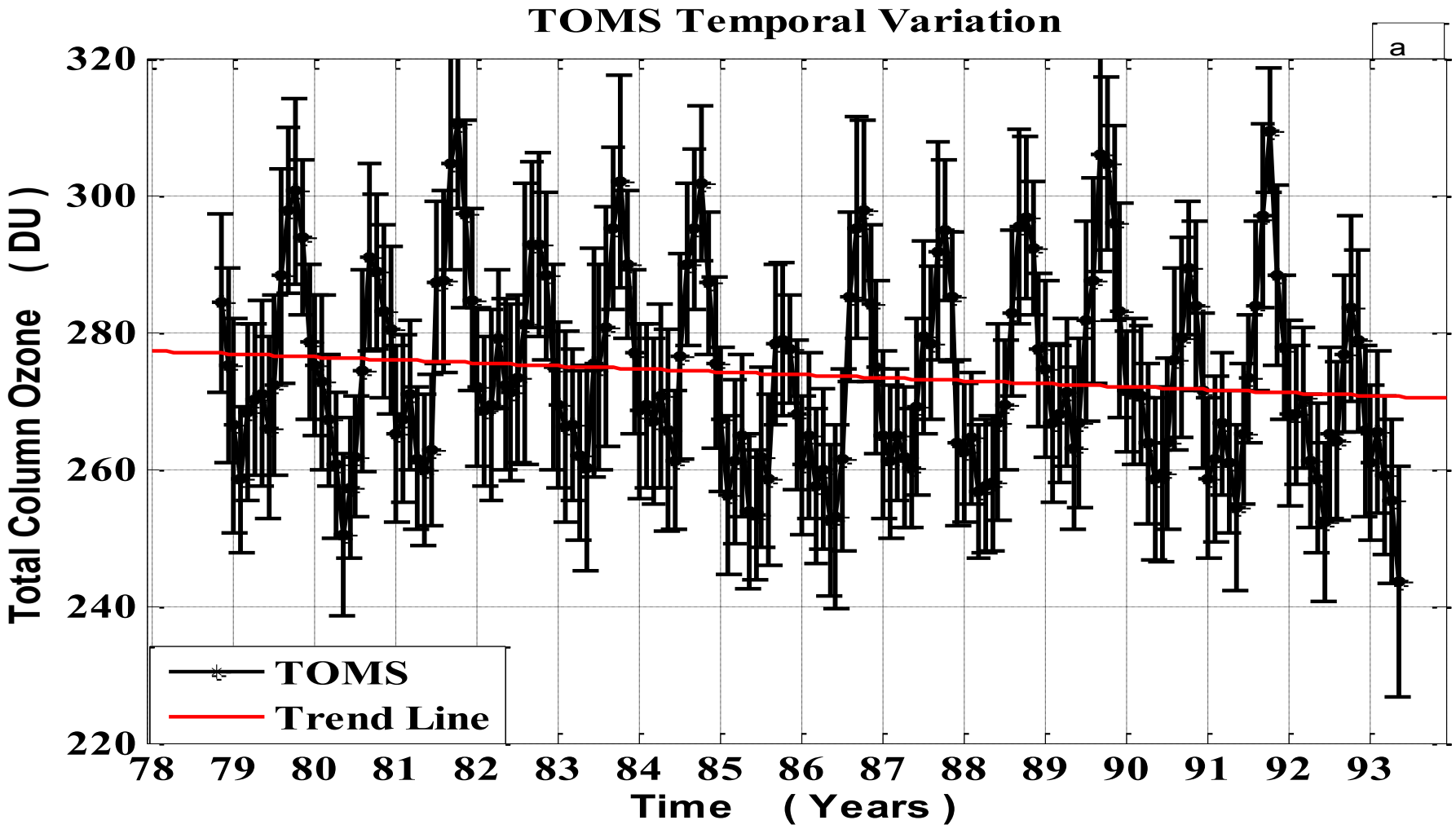

Figure 4.8 Ozone temporal variation trend over Irene from (a) TOMS satellite

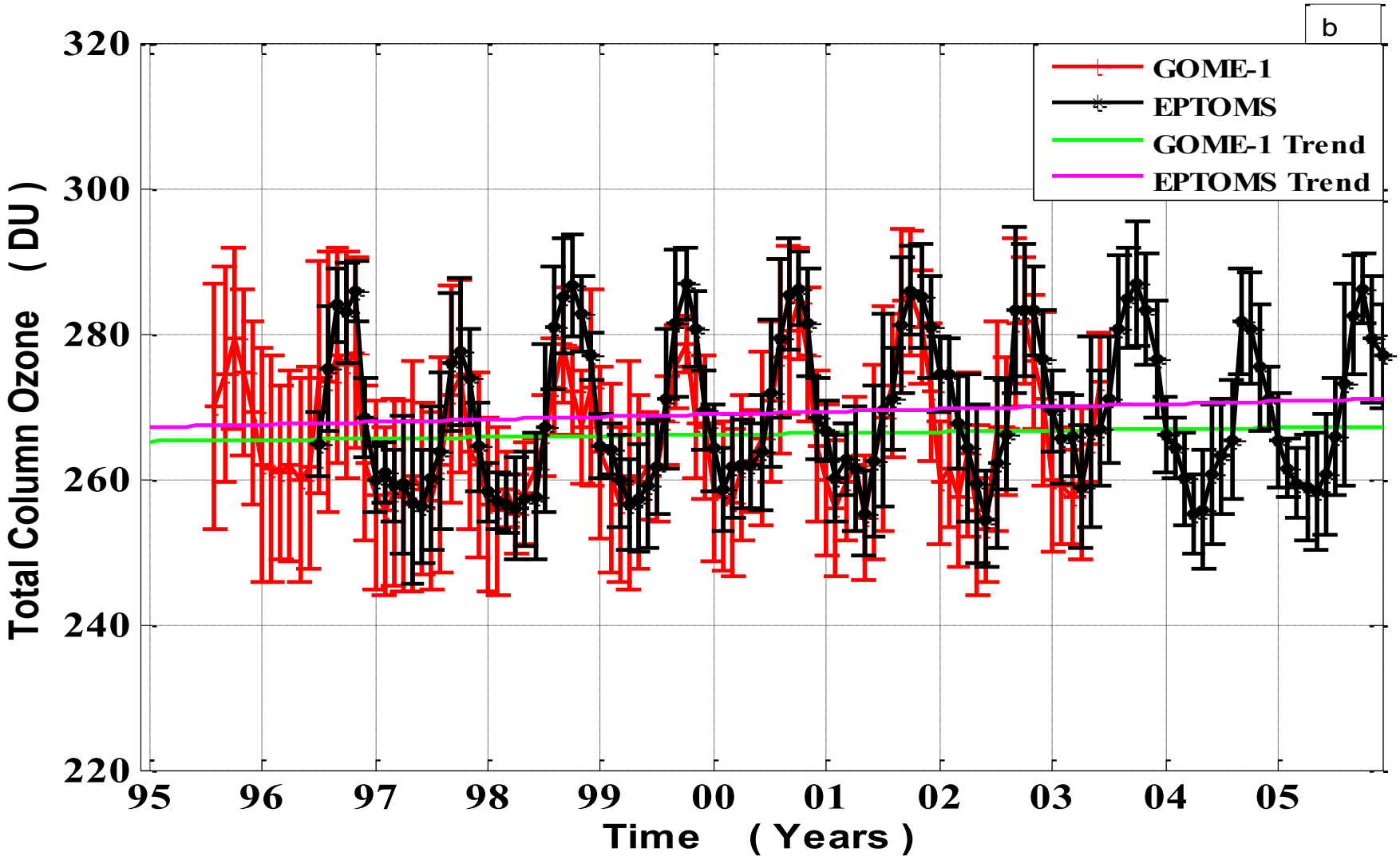

Figure 4.8 Ozone temporal variation trend over Irene from (b) GOME-1 and EPTOMS

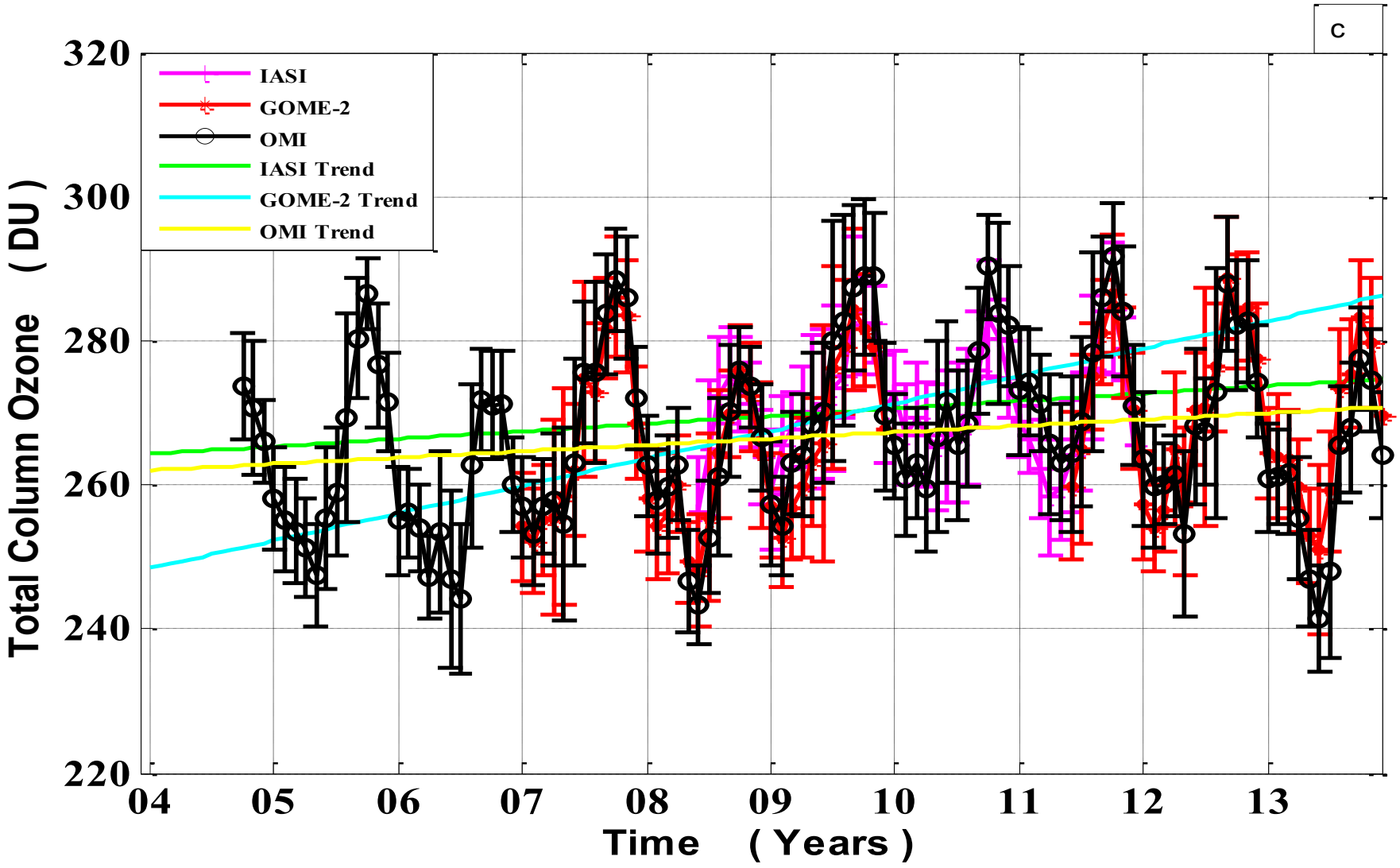

Figure 4.8 Ozone temporal variation trend over Irene from (c) OMI, GOME-2 and IASI satellites.

4.2.2.4 Dobson seasonal variation

The seasonal ozone variations from Dobson measurements analysis are based on a time period of 23 years from August 1989 to December 2011 with just a single monthly measurement. The monthly mean ozone values for Dobson instrument was obtained by grouping the data in terms of monthly measurements irrespective of the years of measurement and their corresponding mean is calculated. The standard deviation was also obtained. Vertical ozone variations are varied from 220 DU to 320 DU. Figure 4.9a shows that maximum value in ToZ during October with 284 DU and minimum ozone was observed in later autumn (260 DU). Most ground-based stations record a negative bias when compared with TOMS measurement (Komhyr et al., 1989). This can be due to site condition such as elevation above sea level. At equatorial and southern mid-latitudinal stations, the bias is ~2 % to 3 % which rises to about 5 % over the Antarctica. Dobson instruments at main southern hemisphere sites agree with the world standard Dobson to within 0.5 % (Fioletov et al., 2002). The standard deviations in the measurements are quite high. This can be due to the frequency of monthly measurements as increase in the number of monthly measurement would give more accurate standard deviation. However, since Dobson is an effective tool with high accuracy and precision in determining TCO, the data are used for analysis. Monthly mean ozone for both the Dobson instrument and each satellite are presented in table 4.3.

Figure 4.9a shows the variation between Dobson measurement and combined satellite measurements. The combined satellite measurements are obtained by adding all monthly measurements from satellites used for this study and their mean is determined. The result shows an agreement between Dobson and satellites to within 1 DU for all seasons except for early summer (December) where there agreement is within 3 DU. Since both GOME-1 and GOME-2 measurements are lower than other satellite measurements, both overpass data are removed from figure 4.9b to examine if there would be better agreement between the remaining satellites and Dobson. The result shows a close agreement between them to within 1 DU for all seasons except during mid-spring where their agreement is between 2 DU. Figure 4.9c shows the variation between Dobson and both GOME satellites. The result reveals agreement only for late autumn and winter. Dobson measurements are ~ 4 DU higher in summer, ~ 2 to 3 DU higher during early to mid-spring and ~ 5 DU higher during late spring. However, despite all these differences in measurements, both measurements in figures 4.9a, 4.9b and 4.9c are within the same standard deviation.

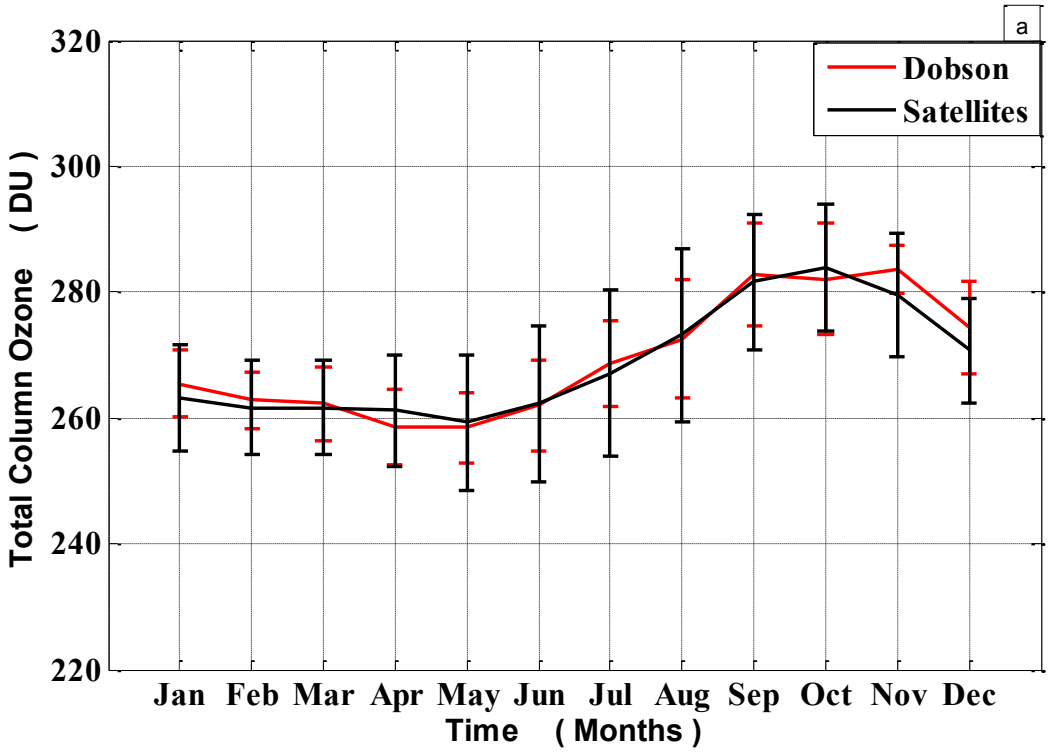

Figure 4.9 Dobson monthly mean ozone variation and standard deviation superimposed with (a) combined all the satellites

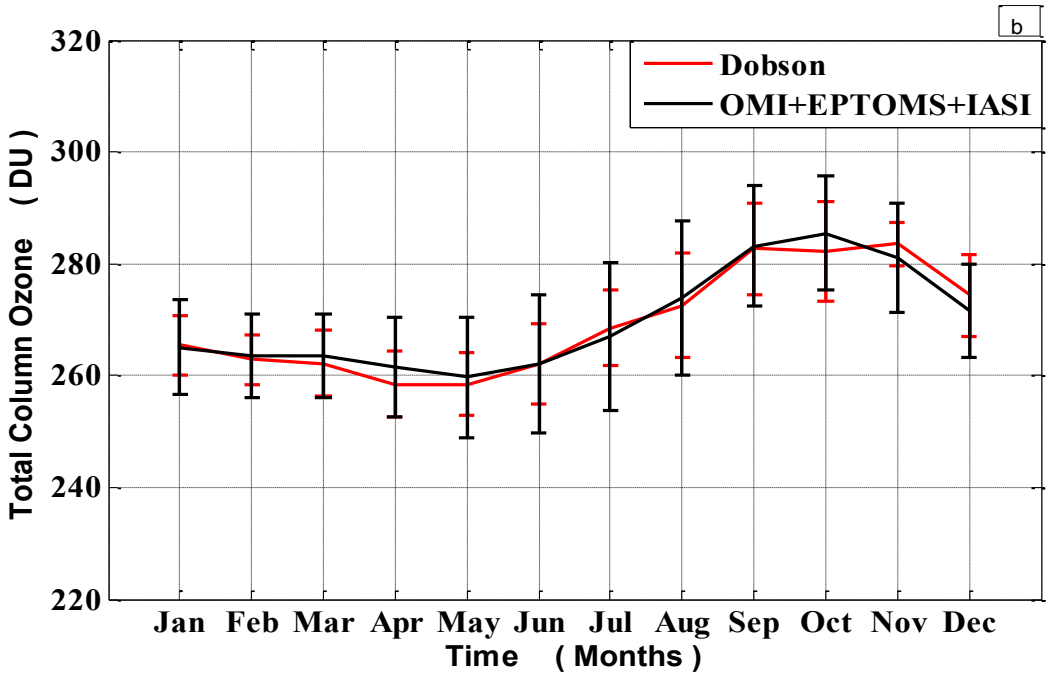

Figure 4.9 Dobson monthly mean ozone variation and standard deviation superimposed with (b) EPTOM, OMI and IASI

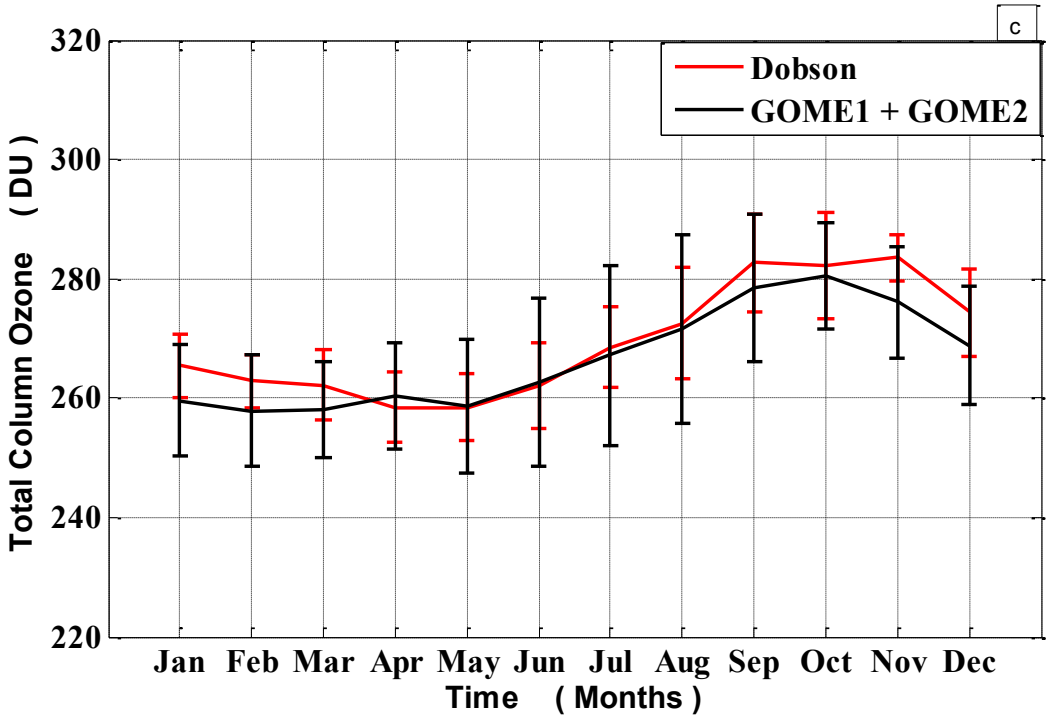

Figure 4.9 Dobson monthly mean ozone variation and standard deviation superimposed with (c) Dobson, GOME-1 and GOME-2

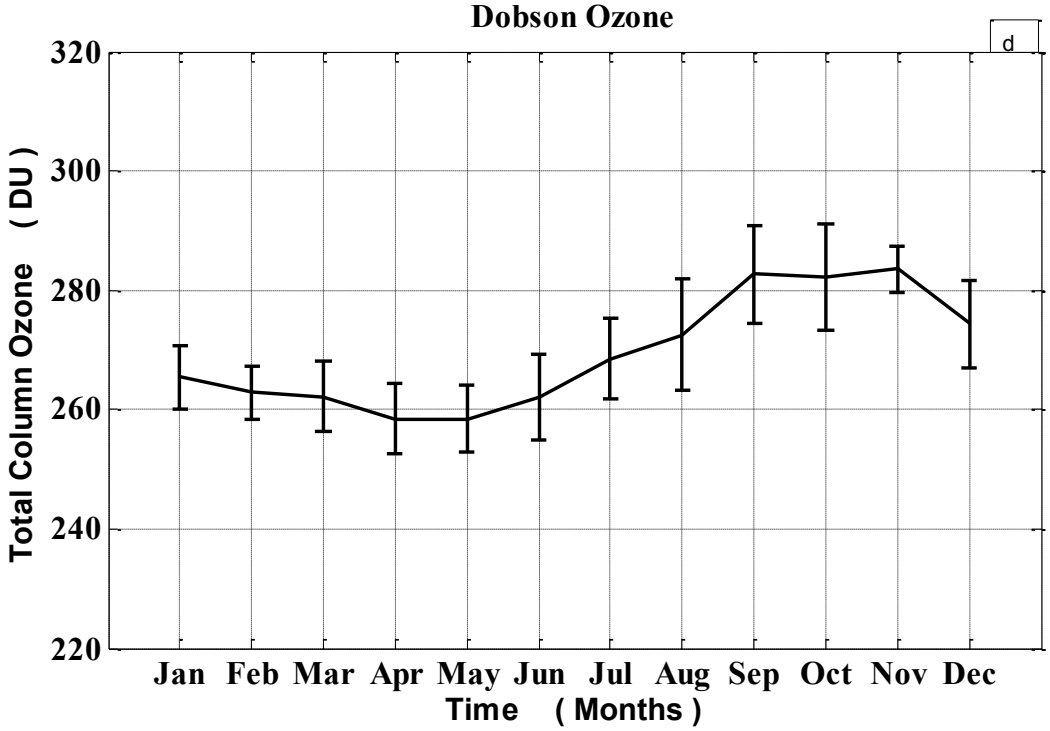

Figure 4.9 Dobson monthly mean ozone variation and standard deviation superimposed with (d) Dobson monthly ozone variation and standard deviation

Instruments	Jan	Feb	Mar	Apr	May	Jun	Jul	Aug	Sep	Oct	Nov	Dec
Dobson	265	263	262	258	257	259	262	273	283	282	284	274
TOMS	267	265	266	247	259	263	272	280	293	297	287	275
GOME-1	260	259	258	261	260	263	267	270	277	278	273	268
EPTOMS	265	263	262	259	259	262	266	273	282	284	280	272
OMI	261	259	260	258	255	258	263	273	281	284	281	270
GOME-2	260	259	258	261	260	263	267	270	277	278	273	268
IASI	266	266	266	265	265	265	268	273	280	280	280	269
Integrated Ozone	255	253	252	251	248	259	268	270	273	274	273	262

Table 4.3. Average monthly ozone for satellite measurements and Dobson instrument for the years

4.2.2.5 Total ozone comparison between integrated ozone and satellite measurements

The monthly mean of SHADOZ and MLS are combined and normalised. The result is then integrated to obtain the column ozone. The monthly mean is presented in table 4.3 along with other satellite measurements. SHADOZ measurements are from 1998 to 2007 while MLS measurements are from 2004 to 2013, so the combined measurements are from 1998 to 2013.the results agree to within ± 10 DU. The result also shows spring time maximum and autumn minimum which is in agreement with the results obtained earlier.

4.3. Geospatial (Latitudinal and Longitudinal) variability of ozone over South Africa

4.3.1 Results

4.3.1.1 Seasonal variations

Ten years of seasonal average is presented in figure 4.10a. The seasonal average was obtained by grouping the data in terms of the four seasons in South Africa irrespective of the years of measurements and then averaged. Monthly ozone variations are from 260 DU to 290 DU for all seasons. For better understanding the monthly variation for winter, the colormap scale is stepped down by 5 DU while those of summer and autumn are further stepped down by 5 DU as shown in figure 4.10b. The result shows maximum total ozone in spring. Spring time ozone has been discussed in earlier chapter. For all seasons, the lower part of South Africa has the highest total ozone. This is expected since ozone concentration is more in higher latitudes than in mid-latitudes and more total ozone in mid-latitudes than in the tropics of both the Northern and Southern Hemispheres (Susan Solomon 1988). This may be one of the reasons for more ozone in lower part of South Africa. As the latitude reduces through north, total ozone also reduces. Diab et al (2004) attributed photochemical reactions, biomass burning, lightning production, and biogenic emissions as some of the reasons for spring maximum over Irene, a South African station. Average spring maximum for lower part corresponds to 290 DU, 285 DU for central part and about 278 DU for upper part. Large photochemical reactions take place in the lower part of South Africa which enhances the ozone level. This ozone is primarily from maritime sources attributed to dominant winds from SE-W (Zunckel et al., 2004). Figure 4.10b shows ozone minimum in autumn corresponding to ~265 DU for lower part but there was no much variation in total ozone for central part and upper part.

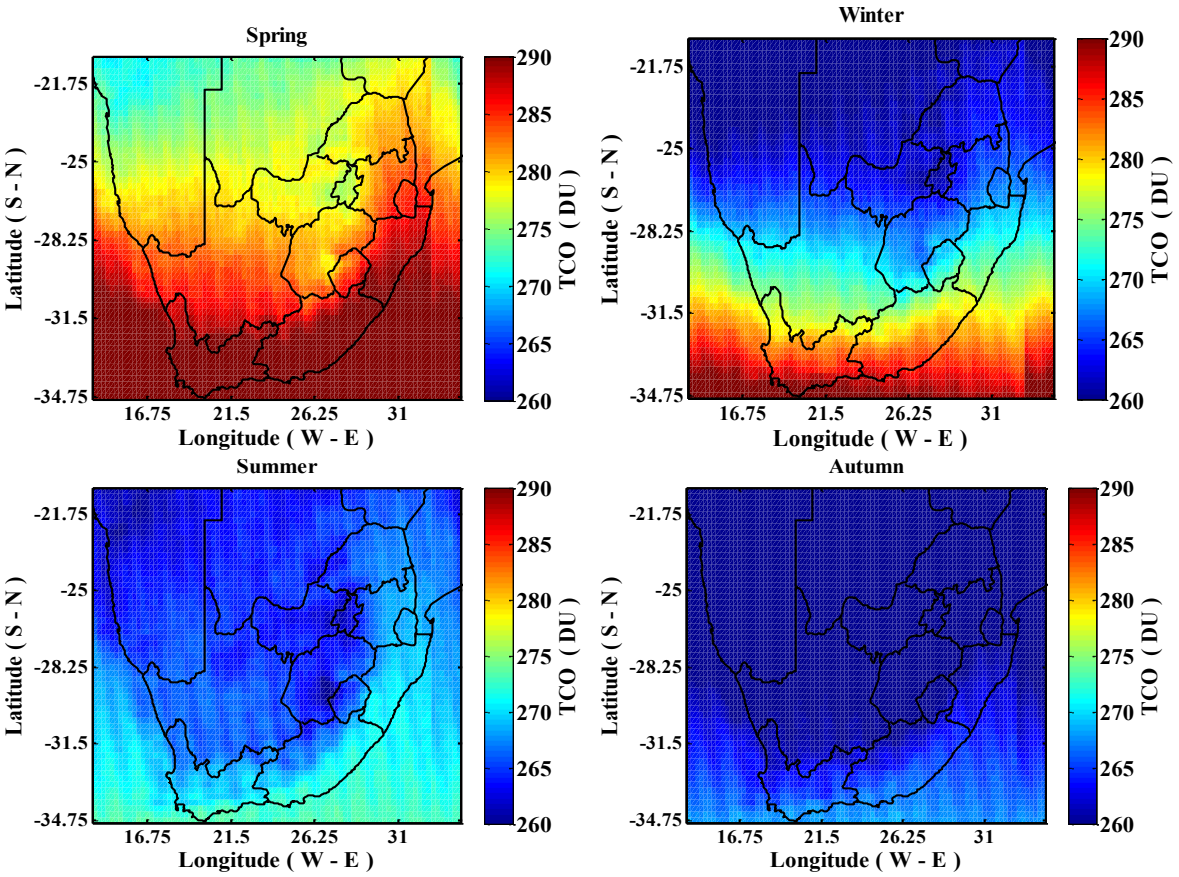

Figure 4.10a. Seasonal variation of ozone over South Africa for (i) spring (ii) winter (iii) summer (iv) autumn

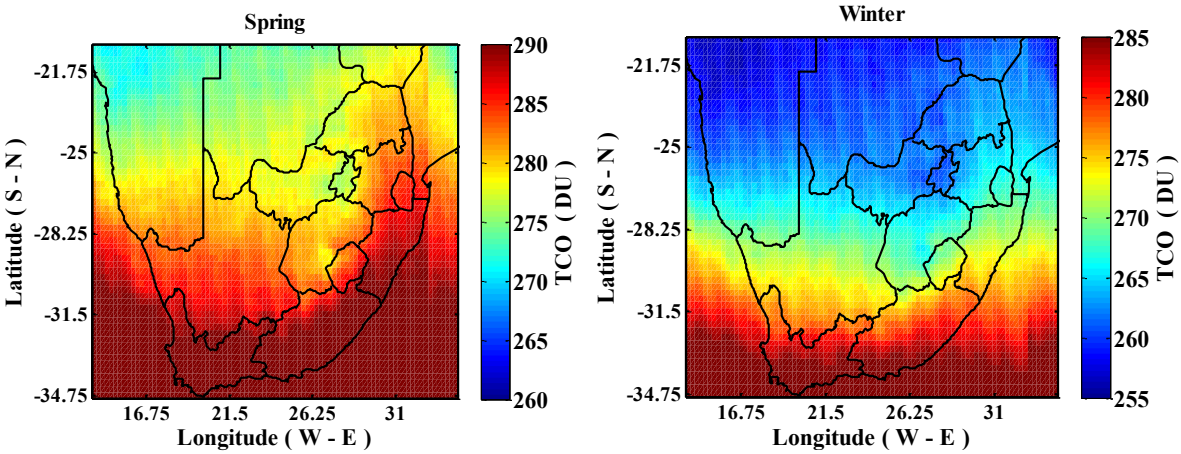

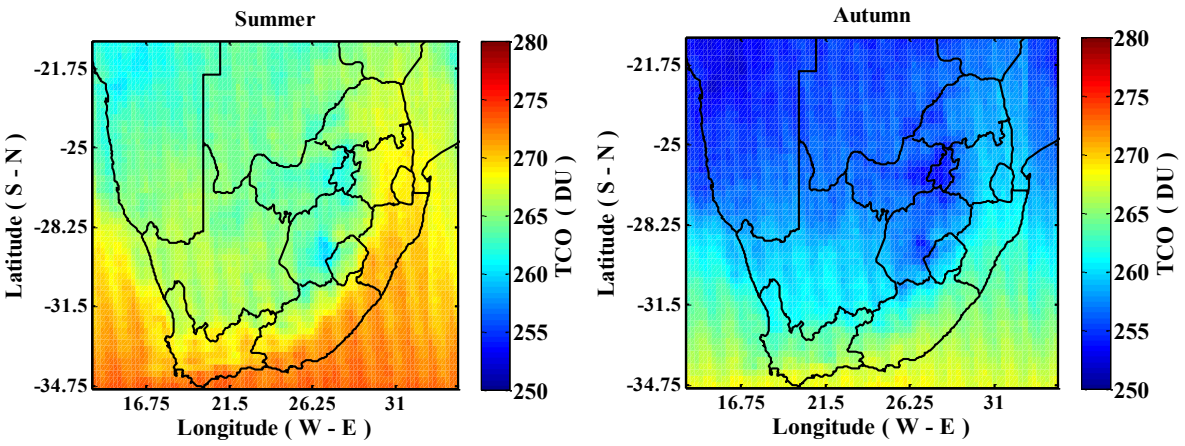

Figure 4.10b. Seasonal variation of ozone over South Africa for (i) spring (ii) winter (iii) summer (iv) autumn (change in colour map scale for better understanding from figure 4.10a).

4.3.1.2 Monthly variation of ozone over South Africa

The monthly ozone distribution was obtained by grouping the datasets into month irrespective of the years and then averaged. All datasets in the lower part, central part and upper part of South Africa were combined individually and their mean was to compare with the results obtained in earlier sections. The monthly variations are from 240 DU to 320 DU as presented in figure 4.11. The result obtained shows that ToZ in the lower part of South Africa corresponds to ~300 DU in during spring while those of the central part and upper parts corresponds to 288 DU and 284 DU respectively. This result is consistent with the result obtained in section two where maximum ToZ over Irene was ~284 DU. Irene is located in the upper part of South Africa. May minimum is observed for measurements in central and upper part of South Africa while for the upper part shows a month early minimum. The wave propagation into the stratosphere when the wind is westerly can be related to the seasonal variation over South Africa.

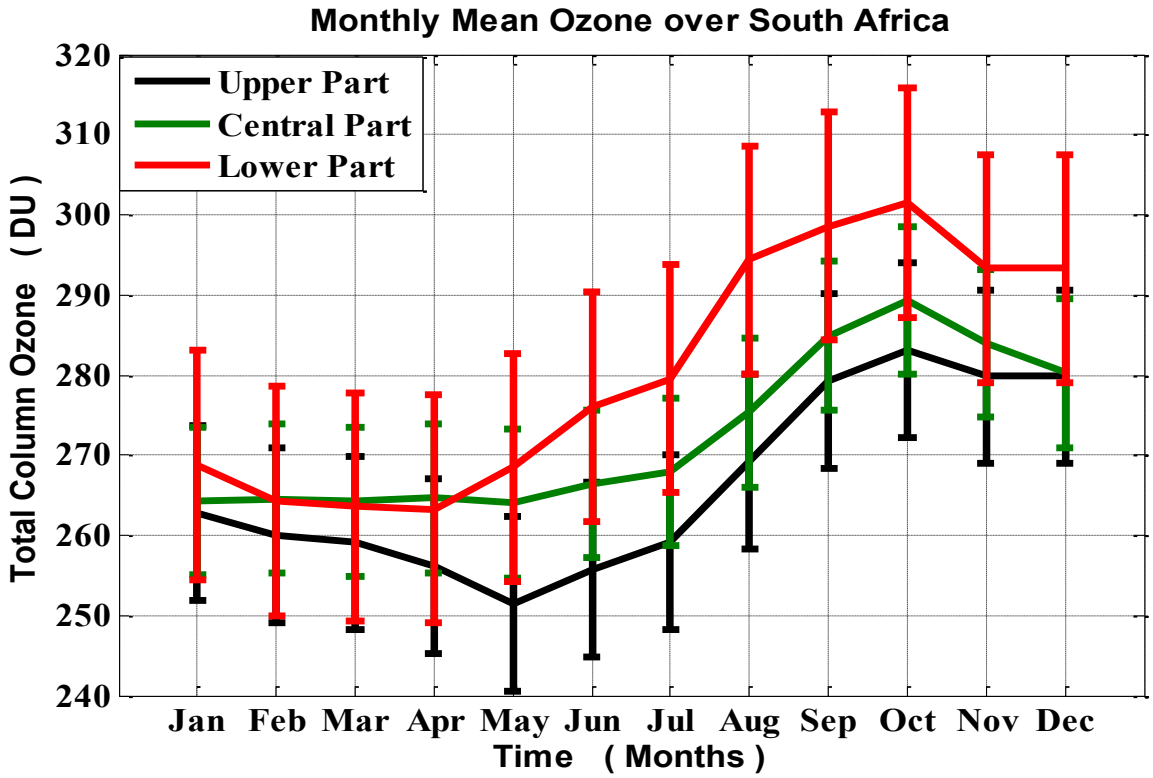

Figure 4.11: Average monthly mean ozone over South Africa

4.3.1.3 Inter-annual variation of total ozone

Figure 4.12 shows ozone variation over South Africa from 2004 to 2013. Overpass data over South Africa was grouped with respect to years and their corresponding mean was determined. The monthly variations are from 255 DU to 285 DU. In section 1, reasons for high ozone observed over Irene compared to other years of recent measurements were discussed. All the results show the same consistency as regards the lower part having the highest total ozone, with central part having more total ozone than upper part. Total ozone in 2006 was quite low compared with other years of measurements with an average of ~265 DU. This low measurement in 2006 has been confirmed by other instruments such as MLS and Ozonesonde profile measurement over one of the South African stations in Irene as discussed in earlier chapters. 2006 also corresponds to the year the largest ozone hole in history was observed. It is evident in all the years of measurements that despite the northern part of South Africa having the lowest ozone concentration, the north eastern part has more ozone concentration than other northern parts of South Africa. This can be due to the pronounced biomass burning in this region leading to higher ozone concentration compared to other northern parts (Clain et al., 2009). The temperature of the Antarctic stratosphere is the major cause of ozone variation from year to year. Temperature and the size of the ozone

hole are inversely proportional as low temperature leads to large ozone hole while warm temperature reduces the size of the ozone hole. The 2013 Antarctic ozone hole was quite larger than 2011 and 2012 and was a little larger than the average ozone hole over the last decade. This resulted in lower total ozone measurement for 2013 compared to 2011 and 2012. 2011 and 2012 have the highest total ozone with values corresponding to ~273 DU in the upper part, ~280 DU in the central part and ~287 DU in the lower part. The 2012 ozone hole is the second smallest in history and the smallest since 2002. This is attributed to warmer temperatures in 2012, thus, high ozone measurements in 2012.

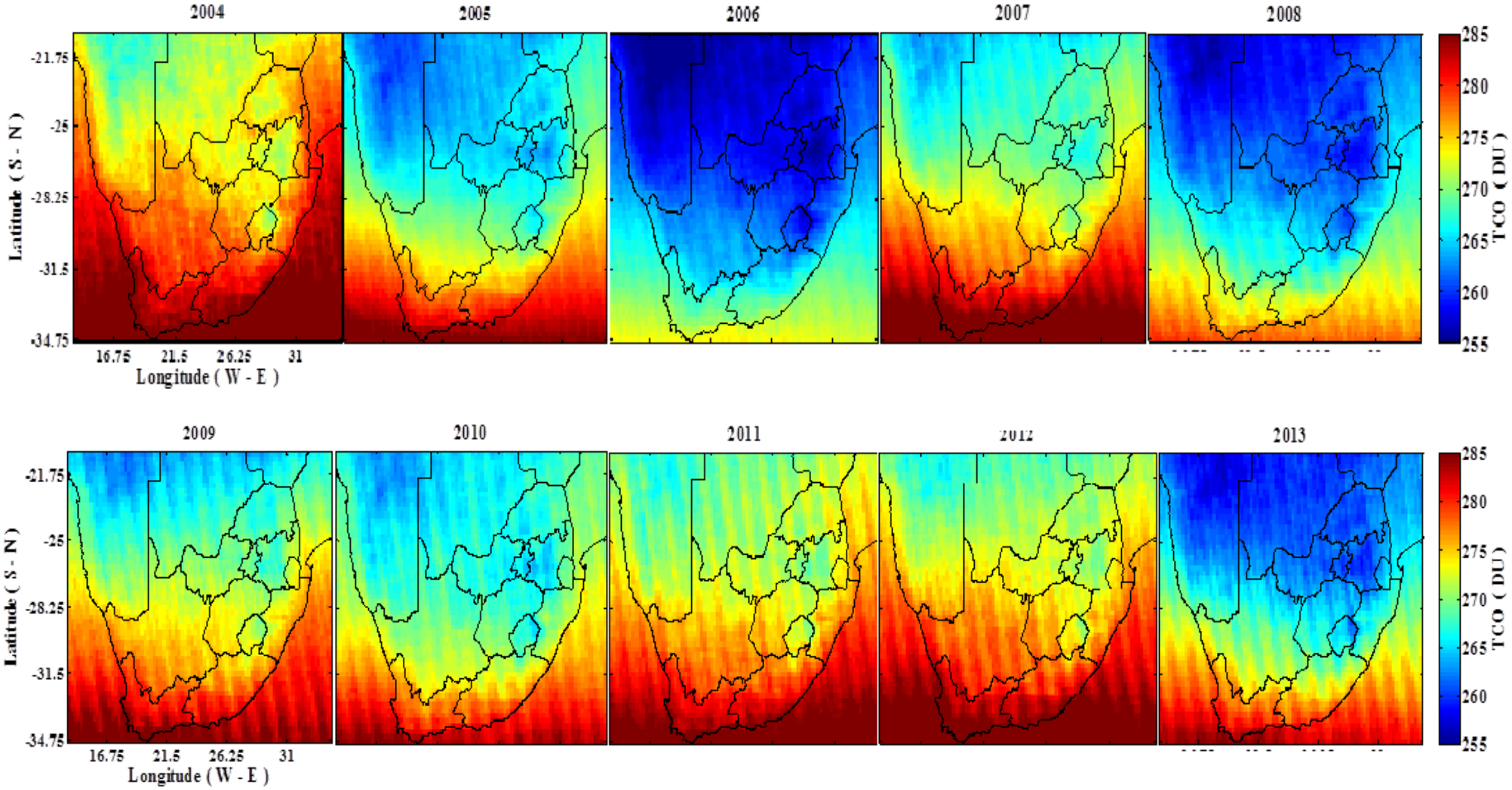

Figure 4.12. Geographical map of South Africa showing yearly distribution of ozone from 2004 to 2013

CHAPTER 5

SUMMARY AND FUTURE STUDIES

Discussion

This research work focused on stratospheric and total column ozone climatology and variability from ground based and satellite observations over Irene from 1978 to 2013 and South Africa from 2004 to 2013. Satellites overpass data from Total Ozone Mapping Spectrometer (TOMS) from November 1978 to May 1993, Earth Probe Total Ozone Mapping Spectrometer (EPTOMS) from January 1997 to December 2005, Global Ozone Monitoring Experiment (GOME-1 and GOME-2) from August 1995 to June 2003 and from January 2007 to December 2013, Ozone Monitoring Instrument (OMI) from October 2004 to December 2013 and the Infrared Atmospheric Sounding Interferometer (IASI) from June 2008 to December 2011 were used for this study and were compared with in situ data from Dobson instrument from 1989 to 2001. Ozonesondes data archived in SHADOZ from 1998 to 2007 were compared with profile measurements from Microwave Limb Sounder (MLS) from 2004 to 2013. TOMS, GOME-1, GOME-2, OMI provided four daily overpass while EPTOMS and IASI had single daily measurements. Dobson data available for this study was the monthly mean measurement while ozonesonde had two monthly measurements.

For stratospheric ozone climatology and variability, ozonesonde and MLS data from 2004 to 2007 were used. The limitation in the years of analysis was attributed to the available data for both years. MLS data was not available between 1998 and 2003 because the satellite had not been launched and ozonesonde data was not available between 2008 and 2012 due to funding problems. These instruments were selected as they provide ozone vertical distribution within the atmosphere. Data obtained from these instruments were in ppmv but were converted to molecules/cm^3 for ozone concentration to be determined. Ozone annual mean from ozonesonde showed an increase in ozone concentration with height till it got to the height region between 22 km and 27 km where ozone maximum concentration is expected (stratospheric maximum). This was replicated for all years of ozonesonde measurements except for 2007 where maximum ozone concentration height stepped down by 1 km to a stratospheric maximum height ranging from 21 km to 26 km. This result of stratospheric ozone maximum in the height region of 22 km to 27 km was also replicated by MLS measurement Ozone seasonal variability from ozonesonde and MLS was also determined by

grouping the data in terms on monthly measurements irrespective of the years of measurements. The result from ozonesonde showed an increase in ozone concentration from $1x10^{12}$ molecules/cm^3 to 2 $x10^{12}$ molecules/cm^3 with an increase in height range between 15 km and 18 km to the height range of 18 km to 21 km. Maximum ozone concentration in the stratospheric maximum was found to be $4.5x10^{12}$ molecules/cm^3. Maximum ozone concentration was found during the spring months (September, October and November) while the minimum was found during autumn months (March, April, May). This seasonal variation is linked with the wave propagation into the stratosphere when the wind is westerly. The monthly standard deviation was also determined as low standard deviation was recorded where maximum ozone concentration was observed. Maximum standard deviation was observed between 17 km and 21 km corresponding to the tropopause height. This may be due to the chemical and dynamical processes taking place in this region. MLS seasonal variation determined was smoother compared to ozonesonde due to its better height resolution. Maximum ozone concentration was found in the height region of 22 km and 28 km corresponding to $4x10^{12}$ molecules/cm^3. These values agree with the global ozone climatology for MLS satellite for 25^oS to 30^oS. Beside this, there is no significant difference between both measurements. The result on the standard deviation between both measurements showed higher standard deviation during spring in lower height region. This may be due to the low accuracy of the instrument at this height region. The difference between ozonesonde measurement and MLS instrument was also obtained. The result showed low difference between the measurements except in the stratospheric height maximum. A difference in the range of $4x10^{11}$ molecules/cm^3 and $8x10^{11}$ molecules/cm^3 was obtained for all seasons.

The vertical distribution and seasonality of tropospheric ozone was also determined using ozonesonde measurements only (this is the only data available for the height region). The result revealed that high surface ozone was likely due to photochemical reactions, biomass burning and anthropogenic activities. This surface ozone however reduced with increasing height as most of them are deposited on the surface while some are titrated by species emmited from the surface. The reduction can also be attributed to part of the ozone having contact with plants and soil. Its seasonal variability reveals maximum concentration during spring and minimum during autumn (May).

Total column ozone overpass from TOMS, EPTOMS, GOME-1, GOME-2, OMI and IASI satellites were compared with Dobson instrument. The yearly ozone variation reveals

significant decrease in column ozone abundant in the atmosphere between the late 1970s and early 1990s. This decrease has been attributed to the ozone hole discovered in 1985 and Mount Pinatubo volcanic eruption in 1992. With varying dynamical processes and transport processes taking place in the atmosphere, ozone values fluctuated within this period. However, column ozone was stable in the late 1990s and early 2000 due to the stability of atmospheric amount of chlorine and bromine as well as the Montreal Protocol which placed a ban on CFC materials being used as revealed from measurements from GOME-1 and EPTOMS. There was however and increase in column ozone over the last decade by ~7 DU to 9 DU measured by OMI, GOME-2 and IASI satellites.

Total column ozone available for these years was divided into three parts with regards to the number of years of overpass. The first was from between 1978 and 1993 where TOMS overpass was used for climatological and variability purposes. The second is between 1995 and 2005 with data from EPTOMS and GOME-1 used while OMI, GOME-2 and IASI were used for the third between 2004 and 2013. TOMS measurements of column ozone were high compared to other satellites. This can be attributed to the years of overpass as some of its measurements had been before the discovery of the ozone hole. Its measurements however showed decreasing trend in column ozone for its 15 years of overpass. GOME-1 measurement was ~5 DU units lower than EPTOMS measurement for all seasons except for late autumn and winter as were similar (although they were within the same standard deviations). They both revealed the well-established spring time ozone maximum and autumn minimum in the southern hemisphere. GOME-2 measurements were lower compared with OMI and IASI measurements but they had a good agreement during spring. IASI measurements were however quite high for the first seven months of the year. This has been attributed to instrumental error as IASI has been found to overestimate ozone in the atmosphere. However, this high ozone measurements are still within the standard deviation obtained for satellites measurements during its overpass.

These satellite measurements were compared with Dobson instrument. The result revealed high correlation between these measurements to within 3 DU for late winter to summer. There measurements were however similar for autumn and early winter. Since GOME-1 and GOME-2 underestimated ozone, there measurements were removed from other satellite measurements and compared. The result showed a better agreement to within 1 DU with Dobson instrument for all seasons. When GOME-1 and GOME-2 measurements were

compared with Dobson, they showed a bias of ~5 DU for all seasons except autumn when it was about 3 DU.

Ozone variability over South Africa was also examined using OMI instrument. The result showed that the lower part of South Africa had higher total ozone compared with different parts of South Africa. Total ozone during spring was maximum over South Africa and it also displayed an autumn minimum. Low ozone was observed in 2006 which was attributed to the large size of the Antarctic ozone hole. This reduced the spring time ozone maximum, which had a resultant effect on total ozone for 2006.

Based on these results, this thesis is summarised below:

Ozone vertical variation

- Irene like other Southern Hemisphere stations agrees with the well-established and documented spring maximum and autumn minimum of both total column ozone and stratospheric ozone.
- The spring maximum can be attributed to biomass burning, its location between two industrialised areas of Johannesburg and Pretoria which is dominated by urban industrial emissions, the use of biofuels (burning of coals for domestic cooking, winter heating) and majorly photochemical sources such as biogenic (microbial and vegetative) emissions, stratospheric injection of ozone rich air and lightning production.
- Maximum ozone concentration obtained from ozonesondes and MLS satellite corresponds to the height region of 22 km and 27 km.
- Ozone concentration at this height region is ~4.5×10^{12} molecules/cm^3.
- Maximum ozone deviation was obtained in the height region of 17 km to 20 km corresponding to the tropopause height where much deviation is expected due to dynamic and chemical processes taking place in that region.
- The monthly temporal variation shows ascending and descending trends in relation to the easterly/westerly QBO phase.
- MLS underestimates ozone on lower altitude regions.

Total column ozone

- TOMS instrument measurement was higher than all other ozone measuring instruments due to its year of overpass as it gives a long term ozone variation

compared to other instruments. Its value was ~10 DU higher than other measurements for the first 10 years of overpass. This can be attributed to the abundance of ozone in the atmosphere before the Mount Pinatubo volcanic eruption in 1991 which caused a major decrease in atmospheric ozone.

- IASI overestimates its measurements by ~7 DU especially during summer and autumn. This can be attributed to the limited number of years of overpass (< 3 years).
- Dobson instrument, EP-TOMS, OMI as well as integrated ozone had the best agreement to ~4 DU in total ozone measurement for all seasons.
- GOME ozone measurement was generally low for all seasons throughout the years of overpass. This is due to the systematic difference of about 2 to 3 % over tropical and equatorial regions and over southern mid-latitudes.
- Total column ozone was uncharacteristically low in May 2002. This unusual decrease has been linked with the isentropic air mass transport over Irene during that period.
- There was also an unusual decrease in total ozone from 285 DU to 275 DU for 2006 and 2008 spring. The reasons for this are yet to be explored.
- Ozone temporal variation reveal significant decrease in total ozone over the last 35 years (before 2000), however, over the last decade, there has been a gradual increase of about 10DU in total ozone as measured by recent instruments such as OMI, IASI and even GOME-2 satellites and confirmed by balloons.
- This gradual increase is attributed to the stability in atmospheric amount of chlorine and bromine. Also, ozone depleting gases such as chlorofluorocarbons are removed from the atmosphere through natural processes.

Ozone variation over South Africa

- The lower part of South Africa has more total ozone compared with the upper part of South Africa. This difference corresponds to ~12 DU.
- Despite the lower values at the upper part of South Africa, the North-eastern part of South Africa has more ozone concentration than other northern part. This is attributed to biomass burning more dominant is the surrounding regions.
- Maximum ozone during spring corresponds to ~290 DU for the lower part of South Africa and ~278 DU for the upper part. Total ozone in the central area during spring is ~285 DU.
- Spring time maximum ozone was more evident in October for all parts of South Africa.

- Autumn minimum recorded over South Africa is ~266 DU in the lower part and ~255 DU in the upper part. Total ozone in the central area during autumn is ~260 DU.
- Autumn minimum was recorded in both the upper and lower part of South Africa in April. The minimum was recorded in the central part of South Africa in May.
- Over the last decade, minimum total ozone recorded was in 2006 attributed to the size of the Antarctic ozone hole (the largest in history) which drastically reduced the spring time maximum of ozone.

This research work has shown the climatological characteristics and variability of both the vertical profile of ozone and total column ozone over Irene. The result showed consistency with the well-established and documented variation over the Southern Hemisphere with spring maximum and autumn minimum. The result also revealed ozone depletion before 1995 of ~10 DU per decade but recent instruments have measured gradual increase in ozone over the last decade. OMI instrument had the best total ozone measurement when compared to other instruments with GOME having the least agreement. IASI instrument was also found to overestimate ozone in the first half of the year. Total ozone over South Africa showed that the lowest part of South Africa had the highest ozone value with the upper part having the least values. The result also reveal low ozone value for 2006 linked with the size of the Antarctic ozone hole being the largest in history.

Recommendations for future studies

- Data in appendix 2 would have to be examined to determine the possible reasons for high and low ozone measurements during the stated dates.
- Low ozone measurement in 2006 over South Africa would be examined to see other possible reasons apart from the Antarctic ozone hole.

Appendix 1A

Ozone Value for Irene

Table A1. Monthly mean (molecules/cm^3)

Height(km)	Jan	Feb	Mar	April	May	June	July	Aug	Sep	Oct	Nov	Dec
1	1.33E+12	1.03E+12	1.08E+12	8.05E+11	8.01E+11	8.52E+11	9.84E+11	9.49E+11	1.11E+12	1.03E+12	1.06E+12	1.13E+12
2	1.26E+12	1.04E+12	1.02E+12	8.36E+11	8.04E+11	8.9E+11	1.04E+12	1.09E+12	1.2E+12	1.15E+12	1.1E+12	1.13E+12
3	1.2E+12	9.38E+11	9.23E+11	7.27E+11	6.95E+11	7.2E+11	9.84E+11	9.82E+11	1.08E+12	1.08E+12	9.78E+11	1.02E+12
4	1.2E+12	9.33E+11	8.49E+11	6.89E+11	6.33E+11	7.32E+11	9.5E+11	8.68E+11	9.45E+11	1.03E+12	9.52E+11	9.54E+11
5	1.21E+12	9.05E+11	8.12E+11	6.44E+11	5.82E+11	7.14E+11	9.11E+11	7.77E+11	8.67E+11	9.73E+11	8.95E+11	8.76E+11
6	1.16E+12	9.17E+11	7.97E+11	6.06E+11	5.5E+11	6.55E+11	8.89E+11	7.04E+11	8.19E+11	8.93E+11	8.16E+11	8.81E+11
7	1.11E+12	8.51E+11	8.02E+11	5.35E+11	4.74E+11	6.08E+11	8.41E+11	7.36E+11	8E+11	8.32E+11	8.14E+11	8.13E+11
8	1.11E+12	8.11E+11	8.08E+11	5.04E+11	4.63E+11	5.76E+11	8.12E+11	6.82E+11	7.73E+11	7.88E+11	7.58E+11	7.62E+11
9	1.08E+12	7.46E+11	7.7E+11	4.56E+11	4.41E+11	5.5E+11	8.06E+11	6.57E+11	7.06E+11	7.8E+11	7.35E+11	7.14E+11
10	7.66E+11	7.07E+11	6.29E+11	6.25E+11	6.05E+11	6.84E+11	6.54E+11	1.05E+12	1.23E+12	1.23E+12	1.18E+12	1.2E+12
11	5.58E+11	5.57E+11	5.1E+11	5.16E+11	4.99E+11	5.89E+11	5.77E+11	9.63E+11	1.05E+12	1.05E+12	9.66E+11	9.58E+11
12	4.83E+11	4.78E+11	4.65E+11	4.76E+11	4.67E+11	5.14E+11	5.42E+11	8.17E+11	9.13E+11	9.45E+11	8.91E+11	8.5E+11
13	4.7E+11	4.13E+11	4E+11	4.36E+11	4.52E+11	4.5E+11	4.99E+11	6.92E+11	8.37E+11	8.52E+11	8.42E+11	8E+11
14	4.37E+11	4.4E+11	4.19E+11	4.46E+11	4.68E+11	5.05E+11	5.33E+11	8.83E+11	9.27E+11	8.95E+11	8.51E+11	7.7E+11
15	4.24E+11	4.73E+11	5.09E+11	4.69E+11	5.34E+11	5.85E+11	5.69E+11	9.9E+11	1.06E+12	9.72E+11	8.68E+11	7.73E+11
16	7.04E+11	6.98E+11	7.07E+11	6.82E+11	8.01E+11	8.4E+11	8.12E+11	1.43E+12	1.69E+12	1.55E+12	1.4E+12	1.26E+12
17	1.01E+12	9.88E+11	9.18E+11	9.63E+11	1.06E+12	1.15E+12	1.22E+12	2.22E+12	2.48E+12	2.4E+12	2.21E+12	1.9E+12
18	1.7E+12	1.68E+12	1.62E+12	1.69E+12	1.81E+12	2.02E+12	2.22E+12	3.57E+12	3.76E+12	3.71E+12	3.55E+12	3.04E+12
19	2.45E+12	2.38E+12	2.36E+12	2.41E+12	2.64E+12	2.99E+12	3.16E+12	4.63E+12	4.86E+12	4.7E+12	4.56E+12	4.09E+12
20	3.14E+12	3.05E+12	3E+12	3.04E+12	3.3E+12	3.75E+12	3.78E+12	5.47E+12	5.74E+12	5.46E+12	5.28E+12	4.96E+12
21	3.56E+12	3.48E+12	3.42E+12	3.48E+12	3.66E+12	4.12E+12	4.04E+12	5.95E+12	6.12E+12	5.87E+12	5.66E+12	5.45E+12
22	3.85E+12	3.81E+12	3.79E+12	3.83E+12	3.86E+12	4.13E+12	3.99E+12	5.94E+12	5.97E+12	5.89E+12	5.78E+12	5.68E+12
23	4.06E+12	4.05E+12	4.08E+12	4.07E+12	3.93E+12	3.96E+12	3.85E+12	5.69E+12	5.67E+12	5.78E+12	5.78E+12	5.82E+12
24	3.98E+12	4.01E+12	4.05E+12	3.97E+12	3.73E+12	3.62E+12	3.6E+12	5.21E+12	5.28E+12	5.49E+12	5.56E+12	5.65E+12

25	3.71E+12	3.77E+12	3.8E+12	3.62E+12	3.39E+12	3.2E+12	3.27E+12	4.6E+12	4.81E+12	5.07E+12	5.19E+12	5.28E+12
26	3.37E+12	3.42E+12	3.44E+12	3.2E+12	3.05E+12	2.86E+12	3E+12	4.12E+12	4.41E+12	4.69E+12	4.82E+12	4.88E+12
27	2.94E+12	2.97E+12	2.94E+12	2.7E+12	2.64E+12	2.51E+12	2.69E+12	3.65E+12	3.94E+12	4.22E+12	4.3E+12	4.35E+12
28	2.74E+12	2.74E+12	2.7E+12	2.49E+12	2.42E+12	2.34E+12	2.47E+12	3.39E+12	3.66E+12	3.93E+12	3.98E+12	4.04E+12
29	2.49E+12	2.47E+12	2.42E+12	2.24E+12	2.18E+12	2.13E+12	2.21E+12	3.09E+12	3.34E+12	3.58E+12	3.61E+12	3.66E+12
30	2.17E+12	2.14E+12	2.09E+12	1.95E+12	1.91E+12	1.89E+12	1.9E+12	2.73E+12	2.96E+12	3.15E+12	3.15E+12	3.17E+12
31	1.92E+12	1.88E+12	1.83E+12	1.73E+12	1.71E+12	1.67E+12	1.65E+12	2.43E+12	2.64E+12	2.77E+12	2.75E+12	2.76E+12
32	1.66E+12	1.63E+12	1.59E+12	1.53E+12	1.52E+12	1.47E+12	1.44E+12	2.15E+12	2.32E+12	2.39E+12	2.36E+12	2.37E+12
33	1.42E+12	1.4E+12	1.37E+12	1.35E+12	1.35E+12	1.29E+12	1.25E+12	1.89E+12	2.01E+12	2.03E+12	1.99E+12	2E+12
34	1.21E+12	1.19E+12	1.18E+12	1.18E+12	1.19E+12	1.14E+12	1.1E+12	1.66E+12	1.73E+12	1.72E+12	1.67E+12	1.68E+12
35	1.01E+12	1E+12	1E+12	1.02E+12	1.03E+12	9.97E+11	9.5E+11	1.42E+12	1.45E+12	1.42E+12	1.36E+12	1.38E+12
36	8.38E+11	8.34E+11	8.46E+11	8.65E+11	8.87E+11	8.7E+11	8.21E+11	1.2E+12	1.19E+12	1.16E+12	1.1E+12	1.12E+12
37	6.89E+11	6.88E+11	7.09E+11	7.3E+11	7.57E+11	7.54E+11	7.08E+11	1E+12	9.72E+11	9.33E+11	8.84E+11	9.05E+11
38	5.67E+11	5.7E+11	5.92E+11	6.1E+11	6.36E+11	6.41E+11	6.04E+11	8.16E+11	7.84E+11	7.48E+11	7.08E+11	7.26E+11
39	4.67E+11	4.72E+11	4.93E+11	5.09E+11	5.34E+11	5.44E+11	5.14E+11	6.65E+11	6.32E+11	6.01E+11	5.68E+11	5.82E+11
40	3.84E+11	3.91E+11	4.1E+11	4.22E+11	4.46E+11	4.58E+11	4.35E+11	5.37E+11	5.07E+11	4.82E+11	4.55E+11	4.64E+11
41	3.22E+11	3.3E+11	3.46E+11	3.54E+11	3.71E+11	3.85E+11	3.69E+11	4.38E+11	4.15E+11	3.96E+11	3.74E+11	3.79E+11
42	2.72E+11	2.8E+11	2.93E+11	2.98E+11	3.1E+11	3.23E+11	3.14E+11	3.59E+11	3.41E+11	3.27E+11	3.09E+11	3.12E+11
43	2.29E+11	2.39E+11	2.48E+11	2.52E+11	2.59E+11	2.71E+11	2.66E+11	2.95E+11	2.8E+11	2.7E+11	2.56E+11	2.57E+11
44	1.97E+11	2.07E+11	2.13E+11	2.15E+11	2.19E+11	2.28E+11	2.27E+11	2.45E+11	2.34E+11	2.27E+11	2.15E+11	2.16E+11
45	1.66E+11	1.75E+11	1.79E+11	1.8E+11	1.84E+11	1.9E+11	1.9E+11	2.02E+11	1.92E+11	1.88E+11	1.78E+11	1.78E+11
46	1.4E+11	1.48E+11	1.48E+11	1.5E+11	1.53E+11	1.57E+11	1.58E+11	1.65E+11	1.57E+11	1.54E+11	1.46E+11	1.46E+11
47	1.15E+11	1.22E+11	1.2E+11	1.21E+11	1.25E+11	1.26E+11	1.28E+11	1.3E+11	1.25E+11	1.22E+11	1.16E+11	1.17E+11
48	9.35E+10	9.75E+10	9.49E+10	9.58E+10	9.91E+10	9.98E+10	1.02E+11	1E+11	9.71E+10	9.44E+10	9.02E+10	9.12E+10
49	7.36E+10	7.53E+10	7.29E+10	7.42E+10	7.61E+10	7.74E+10	8.01E+10	7.43E+10	7.21E+10	7E+10	6.76E+10	6.85E+10
50	6.16E+10	6.14E+10	6.05E+10	6.09E+10	6.27E+10	6.42E+10	6.63E+10	5.95E+10	5.81E+10	5.62E+10	5.5E+10	5.59E+10
51	5.14E+10	5.05E+10	5.01E+10	5.03E+10	5.18E+10	5.33E+10	5.52E+10	4.78E+10	4.69E+10	4.52E+10	4.46E+10	4.54E+10
52	4.3E+10	4.28E+10	4.19E+10	4.27E+10	4.35E+10	4.49E+10	4.67E+10	3.93E+10	3.86E+10	3.74E+10	3.67E+10	3.72E+10
53	3.75E+10	3.7E+10	3.69E+10	3.74E+10	3.89E+10	3.98E+10	4.07E+10	3.43E+10	3.34E+10	3.19E+10	3.2E+10	3.22E+10

54	3.28E+10	3.19E+10	3.3E+10	3.29E+10	3.54E+10	3.57E+10	3.56E+10	3.04E+10	2.93E+10	2.72E+10	2.83E+10	2.82E+10
55	2.65E+10	2.63E+10	2.63E+10	2.73E+10	2.81E+10	2.92E+10	2.93E+10	2.35E+10	2.29E+10	2.22E+10	2.29E+10	2.23E+10
56	2.46E+10	2.47E+10	2.5E+10	2.62E+10	2.68E+10	2.77E+10	2.74E+10	2.16E+10	2.13E+10	2.13E+10	2.16E+10	2.09E+10
57	2.38E+10	2.42E+10	2.52E+10	2.64E+10	2.72E+10	2.75E+10	2.67E+10	2.12E+10	2.1E+10	2.14E+10	2.14E+10	2.07E+10
58	2.31E+10	2.37E+10	2.54E+10	2.66E+10	2.76E+10	2.73E+10	2.61E+10	2.07E+10	2.08E+10	2.16E+10	2.11E+10	2.06E+10
59	2.35E+10	2.4E+10	2.55E+10	2.74E+10	2.85E+10	2.83E+10	2.65E+10	2.12E+10	2.07E+10	2.2E+10	2.12E+10	2.09E+10
60	2.41E+10	2.43E+10	2.55E+10	2.82E+10	2.95E+10	2.95E+10	2.7E+10	2.17E+10	2.06E+10	2.23E+10	2.14E+10	2.12E+10
61	2.46E+10	2.46E+10	2.56E+10	2.9E+10	3.05E+10	3.06E+10	2.76E+10	2.23E+10	2.06E+10	2.27E+10	2.15E+10	2.16E+10
62	2.63E+10	2.45E+10	2.51E+10	2.92E+10	2.88E+10	2.25E+10	2.78E+10	2.25E+10	2.05E+10	1.46E+10	2.2E+10	2.23E+10
63	2.86E+10	2.4E+10	2.43E+10	2.92E+10	2.57E+10	2.15E+10	2.77E+10	2.24E+10	2.05E+10	1.41E+10	2.27E+10	2.31E+10
64	3.09E+10	2.36E+10	2.35E+10	2.91E+10	2.25E+10	2.04E+10	2.77E+10	2.23E+10	2.05E+10	1.36E+10	2.33E+10	2.4E+10
65	4.49E+10	1.43E+10	2.29E+10	9.76E+08	8.18E+09	NaN	NaN	2.06E+10	1.78E+10	9.64E+08	5.11E+10	9.37E+08
66	5.28E+10	1.74E+10	3.32E+10	8.79E+08	1.06E+10	NaN	NaN	1.76E+10	2.04E+10	8.46E+08	6.1E+10	8.04E+08
67	6.06E+10	2.05E+10	4.36E+10	7.82E+08	1.31E+10	NaN	NaN	1.46E+10	2.3E+10	7.27E+08	7.1E+10	6.72E+08
68	6.85E+10	2.36E+10	5.4E+10	6.85E+08	1.56E+10	NaN	NaN	1.16E+10	2.55E+10	6.09E+08	8.09E+10	5.39E+08
69	7.63E+10	2.67E+10	6.44E+10	5.88E+08	1.8E+10	NaN	NaN	8.58E+09	2.81E+10	4.9E+08	9.08E+10	4.07E+08
70	9.51E+10	6.7E+08	NaN	NaN	NaN	NaN	NaN	NaN	NaN	NaN	NaN	3.61E+08

Appendix 1B

Table A2. Standard deviation (molecules/cm^3)

Height(km)	Jan	Feb	Mar	Apr	May	June	July	Aug	Sep	Oct	Nov	Dec
1	7.57E+11	5.13E+11	4.13E+11	2.83E+11	1.9E+11	2.06E+11	4.54E+11	2.47E+11	2.51E+11	2.22E+11	2.73E+11	3.17E+11
2	6.78E+11	4.3E+11	3.42E+11	2.18E+11	1.63E+11	2.51E+11	4.1E+11	2.21E+11	2.46E+11	1.96E+11	1.53E+11	2.88E+11
3	6.5E+11	3.29E+11	3.14E+11	9.86E+10	1.33E+11	1.35E+11	3.21E+11	2.06E+11	2.12E+11	1.94E+11	1.49E+11	2.64E+11
4	6.62E+11	3.42E+11	2.82E+11	1.28E+11	1.33E+11	1.49E+11	3.58E+11	1.41E+11	1.85E+11	1.36E+11	1.54E+11	2.57E+11
5	6.38E+11	3.91E+11	3.54E+11	8.28E+10	1.21E+11	1.49E+11	3.18E+11	1.5E+11	2.27E+11	2.14E+11	1.88E+11	2.38E+11
6	6.74E+11	3.5E+11	3.14E+11	9.02E+10	1.68E+11	1.28E+11	3.19E+11	1.04E+11	2.1E+11	9.6E+10	1.71E+11	2.71E+11
7	7.06E+11	3.48E+11	2.85E+11	1.06E+11	1.33E+11	1.22E+11	2.98E+11	1.09E+11	1.75E+11	1.41E+11	1.38E+11	2.38E+11
8	6.52E+11	3.18E+11	2.63E+11	1.07E+11	9.45E+10	7.89E+10	2.83E+11	1.16E+11	1.16E+11	1.65E+11	1.68E+11	2.78E+11
9	6.64E+11	3.01E+11	2.63E+11	1.06E+11	1.02E+11	7.57E+10	3.13E+11	1.48E+11	9.7E+10	1.41E+11	1.99E+11	2.31E+11
10	1.93E+11	1.94E+11	1.89E+11	1.61E+11	1.68E+11	8.41E+10	8.9E+10	1.56E+11	1.7E+11	1.8E+11	1.86E+11	1.94E+11
11	1.58E+11	1.55E+11	1.61E+11	1.32E+11	1.42E+11	7.43E+10	7.76E+10	1.27E+11	1.63E+11	1.66E+11	1.64E+11	1.55E+11
12	1.35E+11	1.35E+11	1.36E+11	1.15E+11	1.21E+11	6.9E+10	7.01E+10	1.23E+11	1.7E+11	1.53E+11	1.55E+11	1.34E+11
13	1.3E+11	1.16E+11	1.16E+11	1.08E+11	1.2E+11	6.78E+10	6.56E+10	1.38E+11	1.78E+11	1.48E+11	1.43E+11	1.28E+11
141	1.34E+11	1.07E+11	1.16E+11	1.26E+11	1.36E+11	7.61E+10	8.48E+10	1.41E+11	1.96E+11	1.67E+11	1.39E+11	1.24E+11
5	1.53E+11	9.18E+10	1.27E+11	1.43E+11	1.59E+11	9.25E+10	1.12E+11	1.75E+11	2.3E+11	1.86E+11	1.49E+11	1.36E+11
16	1.28E+11	8.88E+10	1.21E+11	1.56E+11	1.81E+11	1.28E+11	1.35E+11	2.68E+11	2.83E+11	2.2E+11	1.72E+11	1.5E+11
17	1.25E+11	1.15E+11	1.28E+11	1.79E+11	1.99E+11	1.64E+11	1.57E+11	3.27E+11	3.01E+11	2.67E+11	2.03E+11	1.74E+11
18	1.33E+11	1.26E+11	1.3E+11	1.71E+11	1.96E+11	1.45E+11	1.77E+11	2.81E+11	2.56E+11	2.55E+11	2.02E+11	1.88E+11
19	1.18E+11	1.15E+11	1.1E+11	1.44E+11	1.8E+11	1.39E+11	1.62E+11	2.29E+11	1.97E+11	1.75E+11	1.71E+11	1.77E+11
20	1.06E+11	9.54E+10	9.89E+10	1.18E+11	1.44E+11	1.51E+11	1.28E+11	2.1E+11	1.46E+11	1.31E+11	1.47E+11	1.55E+11
21	9.17E+10	7.88E+10	9.21E+10	9.99E+10	1.02E+11	1.4E+11	1.11E+11	1.56E+11	1.07E+11	1.1E+11	1.25E+11	1.29E+11
22	7.95E+10	6.84E+10	7.67E+10	8.02E+10	8.5E+10	1.07E+11	9.28E+10	9.91E+10	7.45E+10	7.85E+10	8.75E+10	9.74E+10
23	7.44E+10	6.11E+10	6.45E+10	7.61E+10	1.02E+11	9.01E+10	7.91E+10	9.07E+10	7.1E+10	6.43E+10	7.09E+10	8.72E+10
24	7.16E+10	6.06E+10	7.14E+10	1.02E+11	1.42E+11	9.05E+10	8.84E+10	1.07E+11	8.64E+10	7.58E+10	8.48E+10	9.63E+10
25	7.1E+10	6.6E+10	8.54E+10	1.29E+11	1.79E+11	8.65E+10	1.03E+11	1.18E+11	8.96E+10	8.93E+10	9.72E+10	9.98E+10

26	7.09E+10	6.81E+10	8.62E+10	1.3E+11	1.88E+11	8.3E+10	1.08E+11	1.18E+11	9.09E+10	9.36E+10	1E+11	9.76E+10
27	6.51E+10	6.56E+10	7.79E+10	1.14E+11	1.66E+11	8.4E+10	1.02E+11	1.02E+11	9.3E+10	8.68E+10	8.99E+10	8.8E+10
28	6.19E+10	6.41E+10	7.62E+10	1.05E+11	1.48E+11	8.12E+10	9.66E+10	9.36E+10	9.2E+10	8E+10	7.93E+10	8.41E+10
29	5.79E+10	5.93E+10	7.15E+10	9.15E+10	1.26E+11	7.5E+10	8.86E+10	8.35E+10	8.73E+10	7.23E+10	6.73E+10	7.71E+10
30	5.34E+10	5.01E+10	6.21E+10	7.22E+10	9.84E+10	6.35E+10	7.66E+10	7.12E+10	7.66E+10	6.33E+10	5.37E+10	6.54E+10
31	5.21E+10	4.75E+10	5.36E+10	6E+10	7.45E+10	5.37E+10	6.12E+10	6.12E+10	6.34E+10	5.32E+10	4.5E+10	5.44E+10
32	5.05E+10	4.45E+10	4.38E+10	4.9E+10	5.46E+10	4.56E+10	4.68E+10	5.37E+10	5.06E+10	4.44E+10	3.83E+10	4.58E+10
33	4.82E+10	4.11E+10	3.54E+10	3.96E+10	3.95E+10	3.9E+10	3.5E+10	4.78E+10	4.01E+10	3.73E+10	3.37E+10	3.9E+10
34	4.44E+10	3.69E+10	3.06E+10	3.28E+10	3.11E+10	3.4E+10	2.75E+10	4.31E+10	3.39E+10	3.29E+10	3.14E+10	3.43E+10
35	4.02E+10	3.27E+10	2.77E+10	2.74E+10	2.79E+10	3.19E+10	2.47E+10	3.77E+10	3.33E+10	3.08E+10	2.99E+10	3.17E+10
36	3.53E+10	2.81E+10	2.53E+10	2.37E+10	2.81E+10	3.11E+10	2.3E+10	3.31E+10	3.28E+10	2.84E+10	2.76E+10	2.91E+10
37	2.97E+10	2.37E+10	2.31E+10	2.14E+10	3.01E+10	3.08E+10	2.2E+10	2.93E+10	3.17E+10	2.54E+10	2.47E+10	2.63E+10
38	2.42E+10	2.02E+10	2.07E+10	2.02E+10	3.08E+10	2.97E+10	2.14E+10	2.69E+10	2.86E+10	2.19E+10	2.11E+10	2.24E+10
39	1.97E+10	1.75E+10	1.82E+10	1.91E+10	2.98E+10	2.81E+10	2.06E+10	2.43E+10	2.5E+10	1.88E+10	1.79E+10	1.89E+10
40	1.61E+10	1.52E+10	1.59E+10	1.75E+10	2.76E+10	2.6E+10	1.95E+10	2.18E+10	2.12E+10	1.6E+10	1.5E+10	1.59E+10
41	1.36E+10	1.34E+10	1.38E+10	1.5E+10	2.41E+10	2.34E+10	1.79E+10	1.94E+10	1.75E+10	1.36E+10	1.26E+10	1.35E+10
42	1.23E+10	1.27E+10	1.24E+10	1.28E+10	2.04E+10	2.07E+10	1.66E+10	1.71E+10	1.5E+10	1.22E+10	1.12E+10	1.19E+10
43	1.16E+10	1.24E+10	1.14E+10	1.11E+10	1.69E+10	1.81E+10	1.54E+10	1.51E+10	1.34E+10	1.12E+10	1.03E+10	1.08E+10
44	1.15E+10	1.26E+10	1.09E+10	9.9E+09	1.37E+10	1.59E+10	1.46E+10	1.37E+10	1.27E+10	1.06E+10	9.83E+09	1.03E+10
45	1.17E+10	1.27E+10	1.05E+10	9.34E+09	1.15E+10	1.38E+10	1.35E+10	1.28E+10	1.23E+10	9.69E+09	9.18E+09	1.03E+10
46	1.22E+10	1.29E+10	1.07E+10	9.73E+09	1.09E+10	1.25E+10	1.28E+10	1.25E+10	1.19E+10	9.7E+09	9.33E+09	1.06E+10
47	1.27E+10	1.31E+10	1.1E+10	1.05E+10	1.08E+10	1.16E+10	1.24E+10	1.25E+10	1.15E+10	1.01E+10	9.81E+09	1.11E+10
48	1.21E+10	1.22E+10	1.05E+10	1.03E+10	1.03E+10	1.1E+10	1.15E+10	1.16E+10	1.06E+10	9.81E+09	9.49E+09	1.05E+10
49	1.08E+10	1.05E+10	9.31E+09	9.44E+09	9.38E+09	1.05E+10	1.03E+10	1.01E+10	9.45E+09	9.09E+09	8.67E+09	9.22E+09
50	9.92E+09	9.86E+09	9.21E+09	9.2E+09	9.38E+09	1E+10	1E+10	9.51E+09	9.16E+09	9.04E+09	8.91E+09	8.97E+09
51	9.67E+09	9.68E+09	9.53E+09	9.45E+09	9.64E+09	1.01E+10	1.03E+10	9.46E+09	9.38E+09	9.34E+09	9.48E+09	9.19E+09
52	1.01E+10	1E+10	1.03E+10	1.02E+10	1.02E+10	1.09E+10	1.11E+10	1E+10	1.01E+10	1E+10	1.04E+10	9.93E+09
53	1.12E+10	1.14E+10	1.16E+10	1.16E+10	1.16E+10	1.24E+10	1.25E+10	1.13E+10	1.15E+10	1.15E+10	1.2E+10	1.15E+10
54	1.27E+10	1.31E+10	1.32E+10	1.31E+10	1.34E+10	1.42E+10	1.4E+10	1.29E+10	1.31E+10	1.32E+10	1.38E+10	1.33E+10

55	1.53E+10	1.48E+10	1.49E+10	1.51E+10	1.49E+10	1.62E+10	1.63E+10	1.49E+10	1.47E+10	1.47E+10	1.5E+10	1.52E+10
56	1.64E+10	1.6E+10	1.63E+10	1.63E+10	1.64E+10	1.82E+10	1.81E+10	1.65E+10	1.64E+10	1.61E+10	1.65E+10	1.65E+10
57	1.72E+10	1.72E+10	1.76E+10	1.74E+10	1.78E+10	2.02E+10	1.97E+10	1.79E+10	1.8E+10	1.75E+10	1.82E+10	1.76E+10
58	1.8E+10	1.84E+10	1.89E+10	1.84E+10	1.93E+10	2.22E+10	2.13E+10	1.93E+10	1.96E+10	1.88E+10	1.98E+10	1.87E+10
59	1.95E+10	1.95E+10	2E+10	2E+10	2.08E+10	2.35E+10	2.27E+10	2.07E+10	2.07E+10	2.02E+10	2.1E+10	1.97E+10
60	2.1E+10	2.06E+10	2.1E+10	2.17E+10	2.24E+10	2.47E+10	2.4E+10	2.22E+10	2.16E+10	2.17E+10	2.22E+10	2.07E+10
61	2.26E+10	2.17E+10	2.2E+10	2.33E+10	2.4E+10	2.59E+10	2.53E+10	2.36E+10	2.26E+10	2.31E+10	2.33E+10	2.18E+10
62	2.29E+10	2.26E+10	2.32E+10	2.32E+10	2.3E+10	2.5E+10	2.54E+10	2.45E+10	2.41E+10	2.27E+10	2.34E+10	2.21E+10
63	2.27E+10	2.35E+10	2.46E+10	2.43E+10	2.3E+10	2.51E+10	2.61E+10	2.52E+10	2.59E+10	2.35E+10	2.3E+10	2.19E+10
64	2.24E+10	2.43E+10	2.6E+10	2.53E+10	2.29E+10	2.51E+10	2.68E+10	2.58E+10	2.78E+10	2.43E+10	2.26E+10	2.18E+10
65	1.84E+10	1.29E+10	2.31E+10	1.46E+10	5.26E+08	3.87E+10	NaN	2.01E+10	1.22E+10	2.33E+10	2.33E+10	4.76E+08
66	1.45E+10	1.28E+10	2.07E+10	1.14E+10	4.24E+08	2.99E+10	NaN	1.56E+10	1.4E+10	1.98E+10	2.73E+10	6.08E+09
67	1.06E+10	1.26E+10	1.82E+10	8.11E+09	3.22E+08	2.12E+10	NaN	1.1E+10	1.59E+10	1.62E+10	3.12E+10	1.17E+10
68	6.69E+09	1.25E+10	1.58E+10	4.85E+09	2.2E+08	1.24E+10	NaN	6.47E+09	1.77E+10	1.27E+10	3.52E+10	1.73E+10
69	2.78E+09	1.23E+10	1.33E+10	1.59E+09	1.18E+08	3.68E+09	NaN	1.92E+09	1.96E+10	9.15E+09	3.92E+10	2.29E+10
70	NaN	NaN	NaN	NaN	NaN	NaN	NaN	NaN	NaN	NaN	NaN	NaN

Appendix

Days of anomalies and instruments

DAYS	GOME-1	EPTOMS	OMI	GOME-2	IASI
23/08/1995	XX				
24/08/1995	XX				
05/09/1995	XX				
05/10/1995	XX				
26/10/1995	XX				
25/01/1996	XX				
26/01/1996	XX				
17/06/1996	XX				
21/06/1996	XX				
25/09/1996	XX				
26/09/1996	XX				
27/09.1996	XX				
28/09/1996	XX				
17/10/1996	XX				
18/10/1996	XX				
19/10/1996	XX				
21/10/1996	XX				
03/11/1996	XX				
04/11/1996	XX				

22/04/1997	XX	
13/09/1997	XX	
27/07/1998	XX	
10/08/1998	XX	
01/09/1998	XX	
11/10/1998	XX	
18/10/1998	XX	
25/10/1998		XX
16/06/1999	XX	
11/09/1999	XX	
12/09/1999	XX	
31/10/1999	XX	
07/11/1999		XX
15/08/2000	XX	
16/08/2000	XX	
17/08/2000	XX	
28/08/2000	XX	
29/08/2000	XX	
30/08/2000	XX	
31/08/2000	XX	
01/09/2000	XX	
25/09/2000	XX	

26/09/2000	XX	
27/09/2000	XX	
11/10/2000		XX
15/10/2000		XX
15/11/2000		XX
28/12/2000		XX
24/07/2001	XX	
22/09/2001	XX	
14/10/2001	XX	
17/10/2001	XX	
23/11/2001		XX
05/01/2002		XX
06/01/2002		XX
15/05/2002	XX	
05/09/2002	XX	
05/09/2002	XX	
06/09/2002	XX	
10/9/2002	XX	
11/09/2002	XX	
15/11/2002		XX
23/12/2002		XX
16/10/2003		XX

04/11/2004	XX		
05/11/2004	XX		
08/12/2004	XX		
07/12/2005	XX		
08/12/2005	XX		
08/06/2006		XX	
12/06/2006		XX	
22/06/2006		XX	
26/06/2007			XX
17/08/2007		XX	XX
18/08/2007		XX	XX
19/08/2007			XX
30/08/2007			XX
27/09/2007			XX
13/10/2007			XX
14/10/2007			XX
14/11/2007			XX
29/01/2009			XX
18/07/2009		XX	
24/07/2009		XX	XX
25/07/2009		XX	XX
26/07/2009		XX	XX

01/08/2009	XX	XX	
02/08/2009	XX	XX	
20/08/2009	XX	XX	XX
21/08/2009	XX	XX	XX
24/08/2009	XX		
26/08/2009		XX	
24/09/2009		XX	
25/09/2009	XX	XX	
26/09/2009	XX	XX	
27/09/2009	XX		
04/10/2009			XX
17/10/2009	XX	XX	
18/10/2009	XX		
28/10/2009	XX		
29/10/2009	XX		
30/10/2009	XX		
20/11/2009	XX	XX	
24/04/2010		XX	
20/10/2010			XX
02/11/2010	XX		
03/11/2010	XX		
17/11/2010	XX		

15/08/2011	XX	XX	
16/08/2011	XX	XX	
06/09/2011			XX
07/09/2011	XX		XX
08/09/2011			XX
09/09/2011			XX
19/09/2011			XX
12/10/2011	XX		XX
25/10/2011	XX		
26/10/2011	XX		
02/11/2011	XX	XX	XX
06/08/2012	XX		
07/08/2012	XX	XX	
08/08/2012	XX	XX	
09/08/2012	XX	XX	
06/09/2012	XX	XX	
07/09/2012	XX	XX	
22/09/2012		XX	
23/09/2012		XX	
24/09/2012		XX	
08/11/2012		XX	
30/09/2013		XX	

References

Antón, M., D. Loyola, C. Clerbaux, M. López, J.M. Vilaplana, M. Bañón, J. Hadji-Lazaro, P. Valks, N. Hao, W. Zimmer, P.F. Coheur, D. Hurtmans and L. Alados-Arboledas (2011), Validation of the MetOP-A Total Ozone Data from GOME-2 and IASI Using Reference Ground-Based Measurements at the Iberian Peninsula, *Remote Sensing Environment 115 (2011), 1380 - 1386*

Anton, M., M.E. Koulouli, M. Kroon, R.D. McPeters, G.J. Labow, D. Balis and A. Serrano (2010), Global validation of empirically corrected EP-Total Ozone Mapping Spectrometer (TOMS) total ozone column using Brewer and Dobson ground-based spectrometer, *J. Geophys. Res,. 112, JD006823*

Balis, D., M. Kroon, M.E. Koukouli, E.J. Brinksma, G. Labow, J.P. Veefkind and R.D. McPeters (2007), Validation of Ozone Monitoring Instrument total ozone column measurements using Brewer and Dobson ground-based spectrometer, *J. Geophys. Res., 112, JD008796*

Barnes, R.A., A.R. Bandy and A.L. Torres (1985), Electrochemical Concentration Cell Ozonesonde Accuracy and Precision, *J. Geophys. Res.,90, 7881-7887*

Bhartia et al (1984), Intercomparison of the Nimbus 7 SBUV/TOMS Total Ozone Data with Dobson and M83 Results. *Jour. Geophys. Res.Vol 89, pp. 5239-5247*

Bodeker, G.E., H. Garny, D. Smale, M. Dameris and R. Deckert (2007), The 1985 Southern Hemisphere Mid-Latitude Total Column Ozone Anomaly, *Atmos.Chem.Phys.Discuss.,7, 7137-7169*

Bodeker, G.E., J.C.Scott, K.Kresher and R.L. McKenzie (2001), Global Ozone Trends in Potential Vorticity Coordinates Using TOMS and GOME Inter-Compared Against the Dobson Network *J. Geophys. Res., 106, 23029-23042*

Bojkov R., M. Bishop, W.J. Hill, G.C. Reinsel and G.C. Tiao (1990), A statistical Trend Analysis of Revised Dobson Total Ozone Data Over the Northern Hemisphere, *J. Geophys. Res., Vol.95, pp. 9785-9807*

Bonawentura Rajewska-Wiech, Malgorzata Bialek and Janusz W. Krzyscin (2006), Quality Control of Belsk's Spectrometer: Comparison with the European Sub-Standard Dobson

Spectrophotometer and Satellite (OMI) Overpass, *Publs.inst.Geophys.Pol.Acadosc., D-67(382)*

Boynard, A., C. Clerbaux, P.E. Coheur, D. Hurtmans, S. Turquety, J. Hadji-Lazaro, C. Keim and J. Meyer-Arnek (2009), Measurements of Total and Tropospheric Ozone from IASI: Comparison with Correlative Satellite, Ground-Based and Ozonesonde Observation. *Atmos. Chem. Phys. 9, 6225 – 6271*

Bramstedt, K., J. Gleason, D. Loyola, W. Thomas, A. Bracher, M. Weber and J.P. Burrows (2003), Comparison of Total Ozone from the Satellite Instruments GOME and TOMS with Measurements from Dobson Network 1996 – 2000, *Atmos. Chem., 3, 1409 – 1419*

Browell V. Edward (2003), Large Scale Ozone and Aerosol Distributions, Air Mass Characteristics and Ozone Fluxes Over the Western Pacific Ocean in Late Winter/ Early Spring, *J. Geophys. Res., Vol.108, No. D20,8805 JD003290*

Cai W. (2006), Antarctic Ozone Depletion Causes an Intensification of the Southern Ocean Super-Gyre Circulation, *J. Geophys. Res., Vol.33 GL024911*

Calkins John and Thorunn Thordardottir (1980) The Ecological Significance of Solar UV Radiation on Aquatic Organisms, *Nature 283, 563-566*

Chan E. and Vet (2010), Baselie Levels and Trend of Ground Level Ozone in Canada and the United States, *Atmos. Chem. Phys., 10, 8629-8647*

Chandra S., C. Varotsos and L.E. Flynn (1996), The Mid-Latitude Total Ozone Trend in the Northern Hemisphere, *Geophysical Research Letters, Vol. 23, No. 5, pp. 555-558*

Charles Welch (2014), The Ozone Hole, http://www.theozonehole.com/contactus.htm

Clain, G., J.L. Baray, R. Delmas, R. Diab, J. Leclair de Bellevue, P. Keckhut, F. Posny, J.M. Metzger and J.P. Cammas (2009), Tropospheric Ozone Climatology at two Southern Hemisphere Tropical/Subtropical Sites (Reunion Island and Irene, South Africa) from Ozonesondes, LIDAR and In-Situ Measurements, *Atmos.Chem.Phys.,9,1723-1734*

Clarisse, L., P. F. Coheur, A. J. Prata, D. Hurtmans, A. Razavi, T. Phulpin, J. Hadji-Lazaro, and C. Clerbaux (2004) Tracking and quantifying volcanic SO2 with IASI, the September 2007 eruption at Jebel at Tair, *Atmos. Chem. Phys., 8, 7723–7734*

Coetzee Gerrie, Casper Labuschagne, Anne Thompson, Gregor Geig (2012), Ozone Measurements over South Africa

DeCaria J. Alex, Kenneth E. Pickering, Georgiy L. Stenchikov, Lesley E. Ott (2012) Lightning-generated NO_X and its impact on tropospheric ozone production: A three-dimensional modeling study of a Stratosphere-Troposphere Experiment: Radiation, Aerosols and Ozone (STERAO-A) thunderstorm, *Journal of Geophysical Research: Atmospheres (1984–2012) Vol. 110,D14*

Damiani, A., P. Diego, M. Laurenza, M. Storini, C. Rfanelli (2009), Ozone variability related to SEP events occurring during solar cycle no23. *Ad. Space Res, 43, 28-40*

David W.J. Thompson and Susan Solomon (2002), Interpretation of Recent Southern Hemisphere Climate Change, *Science 296, doi:10.1126/science.1069270*

De Laat, A.T.J. and M. VanWeele (2011), The 2010 Antarctic Ozone Hole: Observed reduction in ozone destruction by minor sudden stratospheric warnings, *Atmos. Sc. Earth and Environ Sc.*

Diab, R.D , A.M. Thompson, M. Zunckel, G.J.R. Coetzee, J. Combrink, G.E. Bodeker, J. Fishman, F. Sokolic, D.P. McNamara, C.B. Archer and D. Nganga (1996), Vertical Ozone Distribution Over Southern African and Adjacent Oceans During SAFARI-92, *J. Geophys. Res.,Vol 101, D19, pp 23823-23833*

Diab, R.D., A. Raghunandan, A.M. Thompson and V. Thouret (2003), Classification of Tropospheric Ozone Profile over Johannesburg based on mosaic aircraft data, *Atmos. Chem. Phys., 3, 713-72*

Diab, R.D., A.M. Thompson, K. Mari, L. Ramsay and G.J.R. Coetzee (2004), Tropospheric ozone climatology over Irene, South Africa from 1990 to 1994 and 1998 to 2000, *J. Geophys. Res., 109, JD00479*

Dobber R. Marcel, Ruud J. Dirksen, Pieternel F. Levelt, G.H.J. van den Oord, Robert H.M. Voors, Quintus Kleipool, Glen Jaross, Matthew Kowalewski, Ernest Hilsenrath, Gilbert W. Leppelmeier, Johan de Vries, Werner Dierssen and Nico C. Rozemeijer (2006), Ozone Monitoring Instrument Calibration, *IEEE Transaction on Geoscience Remote Sensing, Vol. 44, No5*

Dufour, G., M. Eremenko, A. Griesfeller, B. Barret, E. Leflochmoen, C. Clerbaux, J. Hadji-Lazaro, P.-F. Coheur and D. Hurtmans (2012), Validation of Three Different Scientific Products Retrieved From IASI Spectra Using Ozonesondes, *Atmos. Meas. Tech., 5, 611-630*

Drew T. Shindell, Gavin A. Schmidt, Ron L. Miller and David Rind (2001), Northern Hemisphere Winter Climate Response to Greenhouse Gas, Ozone, Solar, and Volcanic Forcing, *J. Geophys. Res., Vol.106, pp. 7193-7210*

Drew T. Shindell and Gavin A. Schmidt (2004), Southern Hemisphere Climate Response to Ozone Changes and Green House Gases, *Geophysical Research Letters, Vol. 31, doi:10.1029/2004GL020724*

Edward V. Browell et al (2003), Large Scale Ozone and Aerosol Distributions, Air Mass Characteristics and Ozone Fluxes Over the Western Pacific Ocean in Late Winter/ Early Spring, *J. Geophys. Res., Vol.108, No. D20,8805 JD003290*

Fahey W. David and Michaela I. Heggling (2010), Twenty Questions and Answers about the Ozone Layer: 2010 Update, *Q10*

Fiotetov, V.E., J.B. Kerr and E.W.Hare (1999), An assessment of the world ground-based total ozone network performance from the comparison with satellite data, *J. Geophys. Res., 104, 1737-1747*

Fiotetov, V.E., G.E. Bodeker, A.J. Miller, R.D. McPeters and R. Stolanski (2002), Global and zonal variations estimated from ground-based and satellite measurements: 1964-2000, *J. Geophys. Res.,* 107, JD001350

Fiotetov, V.E., G. Labow, R. Evans, E.W. Hare, U. Kohler, C.T. McElroy, K. Miyagawa, A. Redondas, V. Savastiouk, A.M Shalamyansky, J. Staehelin, K. Vanicek and M. Weber (2008), Performance of the Ground-Based Total Ozone Network Assessed Using Satellite Data. *J. Geophys. Res., 113 D14313, JD00980*

Gareth J. Marshall et al (2004), Causes of Exceptional Atmospheric Circulation Changes in the Southern Hemisphere, *Geophysical Research Letters, Vol. 31, doi:10.1029/2004GL019952*

Gauss, M., G. Myhre, G. Pitari, M. J. Prather, I. S. A. Isaksen, T. K. Berntsen, G. P. Brasseur, F. J. Dentener, R. G. Derwent, D. A. Hauglustaine, L. W. Horowitz, D. J. Jacob, M. Johnson, K. S. Law, L. J. Mickley, J.-F. Muller, P.-H. Plantevin, J. A. Pyle, H. L. Rogers, D. S. Stevenson, J. K. Sundet, M. van Weele and O. Wild (2003), Radiative Forcing in the 21st Century Due to Ozone Changes in the Troposphere and Lower Stratosphere, *J. Geophys. Res., Vol 108, No. D9, 4292, JD002624*

Gleanson, J.F., P.K. Bhartia, J.R. Herman, R. McPeters, P. Newman, R.S. Stolarski, L. Flynn, G. Labow, D. Larko, C. Seftor, C. Wellemeyer, W.D. Komhyr, A.J. Miller and W. Planet (1993), Record Low Global Ozone in 1992, *Science, vol. 260, no. 5107, pp. 523-526*

Gregory, C.R., G.T. Tiao, D.J. Wubbles, J.B. Kerr, A.J. Miller, R.M. Nagatani, L. Bishop and L.H. Ying (1994), Seasonal Trend Analysis of Published Ground-Based and TOMS Total Ozone Data Through 1991, *J. Geophys. Res., 99, 5449-5464*

Hamill Patrick and Owen Brian Toon (1991), Stratospheric Clouds and the Ozone Hole, *Atmos.Inst.Phys. pp. 34-42*

Harremoes Paul, David Gee, Malcoim MacGarvin, Andy Stirling, Jane Keys, Brian Wynne, Sofia Guedes Vaz (2012), The Precautionary Priciple in the 20th century: Late Lessons from Early Warnings, *Published byEarthscan Publications ltd. p 79*

Hegglin, M.I., C. D. Boone, G. L. Manney, T. G. Shepherd, K. A. Walker, P. F. Bernath, W. H. Daffer,P. Hoor and C. Schillerl (2008), Validation of ACE-FTS satellite data in the upper troposphere/lower stratosphere (UTLS) using non-coincident measurements, *Atmos. Chem. Phys., 8, 1483-1499*

Herman, J.R. et al (1996), Meteor-3, Total Ozone Mapping Spectrometer (TOMS) Data Product User's Guide, 1996, URL:ftp://gsfc.nasa.gov/pub/meteor3/METEOR3_USERGUIDE.PDF

Hofmann, D. J.,S.J. Oltmans, W.D. Komhyr, J.M. Harris, J.A. Lathrop, A.O. Langford, T. Deshler, B. J. Johnson, A. Torres and W.A Matthew (1994), Ozone Loss in the Lower Stratosphere Over the United States in 1992-1993: Evidence for Heterogeneous Chemistry in the Pinatubo Aerosol, *Geophysical Research Letters, Vol. 21, No. 1, pp. 65-68*

Houghton et al (2001), Climate Changes 2001: The Scientific Basis, Cambridge University, *Pres, the Edinburg Building, Cambridge CB2, 2RU, UK*

Jack Fisherman, Catherine E. Watson, Jack C. Larsen and Jennifer A. Logan (1990), Distribution of tropospheric ozone determined from satellite data, *J. Geophys. Res., 95, 3599-3617*

Jaross, G., A. Krueger, R.P. Cebula, C. Seftor, U. Hartmann, R. Haring and D. Burchfield (1995). Calibration and Postlaunch Performance of the Meteor 3/TOMS Instrument.*Journal of Geophysical Research*, Vol 100, 2985-2995

Jiang, Y.B., L. Froidevaux, A. Lambert, N.J Livessey, W.G. Read, J.W. Waters, B. Bojkov, T. Leblane, I.S. McDermid, S. Godin-Beekmann, M.J. Filipiak, R.S. Harword, R.A. Fuller, W.H. Daffer, B.J. Drouin, R.E. Cofield, D.T. Cuddy, R.F. Jarnot, B.W. Knosp, V.S. Perus, M.J. Schwartz, W.V. Snyder, P.C. Stek, R.P. Thurstans, P.A. Wagner, M.A. Hart, S.B. Anderson, C. Bodeker, B. Calini, H. Claude, G. Coetzee, J. Davies, H. De Backer, H. Dier, M. Fujiwara, B. Johnson, H. Kelder, N.P. Leme, G. Konig-Langlo, E. Kyro, G. Laneve, L.S. Fook, J.Merrill, G. Morris, M. Newchurch, S. Oltmans, M.C. Parronds, F. Posny, F. Schmidlint, P. Skrivankova, R. Stubi, D.Tarasick, A. Thompson, V. Thouret, P. Viatte, H. Vomel, P. Von Der Gathen, M. Yela and G. Zablocki (2007), Validation of Aura Microwave Limb Sounder Ozone by ozonesonde and lidar measurements, *J. Geophys. Res., 112, JD008776*

Johnson, F.S., J.D. Purcell and R. Tousey (1951), Measurement of the Vertical Distribution of Atmospheric Ozone from Rockets, *J. Geophys. Res., No. 16*

Jones, A.E. and J.D. Shanklin (2002), Continued Decline of Total Ozone over Halley, Antarctica since 1985, *Nature, 376, 409-411*

Keim, C., M. Eremenko, J. Orphal, G. Dufour, J.-M. Flaud, M. Hopfner, A. Boynard, C. Clerbaux, S. Payan, P.-F. Coheur, D. Hurtmans, H. Claude, H. Dier, B. Johnson, H. Kelder, R. Kivi, T. Koide, M.L. Bartolome, K. Lambkin, D. Moore, F. J. Schmidlin and R. Stubi (2009). Tropospheric Ozone from IASI : Comparisonof different Inversion Algorithm and Validation with Ozonesondes in the Northern Middle Latitudes. *Atmospheric Chemistry and Physics,* 9, 9329-9347

Kirchhoff, V.W., R.A.Barnes and A.L. Torres (1991), Ozone Climatology at Natal, Brazil from In Situ Ozonesonde Data, *J. Geophys. Res., Vol. 96, No. D6, pp. 10, 899-10,909*

Komhyr, W.D., Grass R.D. and Leonard R.K. (1989), Dobson Spectrophotometer 83: A Standard for Total Ozone Measurements, *J. Geophys. Res., Vol.94, pp. 9847-9861*

Laakso, L., V. Vakkari, A. Virkkula, H. Laakso, J. Backman, M. Kulmala, J.P. Beukes, P.G, van Zyl, P. Tiitta, M. Josipovic, J.J Pienaar, K. Chiloane., S. Gilardoni, E. Vignati, A. Wiedensohler, T. Tuch, W. Birmili, S. Piketh, K. Collett, G.D. Fourie, M. Komppula, H. Lihavainen, G.de Leeuw and V.M. Kerminen (2012), South Africa EUCAARI Measurements: Seasonal Variation of Trace Gases and Aerosol Optical Propertices. *Atmos.Chem.Phys., 12, 1847-1864*

Levelt, P.F., G.H. J. Van Den Oord, M.R. Dobber, A. Mälkki, H. Visser, Johan de Vries,Piet Stammes, J.O.V. Lundell and Heikki Saari (2006), The Ozone Monitoring Instrument, *IEEE Transaction on Geoscience and Remote Sensing, Vol. 44, No. 5*

Liu, X, P.K. Bhartia, K. Chance, R.J.D. Spurr and T.P. Kurosu (2009), Ozone Profile Retrievals from Ozone Monitoring Instrument, *Atmos.Chem.Phys.Discuss., 9, 22693-22738*

Livesey, N.J., M. J. Filipiak, L. Froidevaux, W. G. Read, A. Lambert, M. L. Santee, J. H. Jiang, H. C. Pumphrey, J. W. Waters, R. E. Cofield, D. T. Cuddy, W. H. Daffer, B. J. Drouin, R. A. Fuller, R. F. Jarnot, Y. B. Jiang, B. W. Knosp, Q. B. Li, V. S. Perun, M. J. Schwartz, W. V. Snyder,P. C. Stek, R. P. Thurstans, P. A. Wagner, M. Avery, E. V. Browell, J.-P. Cammas, L. E. Christensen, G. S. Diskin, R.-S. Gao, H.-J. Jost, M. Loewenstein, J. D. Lopez, P. Nedelec, G. B. Osterman,G. W. Sachse, and C. R. Webster (2008), Validation of AURA Microwave Limb Sounder O_3 and CO Observation in the Upper Troposphere and Lower Stratosphere*, J. Geophys., Res., Vol. 113 JD008805*

Lu, Q.B. and L. Sanche (2001), Effects of Cosmic Rays on Atmospheric Chlorofluorocarbon Dissociation and Ozone Depletion, *Physical Review Letters, Vol. 87, No. 7*

Lucien, Froidevaux et al (2006), Early Validation Analysis of Atmospheric Profilesfrom EOS MLS on the AURA Satellite, *IEEE Transaction on Geoscience Remote Sensing, Vol. 44, No5*

Mahendranth, B. and G. Bharathi (2002), Inter-annual Variability and Temporal Variation of Total Column Ozone in Visakhapatnam from Ground-Based Observations, Asia-Pacific, *J. Atmos. Sci., 48(2), 191-195*

Marenco Alain, Valérie Thouret, Philippe Nédélec, Herman Smit, Manfred Helten, Dieter Kley, Fernand Karcher, Pascal Simon, Kathy Law, John Pyle, Georg Poschmann, Raner Von Wrede, Chris Hume, Tim Cook (1998), Measurement of ozone and water vapor by Airbus in-service aircraft: The MOZAIC airborne program, an overview, *Journal of Geophysical Research: Atmospheres (1984–2012), Volume 103, Issue D19, pages 25631–25642*

Mark, R. Schoeberl et al (2006), Overview of the EOS AURA Mission, *IEEE Transaction on Geoscience and Remote Sensing, Vol. 44, No. 5*

Masserot, D., J. Lenoble, C. Brogniez, M. Houet, N. Krotkov and R. McPeters (2002), Retrieval of ozone column from global irradiance measurements and comparison with Toms data. A year of data in the Alps, *Geophys. Res. Let., 29, 9, 1309, 10.1029/2002gl014823*

Mckenzie, R.L., G. Seckmeyer, A.F. Bais, J.B. Kerr and S. Madronich (2001), Satellite Retrieval of Erythemal UV Dose Compared with Ground-Based Measurements at Northern and Southern Mid-Latitudes, *J. Geophys. Res., Vol. 106, No. D20, pp. 051-24, 062*

McPeters, R.D., S.M. Hollandsworth, L.E. Flynn, J.R. Herman and C.J. Seftor (1996), Long-term Ozone Trends Derived from the 16-year Combined Nimbus 7/ Meteor 3 TOMS Version 7 Record, *Geophysical Research Letters 23:doi.10.1029/96GL03540*

McPeters, R.D., Gordon J. Labow and B.J. Johnson (1997), A Satellite Ozone Climatology for Balloonsonde Estimation of Total Column Ozone, *J. Geophys. Res., Vol. 102, No. D7, pp. 8875-8885*

McPeters, R.D., Gordon J. Labow and Jennifer A. Logan (2007), Ozone climatological profiles for satellites retrieval algorithm, *J. Geophys. Res., 112, JD00682*

Nair, P.J., S. Godin-Beekmann, J. Kuttipurath, G. Ancellent, F. Goutail, A. Pazmino, L. Froidevaux, J.M. Zawodny, R.D. Evans, H.J. Wang, J. Anderson and M. Pastel (2013),

Ozone Trends Derived from Total Column and Vertical Profiles at a Northern Mid-Latitude Station, *Atmos.Chem. Phys., 13, 10373-10384*

Nassar, R., J.A. Logan, H.M. Worden, I.A. Megretskaia, K.W. Bowman, G.B. Osterman, A.M. Thompson, D.W. Tarasick, S. Austin, H. Claude, M.K. Dubey, W.K. Hocking, B.J. Johnson, E. Joseph, J. Merrill, G.A. Morris, M. Newchurch, S.J. Oltmans, F. Posny, F.J. Schmidlin, H. Vomel, D.N. Whiteman and J.C. Witte (2008), Validation of Tropospheric Emission Spectrometer (TES) Nadir Ozone Profiles Using Ozonesonde Measurements, *J. Geophys. Res., 113, JD008819*

Newman, P.A., J.F. Gleason, R.D. McPeters and R.S. Stolarski (1997), Anomalously Low Ozone over the Artic, *Geophysical Research Letters, Vol. 24, No. 22, pp. 2689-2692*

Nickolay A. Krotkov et al (2006), Band Residual Difference Algorithm for Retrieval of SO_2 from the Aura Ozone Monitoring Instrument (OMI) , *IEEE Transaction on Geoscience and Remote Sensing, Vol. 44, No. 5*

Norval, M. et al (2007), The effects on human health from stratospheric ozone depletion and its interaction with climate change, *Photochem.Photobiol.Sci, 6, 232-251*

Oum, K.W (1998), Formation of Molecular Chlorine from the Photolysis of Ozone and Aqueous Sea-Salt Particles, *Science 279.5347,74*

Paul A. Newman, Leslie R. Lait and Mark R. Schoeberl (1998), The Morphology and Meteorology of Southern Hemisphere Spring Total Ozone Mini-Holes, *Geophysical Research Letters Vol. 15, pp. 923-926*

Paul, J.F. Fortuin and Hennie Kelder (1998), An Ozone Climatology Based on Ozonesonde and Satellite Measurements, *J. Geophys. Res., 103, 709-734*

Poberaj, C.S., J. Staehelin, D. Brunner, V. Thouret, H. De Backer, and R. Stübi (2009), Long-term changes in UT/LS ozone between the late 1970s and the 1990s deduced from the GASP and MOZAIC aircraft programs and from ozonesondes, *Atmos. Chem. Phys., 9, 5343-5369*

Pyle John and Theodore Shepherd (2007), Ozone Climatology and Review: A Review of Interconnections

Rod Jekins (2006), A Comparative Guide to Stratospheric Ozone Depletion

Roxanne Vingarzan (2004), A View of Surface Ozone Background Levels and Trends, *Atmospheric Environment 38 (2004), 3431 - 3442*

Rumen D. Bojkov and Vitali E. Fioletov (1995), Estimating the Global Ozone Characteristics During the Last 30 Years. *J. Geophys. Res., Vol 100, D8, pp.16, 537 – 16, 551*

Rusch, D.W. and R.T. Clancy (1994), Comparison of satellite measurements of ozone and ozone trends *J. Geophys. Res., 99, 501-511*

Semane, N., H. Bencherif, B. Morel, A. Hauchecore and R.D. Diab (2006), An Unusual Stratospheric Ozone Decrease in the Southern Hemisphere Subtropics Linked to Isentropic Air-Mass Transport as Observed Over Irene, (25.5^{o}S, 25.1^{o}E) IN Mid May 2002, *Atmos. Chem. Phys. 6, 1927-1936*

Sivakumar, V., T. Portafaix, H. Bencherif, S. Godin-Beekmann and S. Baldy (2007), Stratospheric Ozone Climatology and Variability Over a Southern Subtropical Site: Reunion Island (21.5S, 55E), *Ann. Geophys, 25, 2321-2334*

Sivakumar,V., J.-L. Baray, S. Baldy and H. Bencherif (2006), Tropopause Characteristics Over Southern Subtropical Site, Reunion Island (21^{o}S, 55^{o}E), Using Radiosonde-Ozonesonde Data, *J. Geophys. Res.,Vol. 111, D19 111, JD006430*

Sivakumar, V., H. Bencherif, N. Begue and A.M Thompson (2011), Tropopause Characteristics and Variability from11yr of SHADOZ Observations in the Southern Tropics and Subtropics, American Meteorological Society, Vol. 50, pp. 1403-1416, JAM2453.1

Staehelin J.N. et al (2001), Ozone Trend: A Review, Rev, *Geophys., 39, 231-290*

Stephen A. Montzka et al (1996), Decline in the Tropospheric Abundance of Halogens from Halocarbons: Implications for Stratospheric Ozone Depletion, *Science, Vol. 272*

Stowe, L.L., R.M. Carey, P.P. Pellegrino (1992), Monitoring the Mount Pinatubo Aerosol Layer With NOAA/II AVHRR Data, *Geophys Res Letter, Vol. 19, No. 2, pp. 159-162*

Susan Solomon (1988), The Mystery of the Antarctic Ozone Hole, *Review of Geophysics, Vol. 26, pp. 131-148*

Sze, N.D et al (1989), Antarctic Ozone Hole: Possible Implications for Ozone Trends in the Southern Hemisphere, *J. Geophys. Res., 94, pp. 11, 521-11,528*

Tesfaye, M., V. Sivakumar., J. Botai and G. Mengistu Tsidu (2011), Aerosol Climatology over South Africa based on 10 years of Multiangle Imaging Spectroradiometer (MISR) data, , *J. Geophys. Res., Vol. 116, D20216*

Theys, N., R. Campion, L. Clarisse, H. Brenot, J. van Gent, B. Dils, S. Corradini, L.Merucci, P.-F. Coheur, M. Van Roozendael, D. Hurtmans, C. Clerbaux, S. Tait and F. Ferrucci (2013), Volcanic SO_2 Fluxes Derived from Satellite Data: A Survey Using OMI, GOME-2, IASI and MODIS, *Atmos. Chem. Phys, 13,5945-5968*

Thompson Anne and Robert Hudson (1999), Tropical Tropospheric Ozone (TTO) Maps From Nimbus-7 and Earth Probe TOMS by the Modified-Residual Method: Evaluation with Sondes, ENSO Signals and Trends from Atlantic Regional Time Series. *J. Geophys. Res., Vol. 27, No. D21, pp. 26, 961-26, 975*

Thompson et al (2000), Tropical Atlantic Paradox: Shipboard and Satellite Views of a Tropospheric Ozone Maximum and Wave One in January – February 1999, *J. Geophys. Res., Vo. 27, No. 20, pp. 3317-3320*

Thompson, A.M., J.C. Witte, R.D., McPeters, S.J. Oltmans, F.J. Schmidlin, J.A. Logan, M. Fujiwara, W.J.H. Kirchhoff, F. Posny, G.J.R. Coetzee, B. Hoegger, S. Kawakami, T. Ogawa, B.J. Johnson, H. Vomel and G. Labow (2003a), Southern Additional Ozonesondes (SHADOZ) 1998-2000 Tropical Ozone Climatology: 1. Comparison with Total Ozone Mapping Spectrometer (TOMS) and Ground-Based Measurements *J. Geophys. Res., 108, JD000967*

Thompson, A.M., J.C. Witte, S.J. Oltmans, F.J. Schmidlin, J.A. Logan, M. Fujiwara,V.W. J. H. Kirchhoff, F. Posny, G.J.R. Coetzee, B. Hoegger, S. Kawakami, T. Ogawa, J. P. F. Fortuin, and H. M. Kelder (2003b), Southern Additional Ozonesondes (SHADOZ) 1998-2000 tropical ozone Climatology: 2. Tropospheric Variability and the Zonal Wave One, *J. Geophys. Res., 108 JD002241*

Thompson, A.M., J.C. Witte, H.G.J. Smit, S.J. Oltmans, B.J. Johnson, V.W. J. H. Kirchhoff, and F. J. Schmidlin (2007), Southern Additional Ozonesondes (SHADOZ) 1998-2004

tropical ozone Climatology: 3. Instrumentation, Station-to-Station Variability and Evaluation with Simulated Flight Profiles, *J. Geophys. Res., 112, JD007042*

Thompson, et al Thompson A.M., S. K. Miller, S. Tilmes, D.W. Kollonige, J.C. Witte, S.J. Oltmans, B.J. Johnson, M. Fujiwara, F. J. Schmidlin, G. J. R. Coetzee, N. Komala, M. Maata, M. Mohamad, J. Nguyo, C.Mutai, S-Y. Ogino, F. Raimundo Da Silva, N. M. Paes Leme, F. Posny, R. Scheele, H.B. Selkirk, M. Shiotani, R. Stübi, G. Levrat, B. Calpini, V. Thouret, H. Tsuruta, J. V. Canossa, H. Vömel, S. Yonemura, J.A. Diaz, N.T. Tan Thanh, and H.T. Thuy Ha (2012), Southern Additional Ozonesondes (SHADOZ) Ozone Climatology 2005-2009: Tropospheric and Tropical Tropopause Layer (TTL) Profiles with Comparisons to OMI-Based Ozone Products, *J. Geophys. Res., 117, JD016911*

Van Der Leun J.C. (2004), The ozone layer, *Photodermatology, Photoimmunology and Photomedicine pp. 159–162*

Van Roozendael et al (1998), Validation of Ground-Based Visible Measurements of Total Ozone by Comparison with Dobson and Brewer Spectrophotometers, *Journal of Atmospheric Chemistry, 29: 55-83*

Varotsos C. (2004), Atmospheric Pollution and Remote Sensing: Implications for the Southern Hemisphere Ozone Hole Split in 2002 and the Northern Mid-Latitude Ozone Trend, *Advances in Space Research 33, pp. 249-253*

Van Roozendael, M., D. Loyola, R. Spurr, D. Balis, J.-C. Lambert, Y. Livschitz, P. Valks, T. Ruppert, P. Kenter, C. Fayt and C. Zehner (2006), Ten Years of GOME/ERS-2 Total Ozone Data- The New GOME Data Processor (GDP) Version 4: 1. Algorithm Description. *J. Geophys. Res., Vol 111, JD006375*

Von Savigny, C., C. S. Haley, C. E. Sioris, I. C. McDade, E. J. Llewellyn, D. Degenstein, W. F. J. Evans, R. L. Gattinger, E. Griffioen, E. Kyrola, N. D. Lloyd, J. C.McConnell, C. A. McLinden, G. Me´gie, D. P. Murtagh, B. Solheim, and K. Strong (2003). Stratospheric Ozone Profiles Retrieved from Limb Scattered Sunlight Radiance Spectra Measured by the OSIRES Instrument on the Odin Satellite, Geophysical Research Letters, Vol. 30, No. 14, 1735, GL016401

Waters, J.W, L. Froidevaux, R.S. Harwood, R.F. Jarnot, H.M. Pickett, W.G. Read, P.H. Siegel, R.E. Cofield, M.J. Filipiak, D.A. Flower, J.R. Holden, G.K. Lau, N.J. Livesey, G.L. Manney, H.C. Pumphrey, M.L. Santee, D.L. Wu, D.T. Cuddy, R.R. Lay, M.S. Loo, V.S. Perun, M.J. Schwartz, P.C. Stek, R.P. Thurstans, M.A. Boyles, K.M. Chandra, M.C. Chavez, Gun-Shing Chen, B.V. Chudasama, R. Dodge, R.A. Fuller, M.A. Girard, J.H. Jiang, Y. Jiang, B.W. Knosp, R.C. LaBelle, J.C. Lam, K.A. Lee, D. Miller, J.E. Oswald, N.C. Patel, D.M. Pukala, O. Quintero, D.M. Scaff, W. Van Snyder, M.C. Tope, P.A. Wagner, and M.J. Walch (2006), The Earth Observing System Microwave Limb Sounder (EOS MLS) on the Aura Satellite, *IEEE Transaction on Geoscience and Remote Sensing, Vol. 44, No. 5*

Wang Jun and Wang Hui-Jun (2010), The relationship between total ozone and local climate at Kunming using Dobson and TOMS data, *Atmos. Oceanic Sc., 3, 207-212*

World Meteorological Organisation (WMO)

Yasmine Calisesi, Heini Wernli and Niklaus Kampfer (2001), Midstratospheric ozone variability over Bern related to planetary wave activity during winters 1994-1995 to 1998-1999, *J. Geophys. Res., 106, 7903-7916*

Ziemke, S. Chandra, B. N. Duncan, L. Froidevaux, P. K. Bhartia, P. F. Levelt and J. W. Waters (2006), Tropospheric Ozone Determined From AURA OMI and MLS: Evaluation of Measurements and Comparison with the Global Modeling Initiative's Chemical Transport Model, *J. Geophys. Res., 111, JD007089*

Ziemke, J.R., S. Chandra and P.K. Bhartia (1998), Two New Methods of Deriving Tropospheric Column Ozone From TOMS measurements: Assimilated UARS MLS/HALOE and Convective-Cloud Differential Techniques, *J. Geophys. Res., 103, 115-127*

Ziemke, J.R., S. Chandra, G.J. Labow, P.K. Bhartia, L. Froidevaux and J.C. Witte (2011), A global Climatology of Tropospheric and Stratospheric Ozone Derived from AURA OMI and MLS Measurement. *Atmos. Chem. Phys, 11, 9237-9251*

Ziemke, J.R. and S. Chandra (2012), Development of a Climate Record of Tropospheric and Stratospheric Ozone from Satellite Remote Sensing: Evidence of an Early Recovery of Global Stratopsheric Ozone. *Atmos.Chem. Phys. Discuss, 12, 3169-3211*

Zunckel, M., K. Venjonoka, J.J. Pienaar, E.G. Brunke, O. Pretorius, A. Koosialee, A. Raghunandan and A.M. van Tienhoven (2004), Surface Ozone over Southern Africa: Synthesis of Monitoring Results during the Cross Border Air Pollution Impact Assessment Project, *Atmos.Enviro. 38, 6139-6147*

Figures References

1.1 https://www.google.co.za/?gfe_rd=cr&ei=aAtzU8rhFoXd8gesw4BQ#q=pie+chart+of+atmospheric+gases visited 18th April, 2014

1.2 https://www.google.co.za/?gfe_rd=cr&ei=aAtzU8rhFoXd8gesw4BQ#q=pictures+of+ozone+formation+and+destruction visited 12th June, 2014

1.3 https://www.google.co.za/?gfe_rd=cr&ei=aAtzU8rhFoXd8gesw4BQ#q=pictures+of+reducing+in+ozone+depleting+substances visited 13th June, 2014

1.4 https://www.google.co.za/?gfe_rd=cr&ei=aAtzU8rhFoXd8gesw4BQ#q=pictures+of+reducing+in+ozone+depleting+substances visited 8th June, 2014

2.1 https://www.google.co.za/?gfe_rd=cr&ei=aAtzU8rhFoXd8gesw4BQ#q=picture+of+dobson+spectrometer visited 5th June, 2014

2.2 https://www.google.co.za/?gfe_rd=cr&ei=rBlzU8z-GY3d8gfk94DwDQ#q=lidar+pictures visited 7th June, 2014

2.3 Ozone sounding with the Vaisala radiosonde RS92-SGP

2.7 https://www.google.co.za/?gfe_rd=cr&ei=aAtzU8rhFoXd8gesw4BQ#q=pictures+of+sbuv+satellite+showing+instruments+on+board visited 10th May, 2014

2.8 https://www.google.co.za/?gfe_rd=cr&ei=aAtzU8rhFoXd8gesw4BQ#q=pictures+of+sbuv+satellite+showing+instruments+on+board visited 23rd May, 2014

2.9 https://www.google.co.za/?gfe_rd=cr&ei=aAtzU8rhFoXd8gesw4BQ#q=pictures+of+aura+satellite+showing+instruments+on+board visited 18th April, 2014

2.10 https://www.google.co.za/?gfe_rd=cr&ei=aAtzU8rhFoXd8gesw4BQ#q=component+of+omi+satellite+images visited 7th June, 2014

2.11 https://www.google.co.za/?gfe_rd=cr&ei=aAtzU8rhFoXd8gesw4BQ#q=component+of+gome+satellite+images visited 7th June, 2014

2.12 https://www.google.co.za/?gfe_rd=cr&ei=aAtzU8rhFoXd8gesw4BQ#q=images+of+iasi+satellite visited 3rd May, 2014